Targeting Oncogenic RAS Signaling in Pancreatic Cancer

Interaction of small molecular inhibitors in the presence and absence of irradiation

Doctoral thesis

to obtain a doctorate (MD/PhD)

from the Faculty of Medicine

of the University of Bonn

Xuan Wang

from Hebei/(PR) China

2023

Written with authorization of

the Faculty of Medicine of the University of Bonn

First reviewer: PD Dr. med. Georg Feldmann

Second reviewer: Prof. Dr. med. Ulrich Spengler

Day of oral examination: 18. 04. 2023

From Medical Clinic 3, Center for
Integrative Medicine of the University of Bonn
Director: Prof. Dr. med. Peter Brossart

Table of Contents

List of abbreviations

AKT (PKB)	Protein Kinase B
APEH	Acyl Peptide Hydrolase
ASTRO	American Society for Therapeutic Radiology and Oncology
BCA	Bicinchoninic Acid
BCR	B-Cell Receptor
BRAF	B-RAF proto-oncogene serine/threonine kinase
BSA	Bovine Serum Albumin
CA19-9	Carbohydrate Antigen 19-9
CEA	Carcinoembryonic Antigen
CFTR	Cystic Fibrosis Transmembrane conductance Regulator
c-MET	Cellular-Mesenchymal-Epithelial Transition Factor
DFS	Disease-Free Survival
DH	Db1 Homolog
DSK	Dual Specificity Kinase
EGFR	Epidermal Growth Factor Receptor
ERAS42	Es cell expressed RAS
ERBB2	ERB-B2 receptor tyrosine kinase 2
ERK	Extracellular-signal-Regulated Kinase
FBP1	Fructose-1,6-Bisphosphatase
FOLFIRINOX	FOLinic acid (leucovorin), Fluorouracil (5-FU), IRINOTECAN and OXaliplatin
G12	Glycine 12
GAP	GTPase-Activating Protein
GDP	Guanosine Diphosphate
GEF	Guanine nucleotide Exchange Factor

Glut1	Glucose Transporter 1
GPCR	G-Protein-Coupled Receptors
GRB2	Growth Factor Receptor Bound Protein 2
GTP	Guanosine Triphosphate
GTPase	Guanosine Triphosphatase
HK	Hexokinase
HVR	Hypervariable Region
HRAS	Harvey Rat Sarcoma Viral Oncogene Homolog
ICMT	Isoprene-cysteine Carboxyl Methyl Transferase
KRAS	Kirsten Rat Sarcoma
Ldha	Lactate dehydrogenase A
Let-7	Lethal-7
MAPK (MEK)	Mitogen-Activated Protein Kinase
miRNA	microRNA
NFDM	NonFat Dry Milk
NK	Natural Killer
NRAS	Neuroblastoma RAS Viral Oncogene Homolog
NRTK	Non-Receptor Tyrosine Kinase
NSCLC	Non-Small Cell Lung Cancer
OS	Overall Survival
P2	Pocket of the switch-II region
PARP	Poly ADP-Ribose Polymerase
PBD	Protein-Binding Domain
PDAC	Pancreatic Ductal Adenocarcinoma
PDK1	Phosphoinositide-Dependent protein Kinase 1
Pfkl	Phosphofructokinase, liver type
PFS	Progression-Free Survival
PH	Pleckstrin Homolog

PI3K	Phosphatidylinositol 3-kinase
PIK3CA	Phosphatidylinositol-4,5-bisphosphate 3-kinase Catalytic subunit Alpha
PS	Phosphattidylserine
PTEN	Phosphatase and Tensin homolog
RAC1	Ras-Associated C3 botulinum toxin substrate 1
RAD	Ras Associated with Diabetes
RAF	V-RAF murine leukemia viral oncogene homolog
RAL	RAS-Linked protein
RalGEF	RAL Guanine nucleotide Exchange Factor
RAP	Ras-Associated Protein
RAS	Rat Sarcoma
RCE1	RAS Convertase converting Enzyme 1
REM	RAS Exchange Motif
RET	REarranged during Transfection proto-oncogene
RHEB	Ras Homolog Enriched in Brain
RT	Room Temperature
RTK	Receptor Tyrosine Kinases
RIT	Ras-like without CAAX (Ras with Inhibitory Threonine)
SBRT	Stereotactic Body Radiation Therapy
SD	Standard Deviation
SOS	Son of Sevenless
SOS1	Son of Sevenless homolog 1
TCR	T-Cell Receptor
TIAM1	Tumor Invasion and Metastasis-inducible protein 1
TK	Tyrosine Kinase
WHO	World Health Organization

1. Introduction

1.1 Pancreatic cancer

1.1.1 Definition

Pancreatic cancer, also known as Pancreatic Ductal Adenocarcinoma (PDAC), represents a group of malignant upper gastrointestinal tract tumors that originate from ductal epithelial or glandular alveolar cells of the pancreas. The five-year overall survival (OS) rate of pancreatic cancer is about 10%, which is among the worst of all human malignancies (Siegel et al., 2019). Incidence is slightly higher in males than in females, and PDAC is more prevalent in patients over the age of 40 years (Ferlay et al., 2015). Primary tumors are located in the head of the pancreas in approximately 70%−80% of cases, while in the remaining cases, it affects the pancreatic body or tail (Yao et al., 2007). The current World Health Organization (WHO) classification histologically distinguishes between epithelial and non-epithelial origins, with ductal adenocarcinoma of glandular duct epithelial origin accounting for the vast majority of 80%−90% of all pancreatic cancers (Ducreux et al., 2015). Less common histological subtypes include mucinous cystic adenocarcinoma, glandular follicular cell carcinoma, adenosquamous carcinoma, neuroendocrine carcinoma and various hybrid tumors (Kamisawa et al., 2016). PDAC represents one of the most devastating human cancers to date, characterized by aggressive local infiltration of surrounding tissues and early metastasis to distant organ sites. Incidence rates closely mirror mortality, and the overall prognosis is extremely poor (Siegel et al., 2018). It is currently the fourth leading cause of cancer-related deaths in Western countries and is on track to become the second leading cause of death in the next decade. Approximately 90% of pancreatic cancers originate from the exocrine pancreas, which forms the majority of the gland and secretes an enzyme-rich alkaline fluid through pancreatic ducts to the duodenum. Despite considerable scientific and clinical efforts over the past decades (Siegel et al., 2017), overall five-year survival rates still remain well below 5%, which is in part due to the fact that the majority of cases is diagnosed at locally advanced or already

metastatic disease stages upon the first presentation (Tuveson and Neoptolemos, 2012), while pancreatic cancer is also highly resistant to most standard chemotherapy or radiotherapy regimens. Therefore, novel molecularly targeted therapeutic approaches are particularly urgently required for this dire disease.

1.1.2 Risk factors and tumor serum markers of pancreatic cancer

The etiology of pancreatic cancer is still not fully understood. Occurrence of pancreatic cancer has been linked to cigarette smoking, alcohol, high-fat and high-protein diets, excessive caffeine consumption, environmental pollution and genetic factors. Recent findings showed that the incidence of pancreatic cancer in diabetic patients was significantly higher than that in the general population, it has also been noted that there is a relationship between patients with chronic pancreatitis and the development of pancreatic cancer, and that the proportion of pancreatic cancer in patients with chronic pancreatitis was significantly higher. There are also additional factors related to the occurrence of this disease, such as occupation, environment, and geography, and others (Kamisawa et al., 2016). Clinically relevant tumor markers used for diagnosis and follow-up of pancreatic cancer include Carbohydrate Antigen 19-9 (CA19-9), Carcinoembryonic Antigen (CEA) and others (E Poruk et al., 2013).

1.2 Definition and classification of RAS gene family members

Rat Sarcoma (RAS) genes comprise a group of proto-oncogenes that can be subdivided into six subfamilies, namely RAS, Ras homolog enriched in brain (RHEB), RAS-Linked protein (RAL), Ras associated with diabetes (RAD), Ras-Associated Protein (RAP) and Ras-like without CAAX (RIT). All family members share a common core G structural domain that provides guanosine triphosphatase (GTPase) and nucleotide exchange functions (Tsuchida et al., 2016). In the context of pancreatic cancer, oncogenic driver variations are most frequently detected in Kirsten Rat Sarcoma (KRAS). Other RAS family members carrying sequence variations in smaller fractions of cases include Harvey rat

sarcoma viral oncogene homolog (HRAS) and neuroblastoma RAS viral oncogene homolog (NRAS), which show a high degree of sequence homology with KRAS.

Structurally, RAS proteins are 160−180 amino acids in length, with a highly conserved enzymatically active G structural domain at the N-terminal end and a hypervariable region (HVR) at the C-terminal end (Song et al., 2019). KRAS encodes a membrane-bound protein with intrinsic guanosine triphosphate (GTP) activity, which will transform from an inactive, guanosine diphosphate (GDP)-bound form into an active, GTP-bound state upon tyrosine kinase receptor binding (Baker et al., 2013, Tan et al., 2019). Di-ubiquitination and acetylation may affect this conversion (Yan et al., 2009, Yang et al., 2013). Downstream signaling pathways affected by KRAS include V-RAF murine leukemia viral oncogene homolog (RAF)/MEK (mitogen-activated protein kinase (MAPK)) and phosphatidylinositol 3-kinase (PI3K)/AKT also known as protein kinase B (PKB). Activation of these pathways by oncogenic KRAS signaling ultimately promotes uncontrolled cancer cell growth and replication (Gimple and Wang, 2019).

Moreover, RAS signaling also modulates the activity of other metabolic pathways such as lipid, nucleotide synthesis, and glycolytic pathways. Apart from this, oncogenic KRAS has been found to promote escape of cancer cells from immune surveillance and to enhance cancer metastasis (Schreiber et al., 2011).

Phenotypic effects of oncogenic RAS signaling may differ across various cancer entities and according to stages of disease.

Of interest, activation of NRAS, HRAS were found to be dependent on palmitoylation modifications (Takahashi et al., 2005, Ahearn et al., 2011).

1.3 KRAS

1.3.1 Characterization of KRAS

Out of all RAS proteins, KRAS is the most frequently mutated isoform (Uprety and Adjei,

2020), accounting for approximately 85% of oncogenic RAS mutations in cancer cells (Hobbs et al., 2016). KRAS mutations are most prevalent in highly aggressive cancers, including pancreatic, lung, colorectal and bile duct cancers (Vasan et al., 2019). The KRAS gene, along with HRAS and NRAS, encodes a family of membrane-bound 21kd GTP-binding proteins that govern tumor cell proliferation, differentiation, and apoptosis by cooperating with numerous effectors (Riely et al., 2009).

KRAS proteins contain four major structural domains. The first structural domain, located at the N-terminal end of the protein, is identical in all three RAS variants, whereas the second structural domain has a low level of sequence homology. These two sections together make up the G-domain, which is critical for KRAS downstream signaling. The GTP-binding pocket is found in the G-structural domain of KRAS proteins, and it is important for the interaction between putative downstream effectors and GTPase-Activating protein (GAP)s. The C-terminus of KRAS proteins contains a highly variable region that governs post-translational modifications and affects plasma membrane anchoring (Pylayeva-Gupta et al., 2011). After covalent attachment of the farnesyl group to cysteine residues catalyzed by farnesyl transferase, inactive KRAS initiates a membrane-bound process, and RAS convertase converting enzyme 1 (RCE1) proteolyzes the last three amino acids at the cell surface of the outer membrane to offset the negative charge and prevent plasma membrane rejection, and isoprene-cysteine carboxyl methyl transferase (ICMT) catalyzes methyl shifts to the C-terminal amino acid (Ahearn et al., 2011).

KRAS cycles between the GTP-bound active state and the GDP-bound inactive state. The activation of RAS family members relies on Guanine nucleotide Exchange Factor (GEF)s, which facilitate the switch to the active state. The activation process is triggered by the binding of ligands to nearby transmembrane receptors, such as receptors of G-protein-coupled, growth factor, and toll-like. This binding event initiates the exchange of GDP for GTP by GEFs, thereby enhancing RAS activation in the intracellular signaling pathway. RAS activates a variety of downstream effectors, including PI3K, serine/threonine kinases,

GAPs and GEFs (Shields et al., 2000). RAS is temporarily inactivated when GTP complexes are reverted back to GDP molecules through hydrolysis of GTP. Oncogenic mutations lead to accumulation of KRAS in the GTP-bound and thus functionally active state by impairment of its intrinsic GTPase activity (Lito et al., 2016).

Oncogenic KRAS mutations preferentially affect codons 12, 13, or 61. Glycine 12 (G12) mutation leads to RAS activation by preventing GAP binding and hydrolysis stimulated by GAP. Codon 13 mutation causes a steric conflict with arginine, reducing GAP binding and hydrolysis. Glutamine 61, on the other hand, plays a direct role in catalysis by aiding to maintain the transitional phase in the hydrolysis reaction (Ostrem and Shokat, 2016). Codon G12 mutations account for 98% of all KRAS mutations in PDAC, resulting in constitutive activation of KRAS and sustained stimulation of downstream signaling pathways that drive many aspects of carcinogenesis, including metabolic reprogramming, sustained proliferation, resistance to apoptosis, evasion of inflammatory processes, tumor microenvironment remodeling, cell migration, and metastatic spread (Pylayeva-Gupta et al., 2011). The mutant cysteine 12 is near to the pockets of nucleotides and switching regions in KRAS proteins, which are crucial for activator interactions. Small compounds that bind covalently to cysteine in mutant KRAS showed the capacity to directly and selectively target oncogenic KRAS and abolish activation of downstream effector signaling. Covalent inhibitors of G12C depend on intact GTPase activity, as drug-bound KRAS G12C is trapped in its GDP-bound and hence inactive form (Shipman, 2016). Following the first discovery of a G12C heterotrimeric modulation region, a growing number of studies on G12C-selective inhibitors have been conducted. One example is the development of ARS-853, a highly specific inhibitor of KRAS G12C with increased bioavailability and potency to block GDP-GTP exchange (Patricelli et al., 2016).

1.3.2 Developments of KRAS research in recent years

KRAS mutations have been linked to a variety of clinical and pathological characteristics, which change depending on tumor histology, race, and smoking history (Ladanyi et al.,

2002). Several studies have discovered a definite link between smoking behavior and prevalence of KRAS mutations, with tobacco smoke appearing to trigger specific types of KRAS mutations and smokers being more likely to carry purine and pyrimidine translocations than nonsmokers. KRAS signaling is tissue specific, which is essential since therapeutic efficacy in one specific KRAS-driven tumor type does not necessarily predict efficacy in other cancers. In a number of recent studies, autocrine and paracrine signaling pathways have been found to be major amplifiers of oncogenic KRAS signaling in a variety of tumors (Ardito et al., 2012). Oncogenic KRAS signaling promotes tumor cell specific up-regulation of aerobic glycolysis (that is, overexpression of glycolytic enzymes including hexokinase (Hk)1, glucose transporter 1 (Glut1), phosphofructokinase, liver type (Pfkl), lactate dehydrogenase A (Ldha) and Hk2), which according to some authors might provide opportunities for targeted therapeutic intervention (Ying et al., 2012). The growth inhibitory role of wild-type KRAS is thought to be mediated via competition of activating or inhibitory regulators for optimal membrane localization (Young et al., 2013). It can block oncogenic KRAS, resulting in ineffective cell transformation and a reduction in tumor burden in some cancers.

KRAS mutations show pervasive effects on the tumor microenvironment, which aids to promote and maintain malignant cancer growth. Tumor cells harboring overexpression of KRAS support cell growth in a paracrine manner through secretory molecules, which can promote cancer malignancy (Di Magliano and Logsdon, 2013).

In cell culture experiments, inhibitors of ERK1/2 kinase, which mediates signaling down-stream of MEK, were found to confer growth inhibition of approximately 40% in KRAS mutant tumors (Morris et al., 2013). Recent evidence suggests that using microRNAs (miRNAs) that target KRAS could be a suitable way to inhibit oncogenic protein functions. Lethal-7 (Let-7) miRNA family members were found to be significant regulators of KRAS in several studies. Let-7 complementary sites on the 3’-UTR of the RAS gene family allow let-7 miRNAs to bind to KRAS genes and regulate their expression (Johnson et al., 2005). Decreasing let-7 expression in cancer tissues was associated with significantly greater

levels of KRAS mRNA, which was similarly linked to patient prognosis.

1.3.3 KRAS in carcinogenesis

The role of KRAS in pancreatic cancer

Oncogenic KRAS is the major driver of PDAC and modulates various signaling networks affecting numerous cellular functions including immuneregulatory pathways (Collins et al., 2012). In PDAC, oncogenic KRAS signaling is primarily mediated by three guanine nucleotide exchange factor pathways, namely PI3K/ Phosphoinositide-Dependent protein Kinase 1 (PDK1)/AKT, RAF/MEK/ Extracellular-signal-Regulated Kinase (ERK), and RAL (Fig. 1). Current studies in mice suggest that tumor cell-autonomous KRAS-PI3K-PDK1 signaling is required for the onset, development, and maintenance of pancreatic cancer (Bisht and Feldmann, 2018).

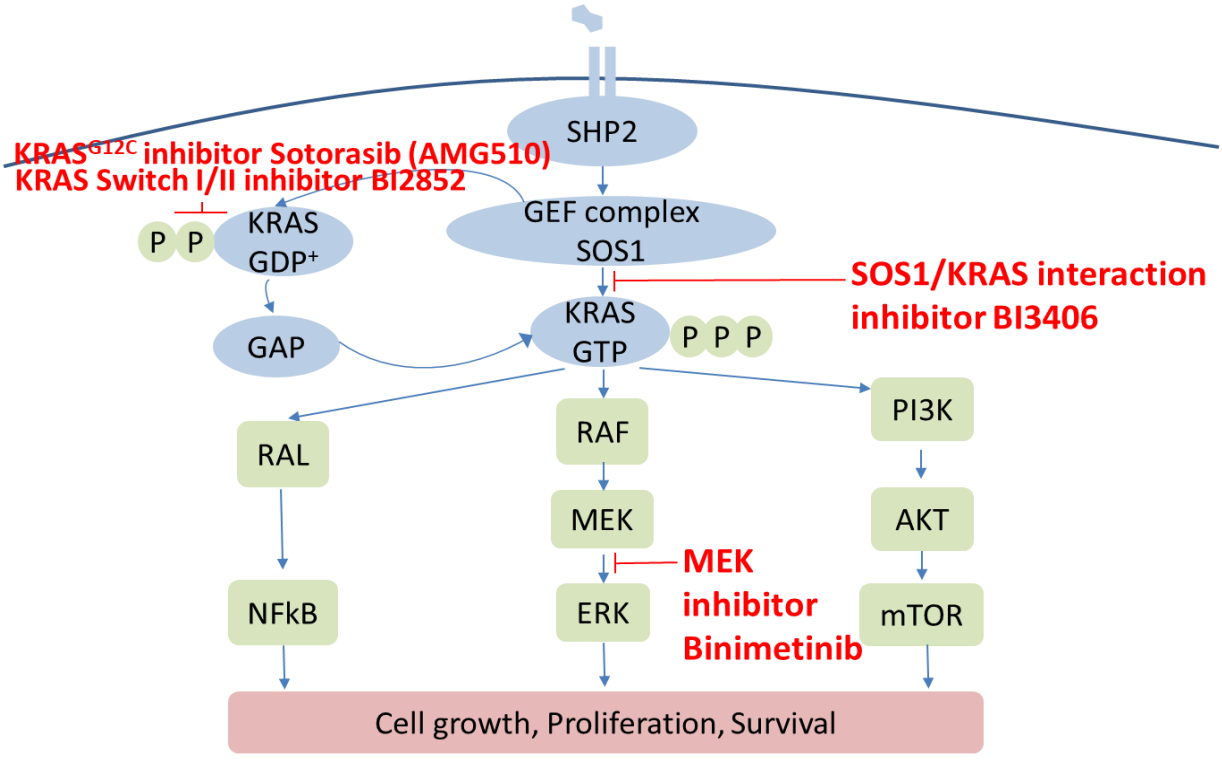

Figure 1: RAS-related pathways of action and the compounds which are mainly explored.

PI3K is an oncogenic class IA constant activator, which exclusively activates the PI3K/

PDK1/AKT pathway in Ptfla-positive cells, conveys oncogenic signaling in KRAS G12D-driven pancreatic cancer progression. The RAL guanine nucleotide exchange factor (RalGEF) pathway regulates pancreatic cancer development by loading GTP onto the RAS superfamily of small GTPases and activates small GTPases RAL-A and RAL-B, which act as mediators for tumor proliferation and metastasis, respectively, in human PDAC cell lines to regulate the development of pancreatic cancer (Brose et al., 2002).
Tumor microenvironment is assumed to be a critical mediator in PDAC progression, with paracrine activation of particular cytokine receptors or Receptor Tyrosine Kinases (RTK)s, potentially determining tissue-specific signaling pathways. Collins et al. (2012) discovered that persistent KRAS activation in the pancreas can cause fibro-inflammation, which promotes tumor growth via paracrine stimulation of activated fibroblasts and pancreatic stellate cells. Inactivation of oncogenic KRAS can entirely reverse fibrotic and inflammatory alterations in early pancreatic tumors by activating fibroblasts, pancreatic stellate cells, and immune cells. Chronic inflammatory stimuli can activate fibroblasts and stellate cells leading to pancreatic tissue remodeling and fibrosis, thus enhancing transforming potential of oncogenic KRAS signaling (Pylayeva-Gupta et al., 2011). Different cancer types, including PDAC, non-small cell lung cancer (NSCLC), and colon cancer, show distinct differences in their respective KRAS-driven signaling networks.

The role of KRAS in lung cancer

KRAS mutations are fairly common in lung adenocarcinoma, accounting for about 30% of cases, with exons 2 and 3 accounting for more than 97% of KRAS mutant cases (G12, G13 and Q61). These mutations reduce the innate GTPase activity of RAS and induce resistance to GTPase activators, thus causing RAS to accumulate in an activated, GTP-bound form and maintain constitutively active RAS signaling (Brose et al., 2002). In NSCLC, mutations within codon 12 of KRAS have been found to be inversely linked to disease-free (DFS) and OS in some studies (Slebos et al., 1990). Furthermore, malfunctioning of natural killer (NK) cells has recently been linked to growth and

progression of KRAS-driven lung cancer. This malfunction was caused by abnormal expression of fructose-1,6-bisphosphatase (FBP1) in NK cells, which inhibits glycolysis and impairs viability. This could point to a potential new route for NK cell-based cancer treatment by directly targeting FBP1 (Kortlever et al., 2017).

The role of KRAS in colorectal cancer

KRAS mutations are found in around 30−40% of colorectal cancers, and have been linked to lower survival, increased aggressiveness, and resistance to certain therapeutic strategies in this disease.

Furthermore, KRAS mutations have been detected in 50% of adenomas and were identified as critical genetic variations occurring early in adenoma-to-carcinoma cascade. Hence, it is widely held that KRAS mutations represent a key factor in the multi-step process of early carcinogenesis. KRAS mutation rates are unaffected by histological stage, tumor grade, geographic region, gender, or age. However, patients with anastomotic recurrence (58.2%) had a higher rate of G to A conversions than those with other forms of recurrence (Andreyev et al., 2001). Treatment of colorectal cancer cells with miR-143 mimetics or by overexpression of miR-143 inhibited KRAS expression levels, lowered ERK1/2 activation, and stopped cell proliferation (Chen et al., 2009), underlining the potential of miRNA-based therapeutics in treating KRAS-driven colorectal cancer.

1.3.4 Related interaction pathways of KRAS

Upstream signals of KRAS

Epidermal Growth Factor Receptor (EGFR) signals upstream of KRAS. Multiple studies found oncogenic mutations within EGFR to be mutually exclusive with KRAS mutations, implying that they share common downstream effectors in lung cancer cells (Kosaka et al., 2004). Upon functional activation EGFR activates and signals through various downstream effectors, including the PI3K/AKT and RAS/RAF/MEK(MAPK)/ERK pathways,

thus promoting cancer progression, neo-angiogenesis and metastatic spread, and ultimately affecting progression-free (PFS) as well as OS in cancer patients with EGFR mutations (Cataldo et al., 2011). KRAS signaling may be activated by different upstream signals involving growth factors (platelet derived and epidermal growth factor, as well as insulin-like growth factor, etc.), hormones, neurotransmitters and cytokines (Jančík et al., 2010). These processes typically depend on distinct KRAS membrane localization and interaction with effector proteins.

Downstream signals of KRAS

RAS-GTP binds directly to RAF proteins, recruiting the RAF kinase family members from the cytoplasm to the membrane, where they dimerize and become active. Activated RAF then phosphorylates and activates other downstream effectors, namely MEK or ERK, and propagates growth signals to regulate cell cycle and proliferation. Meanwhile, PI3K-AKT-mTOR, which also stimulates cell proliferation and suppresses apoptosis, is another route involved. The RAL pathway and tumor invasion and metastasis-inducible protein 1 (TIAM1)-Ras-Associated C3 botulinum toxin substrate 1 (RAC1) are involved in intracellular vesicle trafficking, cytoskeleton organization and tumor growth (Lambert et al., 2002). The RAS/MAPK pathway is considered to be one of the most critical oncogenic signaling axes, finally governing expression of key regulators such as cyclin D controlling cell cycle progression. Oncogenic KRAS dysregulates several metabolic processes, including glutamine catabolism, glycolysis, and redox hemostasis, enhances cancer cell chemoresistance, and plays a vital role in affecting multiple other intracellular signaling pathways (Mukhopadhyay et al., 2021).

1.4 KRAS related inhibitors

1.4.1 KRAS G12C inhibitors

In non-neoplastic cells, KRAS plays a role as a member of the RAS family, also acting as a molecular switch, which is briefly described as being switched "off" when bound to GDP

without enzymatic activity; however, when it receives activation signals from cell surface receptors, RAS binds to GTP and "opens" downstream signaling pathways to regulate cell proliferation, apoptosis, metabolism and angiogenesis (Pai et al., 1989). Various proteins share regulatory roles in this process, including GEF and GAP. GEFs can stimulate its binding to GTP and activate KRAS proteins, while GAPs accelerate GTP hydrolysis and convert KRAS to its inactive state (Dunnett-Kane et al., 2021), which is cycled between these two states at a very low rate. When the KRAS gene is mutated, conformation of the encoded and expressed KRAS protein is altered so that the protein almost completely loses its intrinsic GTPase activity. While affinity for GTP is significantly increased (Haigis, 2017), dissociation of GTP from KRAS is reduced and binding capacity of GDP to KRAS is weakened, so that the concentration of KRAS bound to GTP is increased, leading to sustained activation of downstream signaling pathways and uncontrolled cell growth. Consequently, oncogenic KRAS signaling establishes a major signaling axis for tumor cell proliferation and survival, providing a pivotal target for cancer therapy (Ryan and Corcoran, 2018). Mutant cysteine 12 is located next to the binding pocket of the switch-II region (P2) (Ostrem et al., 2013). In contrast to the wild type form, KRAS mutations disrupt the guanine exchange cycle, thereby locking it into a GDP-bound form that drives pro-tumor signaling (Ostrem et al., 2013).

For more than 30 years, major approaches to inhibit oncogenic KRAS have been to either block its entry into the cell or subcellular shuttling, or by blocking the proteins that interact with it. Unfortunately, none of these efforts led to any tangible, clinically relevant therapeutic success, and hence KRAS has long been considered to be an “undruggable” target. Encouragingly, Lito et al. (2016) recently found that the G12C variant of KRAS retains hydrolytic activity and continues to cycle between its active and inactive states. To address the bottleneck of lacking a binding pocket on the KRAS protein surface, some studies have targeted its cysteine-containing characteristics and used a library of small molecule fragments containing disulfide bonds for screening. With this approach, a small expandable pocket was finally found in the cysteine and molecular switch II region of

KRAS protein near the codon 12 mutation, which became a target for subsequent drug design.

Subsequently, drugs that specifically bind to this mutant protein have been developed. Amgen and Mirati Therapeutics have developed two direct KRAS G12C inhibitors, namely sotorasib (also known as AMG-510 or Lumakras), which is ten times more potent than the original lead compound, as well as adagrasib (also known as MRTX849), which act by selectively forming covalent bonds with cysteine 12 within the KRAS G12C oncoprotein, which is present only in the inactive GDP-binding conformation, so as to lock KRAS in an inactive state, inhibit tumor cell growth and proliferation, and induce apoptosis (Fell et al., 2020). These KRAS G12C inhibitors are highly specific, optimally designed for durable target inhibition with long half-life of up to 24 hours and broad tissue distribution, and are also able to cross the blood-brain barrier. In tumor models, AMG-510 is able to selectively target KRAS G12C, and monotherapy induces tumor regression in a mouse model of KRAS G12C tumors (Canon et al., 2019).

Sotorasib was evaluated as second line systemic therapy as compared to docetaxel in 345 KRAS G12C mutant non-small-cell lung cancer (NSCLS) patients in a prospective randomised, open-label, phase 3 clinical trial (Adrianus Johannes de Langen et al., 2023). In this study, sotorasib showed significantly improved median PFS as compared to docetaxel (5.6 months [95% CI 4.3-7.8] versus 4.5 months [95% CI 3.0-5.7]) with a hazard ratio of 0.66 [0.51-0.86] (p=0.0017). Of note, sotorasib showed a favorable toxicity profile with a lower rate of grade 3 or higher toxicity as compared to docetaxel chemotherapy (n=56 [33%] versus n=61 [40%]). Based on these data, sotorasib has recently been approved as second line therapeutic option for metastatic KRAS G12C mutant NSCLC by the FDA and EMA. As opposed to this, clinical data for gastrointestinal cancers including pancreatic cancer is currently less abundant and sotorasib is currently only available for selected individual cases of KRAS mutant pancreatic cancer patients within clinical trials or as off-label therapy (Strickler JH, et al., 2023).

1.4.2 MEK inhibitors

Due to the high affinity of KRAS for GTP and the relative abundance of GDP/GTP in human cells and tissues, early attempts to target KRAS with drug therapy did not achieve the desired results. This led to numerous efforts to target KRAS downstream effectors such as RAF, MEK, PI3K, AKT, mTOR or combinations of these. KRAS transmits upstream signals from cell surface receptors to downstream pathways, including the RAF/MEK/ERK pathway. MEK is the most typical example of a dual specificity kinase (DSK) that are relatively uncommon with RTKs and non-receptor tyrosine kinase (NRTK) activity, which both belong to the tyrosine kinase (TK) family. It activates the downstream sole substrate ERK through phosphorylation of tyrosine and threonine regulatory sites, which initiates a series of cell biological functions such as regulation of cell proliferation, invasion, angiogenesis and apoptosis resistance. There are two MEK family members, MEK1 and MEK2, which show nearly 85% sequence homology and have similar biological functions. The binding site of MEK inhibitors is neither an ATP binding site nor an ERK1/2 competition site, but a position close to the hydrophobic region of MEK, thus preventing ERK phosphorylation. These non-ATP competition inhibitors are rather selective. Mounting evidence suggests that RAS inhibitors have limited clinical efficacy when used as monotherapy, whereas MEK inhibitors may show significant therapeutic efficacy in malignancies caused by KRAS mutations (Martinelli et al., 2017). Currently, several highly selective drugs for MEK are available and dozens of compounds are in clinical development.

1.4.3 SOS1 inhibitors

Son of sevenless homolog 1 (SOS1) encodes a protein that acts as GEF and is widely expressed in various tissues. GEFs interact with GAPs to maintain KRAS homeostasis (Zhao et al., 2007). SOS1 protein consists of several structural domains: The Db1 homolog (DH) domain with specific Ras-GEF activity, the Pleckstrin homolog (PH) domain that forms an auto-inhibitory domain together with the DH, the RAS exchange motif (REM)

of the acting metastable activator, and the CDC25 homologous catalytic structural domain. The REM structural domain and the CDC25 homologous structural domain together constitute the catalytic functional region of SOS1, the DH structural domain and the PH structural domain together form a self-inhibitory domain belonging to the N-terminal regulatory region, and the PH structural domain is closely related to the DH structural domain, interacting with PIP2 and phosphatidic acid, where the DH domain physically blocks the metastable RAS binding site in the crystal structure of SOS1 (Gerboth et al., 2018). The role of SOS1 protein within the RAS signaling pathway is to promote the release of GDP from RAS, which then binds GTP, thus transforming RAS from an inactive to an active state. Therefore, SOS1 acts as a RAS-activating protein. SOS1 interacts with the adapter protein growth factor receptor bound protein 2 (GRB2), and the resulting SOS1/GRB2 complex binds to activated/ phosphorylated receptor tyrosine kinases (e.g., EGFR, ERB-B2 receptor tyrosine kinase 2 (ERBB2), rearranged during transfection proto-oncogene (RET), Cellular-Mesenchymal-Epithelial Transition Factor (c-MET), ALK) (Pierre et al., 2011). SOS1 is also recruited to other phosphorylated cell surface receptors such as T-cell receptor (TCR), B-cell receptor (BCR) and monocyte colony-stimulating factor receptor (Salojin et al., 2000). Localization of SOS1 to the plasma membrane adjacent to RAS family proteins allows SOS1 to interact with RAS protein. One single activated SOS1 molecule will sequentially activate multiple RAS molecules. Therefore, RAS signaling may be greatly amplified by SOS1. SOS1 inhibitors block GEF SOS1 protein binding to KRAS, thus preventing replacement of GDP by GTP, so that ultimately KRAS remains in an inactive state. Since both SOS1 inhibitors and SHP2 inhibitors thus enhance the probability of KRAS to remain functionally inactive, there is an obvious rationale for combinatorial therapeutic approaches that apply these compound together with mutation-specific inhibitors that directly bind oncogenic KRAS, such as the KRAS G12C inhibitors described above. As a matter of fact, preclinical studies proved that SHP2 plus KRAS G12C inhibitor combinations, as well as combinations of SOS1 plus KRAS G12C inhibitors exhibit therapeutic synergism in KRAS-driven cancer cells. Therefore,

such combinatorial regimens are currently undergoing active clinical evaluation (Liu et al., 2019).

1.5 Mechanisms of resistance to inhibition of KRAS effector pathways

Several studies reported compensatory activation of the PI3K/AKT pathway upon MEK1/2 inhibition, which is consistent with previously reported interaction between PI3K and MEK pathways in cancers with KRAS mutations (Collisson et al., 2012). Of Interest, concomitant blockade of MEK1/2 and AKT has the potential to overcome this escape mechanism (Shimizu et al., 2012). Inhibition of nucleotide exchange activity enhances the inhibitory effect of KRAS G12C inhibitors, as discussed above (Hobbs et al., 2016). Combination therapy regimens might therefore have the potential to overcome resistance to KRAS inhibitor monotherapy and confer long lasting, sustained therapeutic response.

As previously discussed, KRAS acts as pivotal mediator within the signaling cascade of EGFR-induced carcinogenesis. In recent years, it has been shown that mutations in KRAS or B-RAF proto-oncogene serine/threonine kinase (BRAF) are correlated with resistance to anti-EGFR directed therapy in colorectal cancer (Di Nicolantonio et al., 2008). Mutations in any of the codons described previously can promote accelerated nucleotide exchange and reduce GAP binding. Either of these could lead to increased GTP binding and KRAS activation. Consequently, in addition to the MAPK/ERK pathway, alterations in other mediators of the EGFR pathway, including mutations in phosphatase and tensin homolog (PTEN), BRAF, and phosphatidylinositol-4,5-bisphosphate 3-kinase catalytic subunit alpha (PIK3CA) are capable of further altering the response to anti-EGFR treatments (Bokemeyer et al., 2011). On the one hand, these additional alterations may confer adverse prognosis, on the other hand this interaction might also indicate that inhibition of KRAS downstream signaling pathways may be a valid approach to prevent resistance against KRAS inhibitor or anti-EGFR therapies, respectively.

1.6 Overcoming KRAS inhibitor resistance

In preclinical studies, nearly half of the cases of NSCLC were resistant to KRAS G12C inhibitors, and the forms of KRAS resistance were classified as primary, adaptive and acquired. In acquired resistance, activation of other pathways and secondary mutation of cells became the main cause of resistance development (Jiao and Yang, 2020). Part of the studies showed that different lung cancer cell lines with oncogenic KRAS mutations and PDAC cell lines have different dependence on KRAS signaling, and in some KRAS non-dependent cell lines, cells can survive even if KRAS is completely inhibited. This implies that a possible reason for resistance of KRAS G12C mutant tumors to G12C inhibitors might be that cancer cells might be less dependent on one particular mutant allele from the beginning and that inhibition of this allele hence confers little therapeutic efficacy. The vast majority of these cells exhibit MAPK pathway activation and sensitivity to MAPK pathway inhibitors (Muzumdar et al., 2017). Therefore, multi-target combinations might open up an avenue to overcome resistance against KRAS inhibitor therapy.

1.7 Radiation therapy in pancreatic cancer

Stereotactic body radiation therapy (SBRT) has increasingly been evaluated in pancreatic cancer due to its obvious advantages of guiding by real-time imaging, the capacity to precisely target tumor tissue with minimal irradiation of adjacent normal tissues, providing high doses of radiation in a short period of time, stimulating the immune system and killing cancer cells, while conferring little toxic side effects. Numerous studies have shown that although high local control rates of 53% to 89% were achieved after SBRT, local recurrence is still one of the reasons for the low survival rate of patients who underwent SBRT. Common sites of recurrence after pancreatic cancer resection include the local site of primary resection, abdominal cavity and the liver. The incidence of local failure ranges from 50% to 90%. Experience with adjuvant chemotherapy plus irradiation after surgery has shown that radio-chemotherapy might reduce the incidence of local failure and subsequently also improves survival (Kaiser and Ellenberg, 1985). Shen et al. (2021)

found that SBRT was able to improve patient survival, mirrored by reduction of CA19-9 serum levels. Simultaneous chemotherapy treatment with radiotherapy in patients with pancreatic cancers may have synergistic effects: On one hand, certain chemotherapy regimens increase the sensitivity towards therapeutic irradiation, on the other hand, chemotherapy drugs themselves treat systemic lesions and even stimulate immune benefits in synergy with radiotherapy for systemic tumor control. Intensive chemotherapy prior to radiotherapy is currently a major trend in radiotherapy combined with systemic chemotherapy, and Auclin et al. (2021) retrospectively analyzed that locally advanced or critically resectable pancreatic cancer treated with folinic acid (leucovorin), fluorouracil (5-FU), irinotecan and oxaliplatin (FOLFIRINOX) followed by concurrent radiotherapy had a significantly longer median OS (21.8 months vs. 16.8 months) compared to the chemotherapy only. Using a mouse model of pancreatic cancer, Ye et al. (2020) demonstrated that simultaneous administration of SBRT with mFOLFIRINOX provided better tumor control than either monotherapy or sequential treatment groups, and this combination regimen increased the extent of immunogenic cell death, which in turn enhanced tumor antigen presentation by dendritic cells and infiltration of intratumoral CD8+ T cells.

1.8 Prospects and outlook

We are still only at the beginning of the long road to conquer KRAS mutant cancers. In recent years, the concept of synthetic lethality has emerged as a possible way to overcome current shortcomings of single agent molecularly targeted therapies; briefly put, this concept describes therapeutic synergism of two targeted approaches, in which neither of the two principles alone shows any tangible therapeutic efficacy (Cory et al., 1991). This also opens up new opportunities to therapeutically target KRAS-driven tumors, for which no targeted options have been available until recently. Luo et al. (1991) discovered several genes in the mitotic pathway that exhibit synthetic lethal interactions with KRAS in a genome-wide screen.

In this current work presented here, we systematically explore effects of various combination regimens as laid out above.

Taken together, the aims of this current study are:

1.) To evaluate therapeutic efficacy of pharmacological KRAS inhibition in suitable in vitro model systems of pancreatic cancer growth and progression. For this, KRAS G12C mutation-specific inhibitor therapy will be tested side-by-side with SOS inhibitors designed to inhibit oncogenic KRAS irrespective of the specific KRAS genotype, thus acting as “pan-KRAS” inhibitors in this study. Pancreatic cancer cells applied in these experiments carry either KRAS G12C or other oncogenic driver variants, respectively, while pancreatic cancer cells with wild type KRAS will be used as controls.
2.) To screen for potential therapeutic synergism of pharmacological KRAS inhibition with inhibition of the MEK signaling pathway by means of the small molecule tyrosine kinase inhibitor binimetinib.
3.) To identify a potential radiosensitation of KRAS driven pancreatic cancer cells conferred by KRAS inhibition with or without concomitant MEK inhibition.

The results of these systematic in vitro studies will help to identify the most promising of these therapeutic strategies as outlined above to subsequently be further evaluated in more advanced and clinically more relevant in vivo model systems in the future.

2. Materials and Methods

2.1 Equipment

Table 1: Equipment

Device	Manufacturer
Air displacement pipettes (0.1-2.5 µl, 0.5-10.0 µl, 2-20 µl, 10-100 µl, 20-200 µl, 100-1000 µl)	Eppendorf AG, Hamburg, Germany
Air displacement pipettes (0.5-10 µl, 20-200 µl, 100-1000 µl)	Biohit mLINE, Sartorius Biohit Liquid Handling Oy, Helsinki, Finland
Autoclave	SHP Electronics GmbH, Suffolk, United Kingdom
Blotting unit	X-Cell SureLock, Thermo Fisher Scientific, Invitrogen, Massachusetts, USA
Cell counter	Scepter 2.0 handheld automated cell counter, Merck Millipore, Billerica, Massachusetts, USA
Cell culture centrifuge	Centrifuge 5810R, Eppendorf AG, Hamburg, Germany
Cell culture incubator	Sanyo MCO18-AIC, Panasonic Healthcare, Osaka, Japan
Electrophoresis chamber	PEQLAB 40-1214 and 40-0708, PEQLAB Biotechnologie GmbH, Erlangen, Germany
Electrophoresis power supply	Consort EV 202, Sigma-Aldrich, St. Louis, Missouri, USA
Elisa plate reader	Fluoroskan™ Microplate Fluorometer, Thermo Fisher Scientific, Invitrogen, Massachusetts, USA
Freezer (-80 ºC)	Forma 905 -86 ºC ULT Freezer, Thermo Fisher Scientific, Waltham, Massachusetts, USA
Freezer (-20 ºC)	Siemens, München, Germany
Freezer (4 ºC)	Siemens, München, Germany
Gel imaging system	ChemiDoc™ XRS+ System with Image Lab™ Software with software, Bio-Rad, Massachusetts, USA
Hemocytometer	OPTIK-Labor Dr.-Ing. Wolf-Dieter Prenzel, Lindenweg 9, Görlitz, Germany
Ice machine	Scotsman AF 20, Scotsman Ice Systems, Vernon Hills, Illinois, USA
Inverted microscope	Nikon Eclipse TS100, Nikon Instruments Europe B.V., Düsseldorf, Germany

Laboratory Water Purification Systems	PureLAB TM classic, ELGA VEOLIA, High Wycombe, United Kingdom
Laminar flow hood, biosafety level II	MSC Advantage (1,8m), Thermo Fisher Scientific, Waltham, Massachusetts, USA
Magnetic stirrer	ARE Heating Magnetic Stirrer, VELP Scientific, Usmate, Italy
Microcentrifuge	Centrifuge 5430R, Eppendorf AG, Hamburg, Germany
Microscope with camera, upright	Nikon H 550S, Nikon Instruments Europe B.V., Düsseldorf, Germany
Microwave	Panasonic NN-E245WB, Panasonic, Osaka, Japan
Mini centrifuge	MiniStar Silverline, VWR, Radnor, Pennsylvania, Germany
Mr. Frosty	Nalgene, Thermo Fisher Scientific, Waltham, Massachusetts, USA
pH Meter	S20 SevenEasy™ pH, Mettler-Toledo GmbH, Gießen, Germany
Pipette controller for serological pipettes	PIPETBOY acu, INTEGRA Biosciences AG, Zizers, Switzerland
Precision balance	Extend ED124S, Sartorius AG, Göttingen, Germany
Spectrophotometer	NanoDrop ND-1000 (PeqLab, Erlangen, Germany)
Suction pump	Membranpumpe MP060E, ilmvac GmbH, Ilmenau, Germany
Tube rotator	Roller mixer SRT9, Bibby Scientific Limited, Staffordshire, United Kingdom
Vortex	2_X3 VELP Scientifica, Usmate, Italy
Water bath	WNB22, Memmert GmbH, Schwabach, Germany
Weighting balance	Sartorius TE601, Sartorius AG, Göttingen, Germany

2.2 Consumables

Table 2: Consumables

Item	Manufacturer
6 well tissue culture plates	Sarstedt AG, Nümbrecht, Germany
12 well tissue culture plates	Sarstedt AG, Nümbrecht, Germany
24 well tissue culture plates	Sarstedt AG, Nümbrecht, Germany
96 well tissue culture plates, flat bottom	Corning Inc., Corning, New York, USA

96 well white plates	Nunc™, Sjælland, Denmark
1.5 ml microcentrifuge tubes	Sarstedt AG, Nümbrecht
8.0 µm cell culture	BD Biosciences, San Jose, California, USA
Autoclavable bags	Nerbe plus GmbH, Winsen, Germany
Beakers (400 ml, 1000 ml)	Schott AG, Mainz, Germany
Cover slips	Engelbrecht Medizin-und Labortechnik, Edermünde, Germany
Cryo tubes, 2.0 mm, PP, sterile	Sarstedt AG, Nümbrecht, Germany
Volumetric cylinders	Brand GmbH, Wertheim, Germany
Disposable scalpel	FEATHER Safety Razor Co., Ltd., Osaka, Japan
Conical flask	Technische Glaswerke Ilmenau GmbH, Minden, Germany
Microscopic slides	Engelbrecht Medizin-und Labortechnik, Edermünde, Germany
Nuclease-free microcentrifuge tubes (0.2 ml, 0.5 ml 1.5 ml)	Nerbe plus GmbH, Winsen/Luhe
Pipettes (2ml, 5 ml, 10 ml, 25 ml, 50 ml)	Greiner Bio-One GmbH, Frickenhausen, Germany
Conical centrifuge tubes, PP (15 ml, 50 ml)	Greiner Bio-One GmbH, Frickenhausen
Parafilm	American National Can Co., Chatsworth, California, USA
Pasteur pipettes, glass	Brand GmbH, Wertheim, Germany
Pipette tips (1-10 µl, 2-200 µl, 100-1000 µl)	Nerbe plus GmbH, Winsen/Luhe, Germany
Plastic Carboy (5 l, 10 l)	Kautex™, Thermo Fisher Scientific, Massachusetts, USA
Kim wipes	Kimtech Science™, Kimberly-Clark GmbH, Koblenz, Germany
PVDF Transfer membrane	Thermo Fisher Scientific, Massachusetts, USA
Filtered pipette tips (10 µl, 200 µl, 1000 µl)	Nerbe plus GmbH, Winsen/Luhe, Germany
Syringes (2 ml, 20 ml)	Becton, Dickinson and Company, Franklin Lakes, New Jersey, USA
Syringe filters, 0.45 µm pore size	Filtropur S 0.45, PES-Membran, Sarstedt AG, Nümbrecht, Germany
Syringe filters, 0.22 µm pore size	Filtropur S 0.2, PES-Membran, Sarstedt AG, Nümbrecht, Germany
Tissue culture flasks (25 cm^2, 75 cm^2)	Sarstedt AG, Nümbrecht, Germany

2.3 Chemicals and reagents

Table 3: Chemicals and reagents

Item	Manufacturer
Acetic acid, glacial	Merck, Darmstadt, Germany
Agarose, standard	Carl Roth, Karlsruhe, Germany
β-mercaptoethanol	Sigma-Aldrich, St. Louis, Missouri, USA
BCA Assay	Thermo Fisher Scientific, Waltham, Massachusetts, USA
Bovine serum albumin, fraction V, molecular biology grade	Carl Roth, Karlsruhe, Germany
CellTiter 96 AQueous One Solution Cell Proliferation Assay	Promega, Fitchburg, Wisconsin, USA
Crystal violet	Sigma-Aldrich, St. Louis, Missouri, USA
Cytoseal 60	Thermo Fisher Scientific, Waltham, Massachusetts, USA
Dimethyl sulfoxide (DMSO), cell culture grade	Sigma-Aldrich, St. Louis, Missouri, USA
Disodium ethylenediaminetetraacetate (Na_2 (EDTA)) dihydrate	Sigma-Aldrich, St. Louis, Missouri, USA
EOSIN Y solution (alcoholic)	Sigma-Aldrich, St. Louis, Missouri, USA
Ethanol, 70%, denatured	Otto Fischar, Saarbrücken, Germany
Ethanol, anhydrous, molecular biology grade	AppliChem, Darmstadt, Germany
Ethidium bromide solution (10 mg/ml)	Sigma-Aldrich, St. Louis, Missouri, USA
Formaldehyde, 37%, analytical grade	Merck, Darmstadt, Germany
Formalin, 4%	Otto Fischar, Saarbrücken, Germany
Hematoxylin solution, Harris modified	Sigma-Aldrich, St. Louis, Missouri, USA
Hydrochloric acid	Carl Roth, Karlsruhe, Germany
Luminol	Sigma-Aldrich, St. Louis, Missouri, USA
Methanol, analytical grade	AppliChem, Darmstadt, Germany
MOPS SDS Running Buffer (20X)	NuPAGETM, Thermo Fisher Scientific, Massachusetts, USA
Napoye loading dye, 4 × loading dye	Carl Roth, Karlsruhe, Germany
Nonfat dry milk	Carl Roth, Karlsruhe, Germany
Nuclease-free water	Life Technologies, Carlsbad, California, USA
Phosphatase inhibitor cocktail 2	Sigma-Aldrich, St. Louis, Missouri, USA
Phosphatase inhibitor cocktail 3	Sigma-Aldrich, St. Louis, Missouri, USA
Ponceau S solution	Sigma-Aldrich, St. Louis, Missouri, USA
Prestained protein marker	ProteinTech, Wuhan, Hubei, P.R.C
Protease inhibitor cocktail	Sigma-Aldrich, St. Louis, Missouri, USA
RalA Activation Assay Biochem Kit	Cytoskeleton, Inc. Acoma St., Denver, Colorado, USA

Sodium acetate trihydrate	Merck, Darmstadt, Germany
Sodium chloride, analytical grade	AppliChem, Darmstadt, Germany
Sodium dodecyl sulfate (SDS), molecular biology grade	AppliChem, Darmstadt, Germany
Sodium hydrogen carbonate ($NaHCO_3$)	Merck, Darmstadt, Germany
Sodium hydroxide, pellets	Sigma-Aldrich, St. Louis, Missouri, USA
Sodium hydroxide solution, 5 N	Carl Roth, Karlsruhe, Germany
Transfer Buffer (20X)	NuPAGE™, Thermo Fisher Scientific, Massachusetts, USA
Trypan Blue (0.4%)	Thermo Fisher Scientific, Invitrogen, Massachusetts, USA

2.4 Antibodies

Table 4: Primary antibodies

Antigen	Clone/Catalogue No.	Manufacturer
ERK	Rabbit monoclonal, clone 4695S	Cell Signaling Technology, Danvers, Massachusetts, USA
pERK	Rabbit monoclonal, clone 9101S	Cell Signaling Technology, Danvers, Massachusetts, USA
MEK	Rabbit monoclonal, clone 8727S	Cell Signaling Technology, Danvers, Massachusetts, USA
pMEK	Rabbit monoclonal, clone 2338S	Cell Signaling Technology, Danvers, Massachusetts, USA
GAPDH	Rabbit monoclonal, clone 14C10/2118	Cell Signaling Technology, Danvers, Massachusetts, USA
PARP	Rabbit monoclonal, clone 9532S	Cell Signaling Technology, Danvers, Massachusetts, USA
Cleaved PARP	Mouse monoclonal, clone 9554P	Cell Signaling Technology, Danvers, Massachusetts, USA
Caspase 3	Rabbit monoclonal, clone 9662S	Cell Signaling Technology, Danvers, Massachusetts, USA
Cleaved caspase 3	Rabbit monoclonal, clone 9664P	Cell Signaling Technology, Danvers, Massachusetts, USA

Table 5: Secondary antibodies

Antigen	Clone/Catalogue No.	Manufacturer
Rabbit IgG	Goat polyclonal, HRP - coupled/ 7074	Cell Signaling Technology, Danvers, Massachusetts, USA
Mouse IgG	HRP-linked antibody	Cell Signaling Technology, Danvers, Massachusetts, USA

2.5 Cell culture supplies

Table 6: Cell culture reagents

Reagent	Manufacturer
DMEM, high glucose (4.5 g/l), stable glutamine	PAA Laboratories, Pasching, Austria
RPMI 1640, stable glutamine	PAA Laboratories, Pasching, Austria
Fetal calf serum (FCS), standard, heat inactivated	PAA Laboratories, Pasching, Austria
Penicillin/Streptomycin, 10,000 I.U./ml and 10,000 µg/ml	PAA Laboratories, Pasching, Austria
Plasmocin, 25 mg/ml	Invivogen, San Diego, California, USA
DPBS without Ca2+ or Mg2+	PAA Laboratories, Pasching, Austria
Trypsin-EDTA, 0.05 %/ 0.02 % in PBS	PAA Laboratories, Pasching, Austria

Table 7: Cell culture media

DMEM full medium		RPMI full medium	
DMEM, high glucose (4.5 g/l), stable glutamine	500 ml	RPMI 1640, stable glutamine	500 ml
FCS, heat inactivated	50 ml	FCS, heat inactivated	50 ml
Penicillin/Streptomycin, 10,000 I.U./ml and 10,000 µg/ml	5.5 ml	Penicillin/Streptomycin, 10,000 I.U./ml and 10,000 µg/ml	5.5 ml
Plasmocin 25 mg/ml	100 µl	Plasmocin 25 mg/ml	100 µl

Table 8: Cell lines

Cell line	Catalogue No./Reference	Source
MiaPaCa-2	ATCC- CRM-CRL-1420	American Type Culture Collection, Manassas, Virginia, USA
Description:	MiaPaCa-2 is a kind of adherent epithelial cell line that was established in 1975 from pancreatic tumor tissue of a 65-year-old male, this cell line has a ploidy time of approximately 40 h, whose colony formation efficiency is approximately 19% in soft agar, and is sensitive to asparaginase.	
Panc-1	ATCC-CRL-1469	American Type Culture Collection, Manassas, Virginia, USA
Description:	Panc-1 is a kind of adherent cell line that was from a pancreatic ductal tumor in a 56-year-old Caucasian male with epithelial pancreatic cancer, whose ploidy time was 52 hours. Chromosomal studies showed that the cell had a chromosome plurality of 63, including 3 uniquely labeled chromosomes and 1 small ring chromosome. The growth of this cell line can be inhibited by 1 unit/ml of L-asparaginase while it can grow on soft agar become tumorigenic on nude mice.	
BxPC-3	ATCC-CRL-1687	American Type Culture Collection, Manassas, Virginia, USA

Description:	BxPC-3 is a kind of adherent cell line that was derived from the pancreatic tumor of a 61-year-old Caucasian female with pancreatic adenocarcinoma, which does not express the Cystic Fibrosis Transmembrane conductance Regulator (CFTR). The cells express mucin, pancreatic cancer-associated antigen and CEA, and are nearly 100% tumorigenic in transplanted nude mice.

Panc-1 and BxPC-3 cell lines were maintained in DMEM full medium, while MiaPaCa-2 cell line was cultured in RPMI full medium (see 2.7).

2.6 Solutions and buffers

Table 9: Tris-HCl

Component and Amount	0.5 M Tris-HCl pH 6.7	1.0 M Tris-HCl pH 8.0	1.5 M Tris-HCl pH 8.8
Trizma base	60.57 g	121.14 g	181.71 g
Ultrapure water	ad 1.0 l	ad 1.0 l	ad 1.0 l
Dissolve the component in approximately 800 ml of ultrapure water, adjust to the desired pH with concentrated hydrochloric acid, and fill up to 1.0 liter with ultrapure water.			

Table 10: 250 mM EDTA, pH 8

Component	Amount
Na_2 EDTA×$2H_2O$	23.26 g
Ultrapure water	ad 250.0 ml
Dissolve in approximately 200 ml ultrapure water, adjust pH to 8 with 5 N NaOH and fill up to 250.0 ml with ultrapure water.	

Table 11: 10% (w/v) SDS

Component	Amount
SDS	10 g
Ultrapure water	ad 100.0 ml
Dissolve in approximately 80 ml ultrapure water and fill up to 100.0 ml with ultrapure water.	

Table 12: 250 mM Luminol

Component	Amount
Luminol	443 mg
DMSO	ad 10.0 ml
Dissolve the luminol in DMSO, distribute them into aliquots and store at -20 ºC.	

Table 13: 90 mM 4-IPBA

Component	Amount
4-IPBA	1115 mg
DMSO	ad 50.0 ml
Dissolve the 4-IPBA in DMSO, distribute them into aliquots and store at -20 ºC.	

Table 14: 0.05% (w/v) Crystal violet solution

Component	Amount
Crystal violet	250 mg
Ultrapure water	ad 500.0 ml
Dissolve the crystal violet in approximately 400 ml ultrapure water, and fill up to 500.0 ml with ultrapure water.	

Table 15: 10×TBS, pH 8.0

Component	Amount	Concentration
1 M Tris HCl, pH 8.0	100.0 ml	100 mM
NaCl	48.15 g	825 mM
Ultrapure water	ad 1.0 l	
Dissolve the components in approximately 800 ml ultrapure water, and fill up to 1.0 l with ultrapure water.		

Table 16: TBST 0.01%

Component	Amount
10×TBS	100.0 ml
Tween 20	1 ml
Ultrapure water	ad 1.0 l
Dilute 10×TBS in 1:10 concentration with ultrapure water and add 1 ml Tween 20.	

Table 17: 50×TAE-buffer

Component	Amount	Concentration
Trizma base	242.0 g	40 mM
Glacial acetic acid	57.1 ml	20 mM
500 mM EDTA, pH 8	100 ml	1 mM
Ultrapure water	ad 1.0 l	
Dissolve the components in approximately 800 ml ultrapure water, and fill up to 1.0 l with ultrapure water.		

Table 18: PMSF

Component	Amount	Concentration
PMSF	871 mg	100 mM
Ethanol, anhydrous	ad 50.0 ml	

Dissolve 871 mg PMSF in anhydrous ethanol to a final volume of 50.0 ml and store at -20 ºC.

Table 19: RIPA lysis buffer

Component	Amount	Concentration
Igepal CA 630	2.5 ml	1%
Sodium deoxycholate	1.25 g	0.5%
10 % SDS	2.5 ml	0.1%
250 mM EDTA	2.0 ml	2 mM
DPBS	ad 250.0 ml	
Dissolve all of the components in DPBS to a final volume of 250.0 ml.		

Table 20: ECL solution

Component	Amount	Concentration
1.5 M Tris-HCl, pH 8.8	3.3 ml	100 mM
250 mM Luminol	250 µl	1.25 mM
90 mM 4-IPBA	1111 µl	2 mM
Ultrapure water	ad 50.0 ml	
Dissolve all of the components in ultrapure water to a final volume of 50.0 ml, store at 4 ºC and avoid the light. Add 0.5 µl of 30% H_2O_2 to each milliliter of solution before each application.		

Table 21: Western blot stripping buffer

Component	Amount
β-Mercaptoethanol	1.74 ml
10% SDS	50 ml
0.5 M Tris HCl, pH 6.7	31.3 ml
Ultrapure water	ad 250.0 ml
Dissolve all of the components in ultrapure water to a final volume of 250.0 ml, store at room temperature (RT) and avoid the light.	

2.7 Software

Table 22: Software

Name	Function	Source
Microsoft© Excel 2016 for Windows, v. 16.0.6965.2053	Data analysis	Microsoft Corporation and Harbin Institute of Technology
Optima Microplate Reader Software Package, v.2.2OR2	Data acquisition	BMG Labtech, Ortenberg, Germany
GraphPad Prism version 6.0. 0 for Windows	Data analysis and graphing	GraphPad Software, San Diego, California USA
SPSS	Data preparing and	IBM, Armonk, State of New York

	analysis	USA
Overleaf	Text editing	https://www. overleaf.com
Image J	Data preparing and analysis	Center for Information Technology National Institutes of Health Bethesda, Maryland USA

2.8 Cell culture methods

2.8.1 Culturing cell lines from cryopreserved freeze backs

Cryopreserved aliquots of cell lines stored at -80 ºC freezers were taken out and rapidly defrosted by incubating in 37 ºC water bath. The liquid cell suspension was then mixed with 9 ml of pre-warmed cell culture medium and pelleted at 1200rpm for 5 minutes. The pelleted cells were resuspended in full growth medium and seeded in sterile T-25 or T-75 tissue culture flasks accordingly and incubated at 37 ºC, 5% CO_2 and 90% relative humidity. The cells were checked every day under the microscope and the medium was changed very 2-3 days.

2.8.2 Subculturing of cell lines

After waking up the cryopreserved cell lines, cells were checked once daily for their healthy growth under the microscope. Once the cells reached 80% confluency, they were subcultured. For subculturing, the old growth medium was removed, the cell monolayer was washed once with DPBS and then incubated with 2 ml of 0.05% Trypsin-EDTA solution at 37 ºC for 5 minutes. After the cells were lifted off the surface, 8 ml of full growth medium was added to neutralize trypsin and the cell suspension was transferred to a sterile 15 ml conical tube. Cells were then pelleted by centrifuging the cell suspension at 1200 rpm for 5 minutes. The pelleted cells were resuspended again in 10 ml of fresh cell culture medium, split at a ratio of 1:10 (1 ml of cell suspension mixed with 9 ml of cell culture medium) in T-75 tissue culture flask and transferred back to the incubator.

2.8.3 Cryopreservation and storage of cell lines

Once the cells reached 80−90% confluency, they were trypsinized and single cell suspensions were made after adding 8ml of full growth medium to 2 ml trypsin solution. The cells were pelleted and resuspended in cryomedium in a way to achieve cell concentration of roughly 1-2 million cells per ml. The cell suspensions were then redistributed to cryotubes fitted inside a cryocontainer (to ensure gradual freezing of -1 ºC /minute) and transferred to -80 ºC freezer for long term storage.

2.8.4 Cell count using Hemocytometer

Cells were trypsinized and single cell suspensions were made. For counting the cells, cell suspension was taken in a microcentrifuge tube to which equal amount of Trypan blue dye was added. After 5 minutes incubation with the dye, cell suspension was loaded in the hemocytometer and the cells were counted under the microscope. The cell numbers were calculated per ml of suspension using the formula: (Total number of cells in 4 quadrants /4)×10,000×2 (adjusted for the dilution factor). The cell counting was repeated at least two times to ensure that the error did not exceed ±5%.

2.9 Cell biology methods

2.9.1 Cell viability assay (MTS-assay)

Principle: Growth inhibition of cell lines was measured using Cell Titer 96 Aqueous One solution Cell Proliferation Assay (Promega). This colorimetric assay is based on the conversion of a tetrazolium compound (MTS abbreviated as 3-(4,5-dimethylthiazol-2-yl)-5-(3-carboxymethoxyphenyl)-2-(4-sulfophenyl)-2H-tetrazolium) to a colored and soluble formazan product. In theory, this conversion is presumably accomplished by reducing equivalents NADH or NADPH produced by dehydrogenase enzymes in metabolically active cells. Since the dying cells lose their ability to reduce tetrazolium salts, the production of the colored formazan product is considered to be directly proportional to the number of viable cells in culture and can be measured spectrophotometrically at 492 nm

(Cory et al., 1991, Barltrop et al., 1991, Buttke et al., 1993).

Procedure: Cells were trpisinized and number of the cells was estimated according to previously described. The cell suspension was then adjusted to a concentration of 25,000 cells/ml and 200 µl of this cell suspension was seeded per well of a flat bottomed 96 well plates. The cells were incubated overnight to ensure complete adherence of cells to the surface. Next day, old media was replaced by 100 µl of fresh medium containing inhibitors or vehicle control accordingly and incubated for the required length of the experiment. After incubation for the desired time point, 10 µl of Cell Titer 96 Aqueous One solution was added to each well and transferred back to incubator for another 2 hours. After 2 hours, the 96 well plate was read and the absorbance at 492 nm was determined using a 96 well plate reader.

2.9.2 Colony formation assay

Principle: Clonogenic assay is an invitro cell survival assay which is based on the ability of a single cell to grow into colonies. Single cell suspensions were diluted to 500-1000 cells per ml and seeded into sterile tissue culture plates at a critically low density to avoid cell-to-cell contact. The cultures were then maintained for a certain period of time and the number of colonies formed by single cells was counted.

Procedure: Cells were trypsinized and the number was estimated according to the above mentioned. The cell density was adjusted to 500 cells/ml and 2 ml of this cell suspension was added to each well of a 6 well plate. After overnight incubation, old media was replaced with growth medium containing inhibitors or vehicle control accordingly for 24 hours. After 24 hours, drug solution was aspirated and the medium containing no drug solution was added to each well. The plate was incubated further for required length of experiment. Once the colonies became visible, cells were washed with PBS, fixed with 70% ethanol for 2 minutes and stained with 0.05% aqueous solution of crystal violet for 2 minutes.

2.9.3 Soft agar colony formation assay

Principle: The soft agar assay for colony formation is an anchorage independent growth assay in soft agar, which is considered to be the most stringent assay for detecting the malignant transformation of cells. This transformation is associated with certain phenotypic changes such as loss of contact inhibition and anchorage independence. The process by which these phenotypic changes occur, is assumed to be closely related to the process of in vivo carcinogenesis and therefore, this assay is believed to be reasonably good predictor or potential indicator of in vivo carcinogenesis. Thus, it is possible to use this assay to measure the ability of cells to form colonies in soft agar matrix without being dependent on the substrate (Schwartz, 1997).

Procedure: Cells were trypsinized and the number was estimated according to the above mentioned. Soft agar assays were set up in 6 well plates with a bottom layer of 1% agarose, an intermediate layer consisting of 0.6% agarose, 10,000 cells per well and inhibitors or vehicle control at respective desired concentrations, and the final layer consisting of medium containing the inhibitors or vehicle controls at respective concentrations. The plates were incubated for 4 weeks at 37 ºC and medium was exchanged once per week. At the end of experiment medium was removed and plates were incubated for 2 hours with 0.005% aqueous solution of crystal violet at 37 ºC and 5% CO_2. Plates were then washed twice with DPBS and colonies were visualized by trans-UV illumination using the gel documentation gel imaging system. Colonies were counted and the colony counts were normalized to the mean colony count of the vehicle control cells.

2.9.4 RealTime-Glo™ Annexin V Apoptosis and Necrosis assay

Principle: Translocation of phosphattidylserine (PS) from the inner to outer membrane leaflet is a hallmark of healthy cells transitioning to apoptosis (Martin et al., 1995). Multiple assays take advantage of Annexin V binding to PS to identify cells undergoing apoptosis. The RealTime-Glo™ Annexin V Apoptosis and Necrosis assay utilizes annexin fusion proteins that contain binary subunits of a luminescent enzyme (Dixon et al., 2016)

(NanoBiTTM). They complement the enzyme when brought into proximity due to their affinity for PS. A time-released substrate is processed by the complemented enzymes to report real-time PS exposure by luminescence. The Necrosis Detection Reagent reports changes in membrane integrity as a result of necrosis. Together, these real-time measures establish the mechanism of action (apoptosis, primary necrosis, or alternative programs) for cell death (Kupcho et al., 2017).

Procedure: Cells were trypsinized and the cell concentration was adjusted to 25,000 cells/ml. 200 µl of this cell suspension was then added into each well of a 96 well flat bottomed white plate and incubated overnight for cell adherence. Next day, old medium was replaced with 100 µl of medium containing inhibitor or vehicle control at desired concentrations respectively and plate was transferred back to incubator for required time point. At the end of the experiment, 100 µl of 2× detection reagent (each time made fresh according to manufacturer's protocol) was added to each well and mixed on a plate shaker for roughly 60 seconds at 300 rpm. Luminescence and Fluorescence signals were measured using plate reader and data was plotted as net luminescence for each concentration.

2.10 Immunological methods

2.10.1 Western blot

Principle: Western blot is a widely used technique for protein detection. It uses antibodies to detect and analyze specific proteins in a given biological sample (tissue or cell culture extracts). This technique uses SDS-Page gel electrophoresis to separate a mixture of proteins, followed by transfer to a PVDF or nitrocellulose membrane. This membrane serves as a platform on which antibodies can be used to probe target proteins. Therefore, western blotting is a combination of several major steps together and includes protein extraction from tissue/cultured cells, SDS-Page gel electrophoresis, transfer, immune-blotting and detection or visualization of target proteins (Towbin et al., 1979).

Preparation of cell extracts and protein estimation: Cells were plated at a cell density of 1 million per T-25 tissue culture flasks and incubated with desired concentrations of inhibitors or vehicle control for different time points respectively. At the end of each time point, cells were washed with PBS and lysed in radioimmunoprecipitation buffer (RIPA) supplemented with phosphatase and protease inhibitors. The lysed pellets were incubated on ice for 30-40 minutes with intermittent vigorous vortexing every 10 minutes. Lysates were cleared by centrifugation at a speed of 13, 000 rpm for 20 minutes and the supernatants were collected for subsequent use. Protein concentrations were estimated using bicinchoninic acid (BCA) assay. Briefly, the protein samples diluted in RIPA buffer at a ratio of 1:4 were added to each well of a 96 well plate in duplicates. Next, 200 µl of BCA mix reagent (reagent A and B mixed at a ratio of 50:1 from the kit) was added to each well and incubated for 30 minutes at 37 ºC. The intensity of the formed purple color was measured colorimetrically at 570 nm. The Bovine Serum Albumin (BSA) standard pre-diluted set containing different protein concentrations lying in the linear range from 0.0625 µg/µl to 2 µg/µl was used for quantification of unknown protein samples. Lysates were aliquoted to avoid multiple freeze-thaw cycles and stored at -80 ºC for long term storage.

SDS-PAGE gel electrophoresis and transfer: For the experiments, premade 4−12% Bis-Tis Nupage gels were used. For each sample, 50 µg of protein sample mixed with loading dye was loaded into each well of the gel and electrophoresed at 200 V for 50 minutes. Separated proteins were transferred from gel to PVDF membranes at 30 V for 1 hour. The membrane containing transferred proteins was then blocked with 5% (w/v) milk powder dissolved in 0.1% TBST for 1 hour at room temperature.

Probing, reprobing and detection: After blocking for 1 hour, the membranes were probed using respective primary antibodies at 4 ºC overnight. Next day, the blots were washed three times with TBST and then reprobed with HRP-conjugated antibodies directed against rabbit or mouse IgG respectively. Detection was performed using a solution of 4-iodophenylboronic acid (4IBPA) and luminol (Haan and Behrmann, 2007). Concentration and medium of antibodies used are shown below.

Table 23: Antibodies and conditions used for Western blot

Antibody	Dilution	Blocking reagent
ERK	1:2000	5% NFDM in TBS-T
pERK	1:2000	5% NFDM in TBS-T
MEK	1:2000	5% NFDM in TBS-T
pMEK	1:2000	5% NFDM in TBS-T
PARP	1:2000	5% NFDM in TBS-T
Cleaved PARP	1:2000	5% NFDM in TBS-T
Caspase 3	1:2000	5% NFDM in TBS-T
Cleaved caspase 3	1:2000	5% NFDM in TBS-T
GAPDH	1:2000	5% NFDM in TBS-T
Rabbit IgG	1:2000	5% NFDM in TBS-T
Mouse IgG	1:2000	5% NFDM in TBS-T

2.10.2 Radiation therapy

Principle: Stereotactic body radiation therapy (SBRT) is an emerging treatment modality, as recently published in the guidelines of the American Society for Therapeutic Radiology and Oncology (ASTRO) and the American College of Radiology, and is defined as a method of delivering treatment to a target site in vivo using a single dose or a small number of fractionated high-dose radiation doses (Towbin et al., 1979). It requires precisely targeted irradiation of the tumor, the ability to achieve radical doses in just a few exposures to destroy the tumor (Zhang and Nagasaka, 2021), and the ability to accommodate a wide range of tumor types and locations (Towbin et al., 1979).

Procedure: For our experimental purposes, Faxitron Multirad 225 X-ray irradiation system (wheeling, IL, USA) was used which is a commercially available X-ray irradiator designed for small animals and cells. Compared with traditional clinical irradiating apparatus, Faxitron MultiRad 225 X-ray irradiation system have lower radiation energy (225 kV vs 6 MV). In addition, this irradiator has a dose monitor, which can accurately measure the radiation dose applied on the experimental subjects (animals or cells) in real time, providing a more stable and uniform irradiation approach (Woo and Nordal, 2006, Ma et al., 2001). For all in vitro functional assays, cells numbers were adjusted accordingly and

plated overnight in 96 well plates for MTS assays, in 6 well plates for clonogenic assays and in T-25 tissue culture flasks for western blot assays. Next day, cells were treated with different inhibitors or vehicle controls and incubated for at least one hour at 37 ºC and 5% CO_2. Post an hour drug treatment, plates were treated with different doses of X-ray irradiation at a rate of 6 Gy/min using Multirad system (225 kV). The plates were then transferred back to incubator for desired time points. At the end of each time point, MTS and clonogenic assays were terminated and data were measured as described in previous sections.

2.11 Ral A activation assay (Bead pull-down format assay)

Principle: GTPases is a family of proteins that serve as molecular regulators in signaling transduction pathways. Ral, a 24 kDa protein of the Ras superfamily, regulates a variety of biological response pathways that include vesicle trafficking, cytoskeletal rearrangment, migration and oncogenesis. Like other small GTPases, Ral regulates molecular events by cycling between an inactive GDP-bound form and an active GTP-bound form. In their active (GTP-bound) state, Ral A and Ral B bind specifically to the protein-binding domain (PBD) of RalBP1 to control downstream signaling cascades. Ral A activation assay utilizes RalBP1 PBD Agarose beads to selectively isolate and pull-down the active form of Ral from purified samples or endogenous lysates. Subsequently, the precipitated GTP-Ral is detected by western blot analysis using an anti-Ral A antibody (Han et al., 2009, Neel et al., 2012).

Procedure: For Ral A activation assay, 1 million cells were plated in T-75 tissue culture flask and incubated overnight. Next day, cells were treated with different inhibitors or vehicle control respectively for 72 hours. At the end of time point, cells were washed with PBS and lysed using cell lysis buffer as provided in the kit. All the steps were performed on ice. Cell lysates were clarified by centrifugation, supernatants were collected and estimated for protein concentration. Around 400 µg of protein lysate was then mixed with 10 µg of RalBP1-PBD beads and incubated at 4 ºC on a rotator for 1 hour. Beads were then

pelleted by centrifugation and washed with wash buffer. The beads mixed with loading dye were then subjected to SDS-Page gel electrophoresis. After running and transfer of protein samples, membranes were probed with Ral A specific primary antibody, HRP-coupled secondary antibody and detected for GTP bound form of Ral A protein.

2.12 Statistical analysis

Two-tailed Student's t-tests were performed using Graph Pad Prism for windows version 6.0. $p<0.05$ was regarded as statistically significant. Unless indicated otherwise, results are shown as mean ± Standard Deviation (SD).

3 Results and Discussion

Activating mutations of RAS genes are among the most commonly detected oncogenic driver alterations and are found in almost a third of all human cancers. Among these, KRAS mutations represent the most predominant subtype and have also been found to be notoriously difficult to target therapeutically. Significant progress has been made with the introduction of clinically active small molecule inhibitors of specific oncogenic KRAS mutations. Namely, AMG-510 (sotorasib) was approved for treatment of KRAS G12C mutant NSCLC only recently (Zhang and Nagasaka, 2021).

3.1 Monotherapy

3.1.1 AMG-510 specifically inhibits the viability of pancreatic cancer cells with KRAS G12C mutation

Here, AMG-510 was administered to KRAS G12C mutant MiaPaCa-2, KRAS G12D mutant Panc-1 or KRAS wild type BxPC-3 pancreatic cancer cells. Cell viability was determined by means of MTS assays. Incubation with AMG-510 at concentrations above 10 nM significantly reduced net viability of KRAS G12C mutant MiaPaCa-2 cells in MTS assays in a dose-dependent manner, and this reduction in cell viability was more pronounced upon concomitant irradiation as a cumulative dose of 2 Gy (Fig. 2A). As opposed to this observation, cell viability of KRAS G12D mutant Panc-1 (Fig. 2B) or KRAS wild type BxPC-3 (Fig. 2C) pancreatic cancer cells was not affected by treatment with AMG-510 alone or in combination with radiotherapy.

3.1.2 AMG-510 specifically inhibits clonogenecity of pancreatic cancer cells with KRAS G12C mutation

In colony formation assays, treatment with AMG-510 significantly reduced clonogenicity of KRAS G12C mutant MiaPaCa-2 (Fig. 3A), but not KRAS G12D mutant Panc-1 (Fig. 3B)

or KRAS wild type BxPC-3 cells (Fig. 3C). Irradiation led to further reduction of colony formation in this assay.

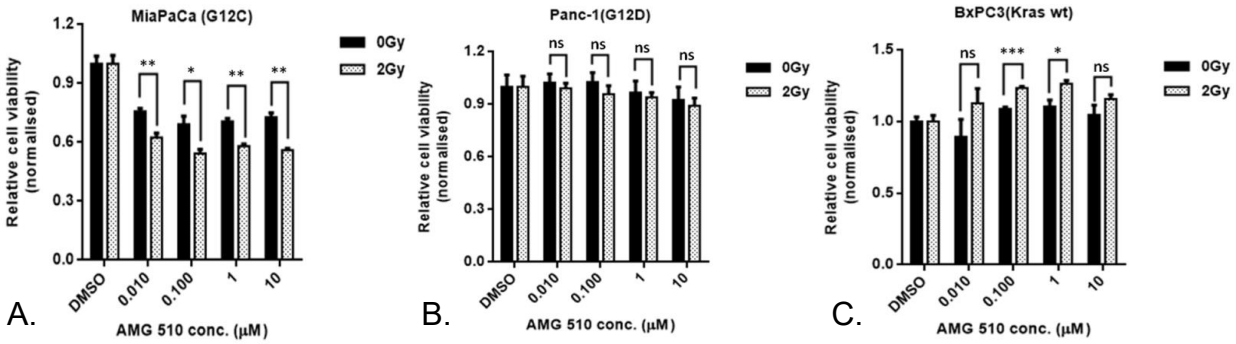

Figure 2: Treatments of MiaPaCa-2 (A), Panc-1 (B), and BxPC-3 (C) with AMG-510, assessed by cell viability (MTS) assays, showed reduced net cell viability of MiaPaCa-2 cells. Relative cell viability of Panc-1 or BxPC-3 cells was not affected. All experiments were repeated three times (* prompts $p<0.05$, ** prompts $p<0.01$, *** prompts $p<0.001$ as compared to mock treated controls respectively).

3.1.3 AMG-510 inhibits growth and clonogenecity of KRAS G12C mutant cells mainly by blocking the MEK/ERK pathway

Western blot assays were performed after treatment of either of the three pancreatic cancer cell lines indicated with AMG-510 alone or in combination with concomitant irradiation at a dose of 2 Gy. Of note, AMG-510 treatment caused reduction of ERK phosphorrylation in a dose-dependent manner starting at a dose of 10 nM, in line with effective MEK/ERK pathway inhibition in both KRAS mutant cell lines (MiaPaCa-2 and Panc-1), while no such effect was observed in the KRAS wild type cell line BxPC-3 (Fig. 4).

3.1.4 Binimetinib inhibits viability of KRAS mutant pancreatic cancer cells

Unlike the genomic landscape observed in NSCLC, where KRAS G12C represents one of the most common KRAS driver mutations found, KRAS G12C mutations represent only a minor fraction of KRAS in pancreatic cancers. Here, roughly two-thirds of all KRAS mutations are G12D, against which no active therapeutic inhibitors are clinically approved as of yet and are currently undergoing preclinical and early clinical investigations.

Previous studies in this situation focused on the use of MEK inhibitors such as binimetinib (a MEK1/2 inhibitor). Here, binimetinib was administered to MiaPaCa-2, Panc-1, or BxPC-3 pancreatic cancer cells. Relative cell viability was determined using MTS assay, binimetinib was found to inhibit net cell viability of both KRAS mutant pancreatic cancer cell lines (Fig. 5).

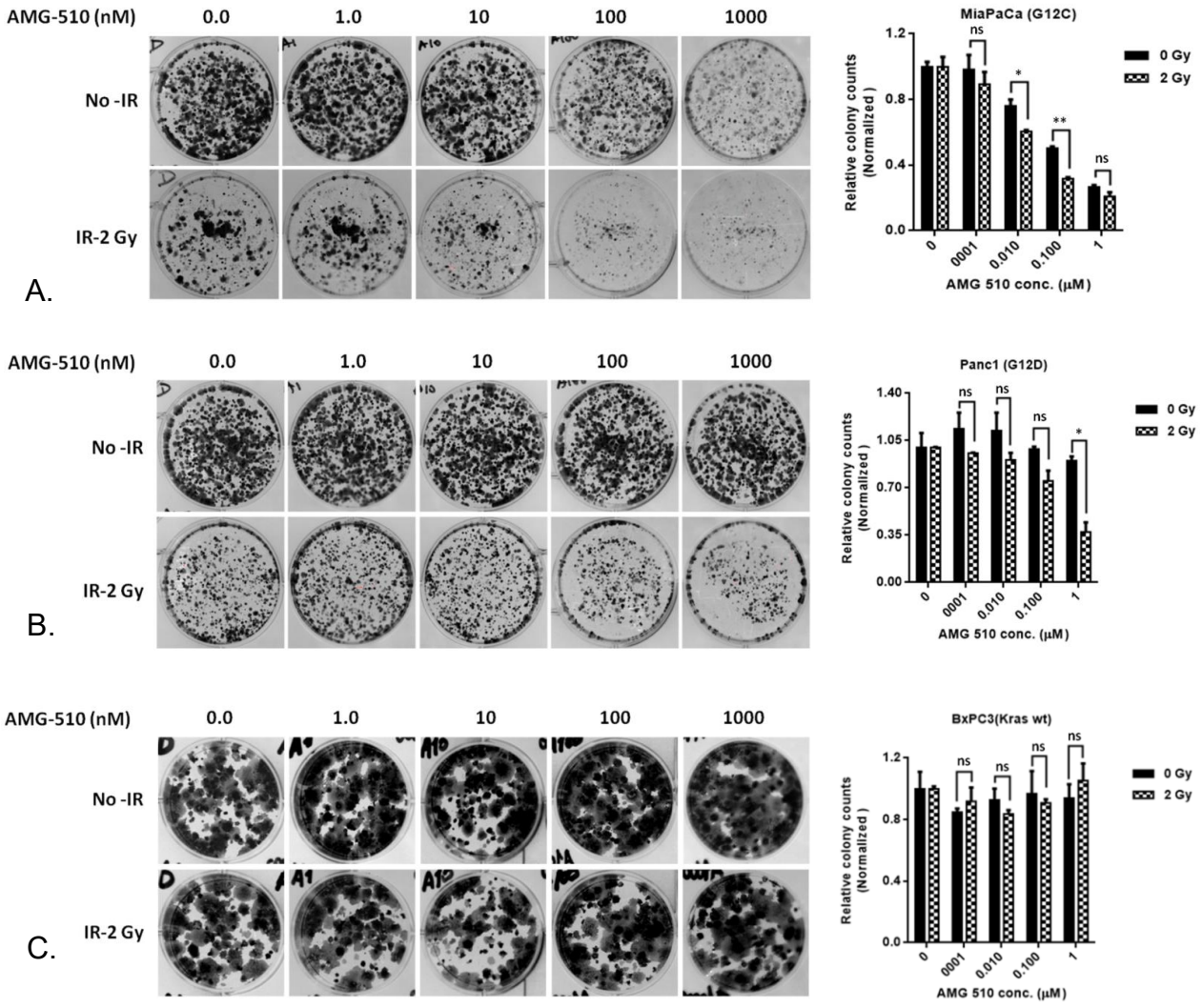

Figure 3: Colony formation assays of MiaPaCa-2 (A), Panc-1 (B), and BxPC-3 (C) with AMG-510. AMG-510 drastically reduced the ability of MiaPaCa-2 cell lines to form colonies at concentrations in the range of 10−1000 nM. Colony formation of Panc-1 or BxPC-3 cells was not affected by treatment with AMG-510, while irradiation further reduced colony counts in MiaPaCa-2 and Panc-1, respectively. The graph on the right shows a representation of three independent experiments, along with their combined colony counts (* prompts $p<0.05$, ** prompts $p<0.01$, *** prompts $p<0.001$ as compared to mock treated controls respectively).

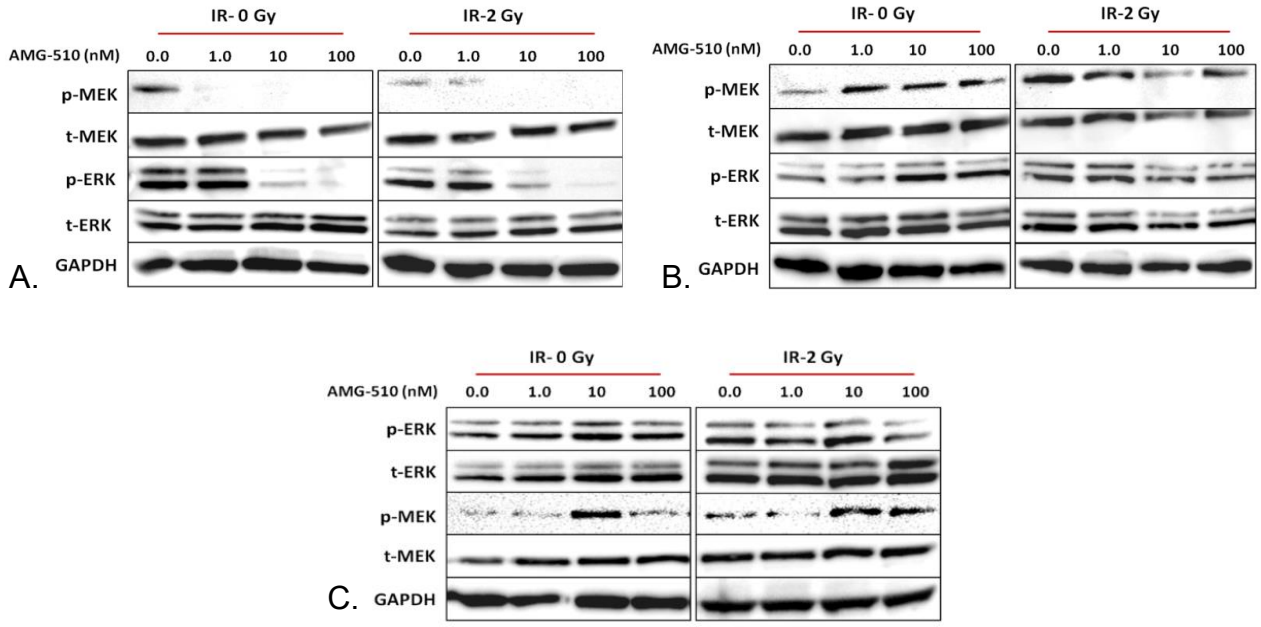

Figure 4: Western blot analysis of KRAS downstream effectors in MiaPaCa-2 (A), Panc-1 (B), and BxPC-3 (C) treated with AMG-510 with or without concomitant irradiation.

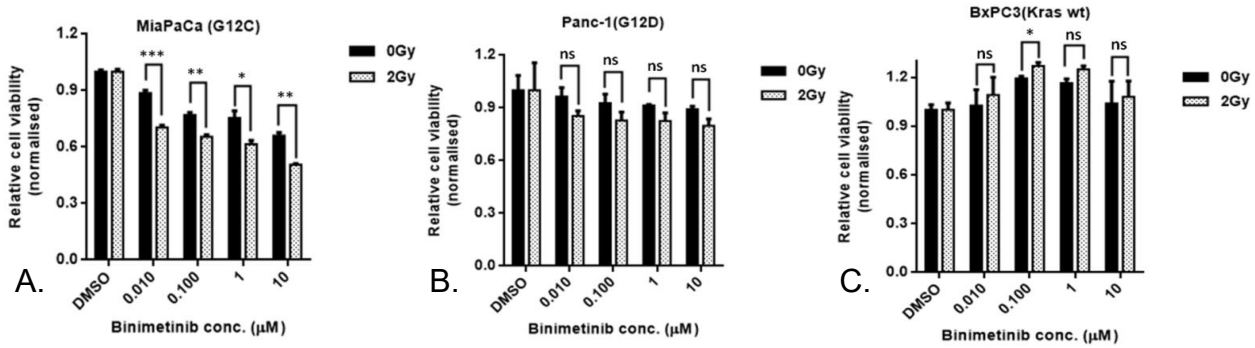

Figure 5: Treatments of MiaPaCa-2 (A), Panc-1 (B), and BxPC-3 (C) with binimetinib, assessed by cell viability (MTS) assays showed that binimetinib reduced cell viability of MiaPaCa-2 or Panc-1 cells in a dose-dependent manner. BxPC-3 cell growth was no affected by treatment with binimetinib with or without concomitant irradiation. All experiments were repeated three times (* prompts $p<0.05$, ** prompts $p<0.01$, *** prompts $p<0.001$ as compared to mock treated controls respectively).

Proliferation and clonogenecity of MiaPaCa-2, Panc-1 and BxPC-3 (Fig. 6) were determined by clonogenic replating assays, irradiation at a dose of 2 Gy had a significant additive effect on whose viability and clonogenecity. These findings suggest that binimetinib inhibited viability of pancreatic cancer cells with KRAS G12C and G12D mutations to a certain extent and enhanced the sensitivity of the cell lines to radiotherapy, while

KRAS wild-type BxPC-3 pancreatic cancer cells were not sensitive to treatment with this compound.

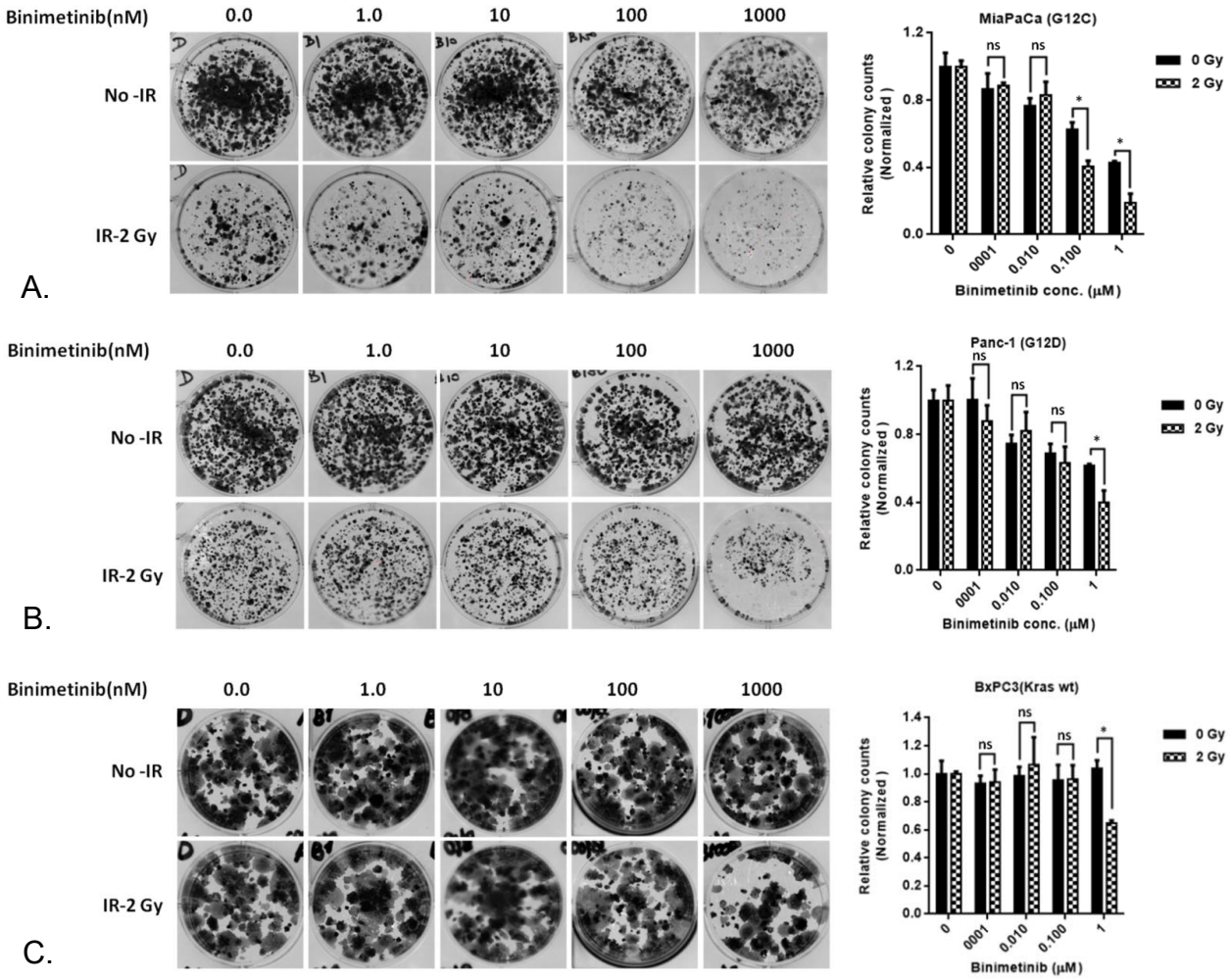

Figure 6: Colony formation assays of MiaPaCa-2 (A), Panc-1 (B), and BxPC-3 (C) showed reduced clonogenecity and colony formation upon the treatment of MiaPaCa-2 or Panc-1 treated by binimetinib, further augmented by irradiation with 2 Gy. Colony formation of BxPC-3 did not change for binimetinib concentrations of up to 1000 nM. Graph on the right shows a representation of three independent experiments, along with their combined colony counts (* prompts $p<0.05$, ** prompts $p<0.01$, *** prompts $p<0.001$ as compared to mock treated controls respectively).

3.1.5 Binimetinib inhibits growth of KRAS mutant cells through inhibition of ERK phosphorylation

Western blot assays were performed after treatment of either of the three cell lines with binimetinib to study effects of KRAS downstream effectors. Overall, alteration of ERK

phosphorylation was consistent with the results of MTS and colony assays, namely, marked dose-dependent inhibition of ERK phosphorylation was observed in MiaPaCa-2 and Panc-1 cells upon binimetinib treatment starting at low concentrations of 10 nM. It is hypothesized that site-specific mutations in the KRAS gene lead to activation of downstream effector pathways in pancreatic cancer cells including the MEK/ERK signaling axis, which may be targeted therapeutically by specific inhibitors such as binimetinib. Meanwhile enhanced MEK phosphorylation might represent a feedback activation caused by inhibition of ERK phosphorylation (Fig. 7).

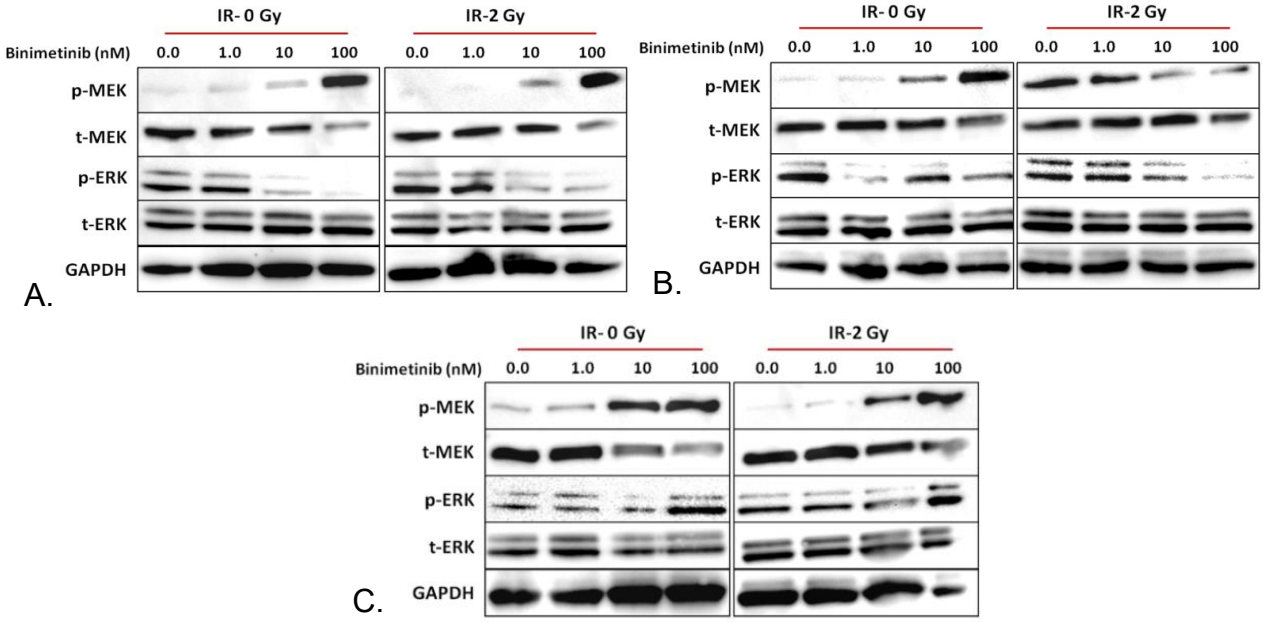

Figure 7: Western blot analysis of MiaPaCa-2 (A), Panc-1 (B), and BxPC-3 (C) treated by binimetinib, with or without concomitant irradiation at a dose of 2 Gy, showed ERK pathway inhibition in KRAS mutant cell lines in line with growth inhibition detected in MTS experiments, and feedback activation of MEK phosphorylation.

3.1.6 BI-3406 in KRAS mutant pancreatic cancer

KRAS activation is regulated binding of SOS1/2 on the membrane, thus activating downstream signaling factors to promote pancreatic cancer development and progression. Given the difficulties in developing direct inhibitors to therapeutically target KRAS mutations discussed above led to the identification of SOS1/2 as potential alternative targets to modulate oncogenic KRAS signaling.

Here the SOS1 inhibitor BI-3406 was applied to MiaPaCa-2, Panc-1 or BxPC-3 pancreatic cancer cells and relative cell viability and proliferation were determined using MTS. Treatment with this compound did not have any significant effect cell viability in either of the three pancreatic cancer cell lines evaluated in MTS assays, and there was no additive growth inhibition by combination of drug treatment plus irradiation in this case (Fig. 8).

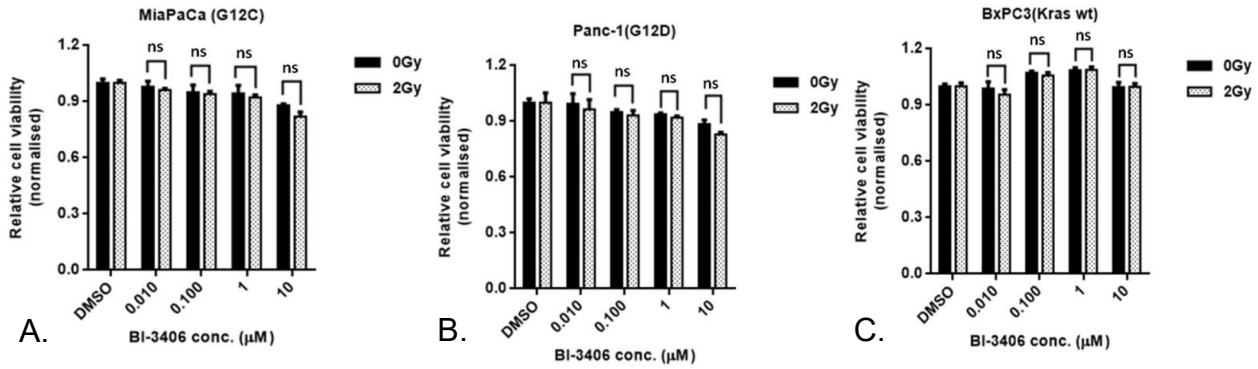

Figure 8: MiaPaCa-2 (A), Panc-1 (B), and BxPC-3 (C) were treated with increasing doses of BI-3406 and cell viability was assessed by (MTS) assays. All experiments were repeated three times (* prompts $p<0.05$, ** prompts $p<0.01$, *** prompts $p<0.001$ as compared to mock treated controls respectively).

Clonogenecity of the three cell lines treated with BI-3406 were assessed by means of colony formation assays. Of note, in replating assays BI-3406 caused significant reduction of colony formation in both KRAS mutant pancreatic cancer cell lines (MiaPaCa-2 and Panc-1), but not the KRAS wild type cancer cell line BxPC-3 (Fig. 9), suggesting that BI-3406 has some potency to overcome oncogenic KRAS signaling caused not only by G12C but also G12D mutations, respectively, in pancreatic cancer cells. However, little additional therapeutic efficacy was documented by combinatorial therapeutic irradiation in this experimental setting.

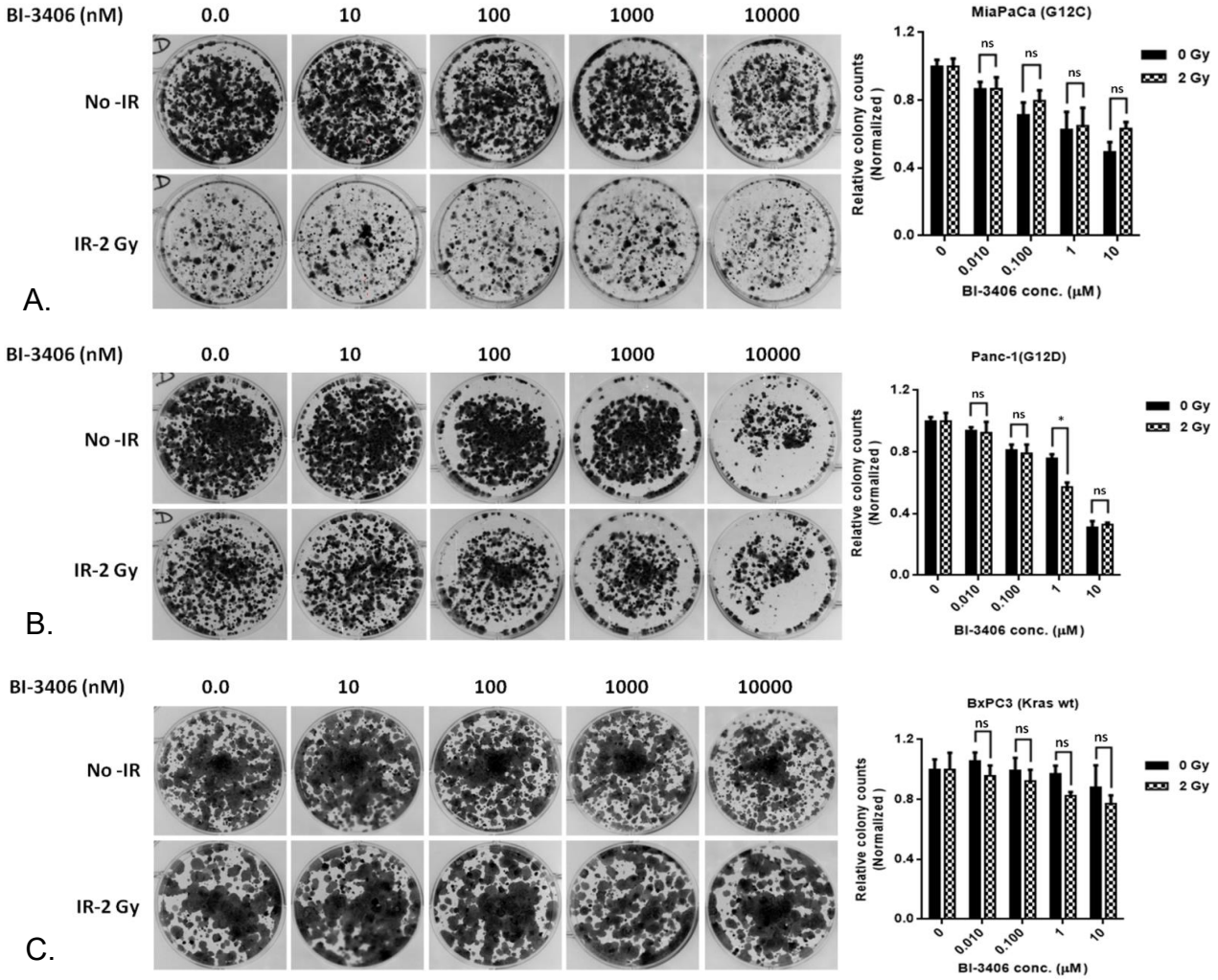

Figure 9: Colony formation of MiaPaCa-2 (A), Panc-1 (B), and BxPC-3 (C) revealed that BI-3406 had the most pronounced inhibitory effect on clonogenecity of Panc-1 followed by MiaPaCa-2 cells, while colony formation of BxPC-3 was not affected. Radiotherapy did not show any tangible additive therapeutic efficacy with this compound. The graph on the right shows a representation of three independent experiments, along with their combined colony counts (* prompts $p<0.05$, ** prompts $p<0.01$, *** prompts $p<0.001$ as compared to mock treated controls respectively).

3.1.7 BI-3406 inhibits ERK phosphorylation in KRAS-mutant pancreatic cancer cells

Western blot analysis of ERK and MEK pathway activation was performed after treatment of MiaPaCa-2, Panc-1 and BxPC-3 cells with increasing doses of BI-3406. Changes in ERK and MEK phosphorylation were overall consistent with the results obtained in MTS and colony formation assays. Thus, dose-dependent downregulation of phosho-ERK and

upregulation of phospho-MEK was observed in all three pancreatic cancer cell lines evaluated (Fig. 10).

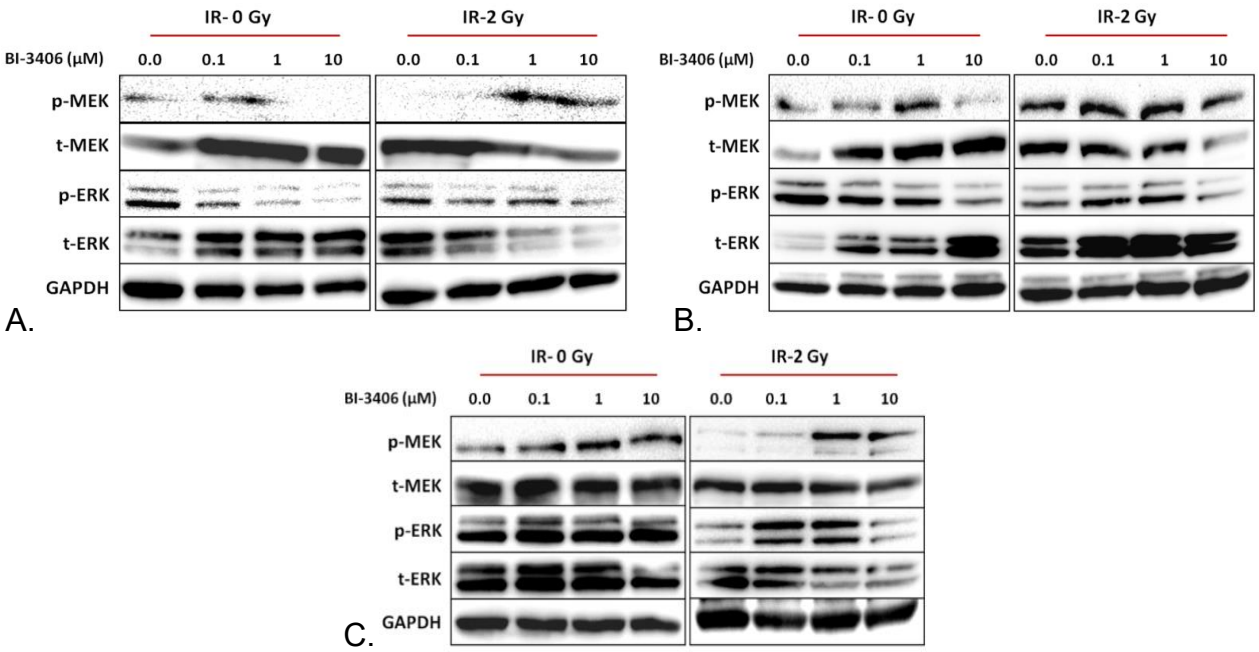

Figure 10: Western blot analysis of MiaPaCa-2 (A), Panc-1 (B), and BxPC-3 (C) treated by BI-3406 with or without combinatorial irradiation at a dose of 2 Gy.

3.1.8 BI-2852 shows limited inhibition of proliferation and colony formation in pancreatic cancer cell lines that is not enhanced by irradiation

SI/II is a region between Switch I and Switch II of the KRAS gene that involves the binding of nucleotide exchange factors, and SII is under the Switch II cycle. BI-2852 is an inhibitor that directly affects GTP-bound KRAS by targeting the switch I/II pocket (SI/II-pocket) with nanomolar affinity. Thus it blocks GEF, GAP and inhibits KRAS downstream signaling.

BI-2852 (a KRAS Switch I/II inhibitor) was administered to MiaPaCa-2, Panc-1, and BxPC-3 pancreatic cancer cells and relative cell viability and proliferation were determined using MTS assays, clonogenecity was assessed by means of colony formation assays.

As depicted in Fig. 11, BI-2852 treatment did not inhibit pancreatic cancer cell viability in either of the cell lines tested, and now additive therapeutic effects was found by combination with radiation therapy.

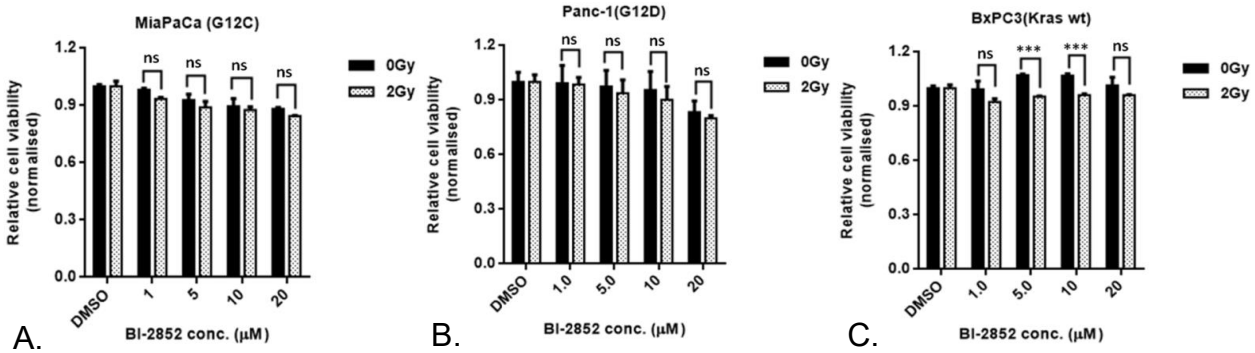

Figure 11: MTS assays of MiaPaCa-2 (A), Panc-1 (B), and BxPC-3 (C) treated with BI-2852. All experiments were repeated three times (* prompts $p<0.05$, ** prompts $p<0.01$, *** prompts $p<0.001$ as compared to mock treated controls respectively).

Of interest, BI-2852 showed slight reduction of clonogenecity and colony formation of all three pancreatic cancer cell lines evaluated here, while concomitant irradiation did not further enhance this effect. The biological relevance however seems limited, since the observed effects across all pancreatic cancer cell lines shown here were rather small (Fig. 12).

3.1.9 BI-2852 monotherapy was not effective in inhibition signaling through the KRAS downstream MEK and ERK effector pathways

Western blot assays were performed after treatment of three pancreatic cancer cell lines with BI-2852 monotherapy. Alterations in MEK and ERK phosphorylation were in line with the results of MTS and colony formation assays as described above, and suggested that BI-2852 monotherapy was not effective in inhibition signaling through the KRAS downstream MEK and ERK effector pathways (Fig. 13).

Concluding from the results of previous experiments presented above, irradiation therapy showed a more pronounced additive therapeutic in vitro efficacy with binimetinib as compared to the other three drugs targeting oncogenic KRAS signaling evaluated. Therefore, in order to screen for further potential therapeutic synergisms, combination regimens of either of these three compounds with binimetinib were systematically evaluated in next steps.

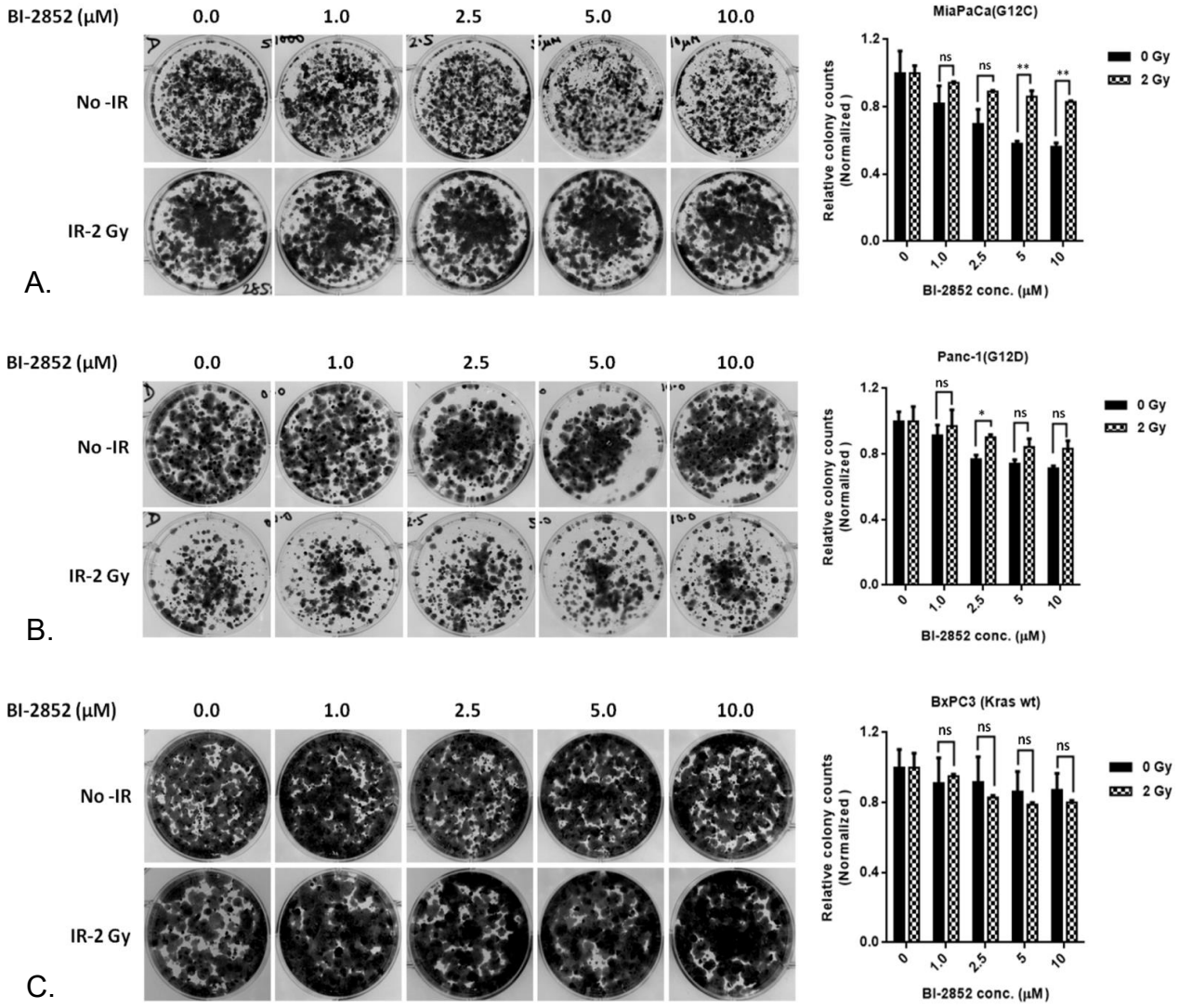

Figure 12: Colony formation of MiaPaCa-2 (A), Panc-1 (B), and BxPC-3 (C) treated with increasing doses of BI-2852. In the absence of irradiation treatment, BI-2852 had the most pronounced inhibitory effect on colony formation in MiaPaCa-2 cells, followed by Panc-1. Clonogenecity and colony formation of BxPC-3 cells was not affected, either with or without concomitant irradiation. The graph on the right shows a representation of three independent experiments, along with their combined colony counts (* prompts $p<0.05$, ** prompts $p<0.01$, *** prompts $p<0.001$ as compared to mock treated controls respectively).

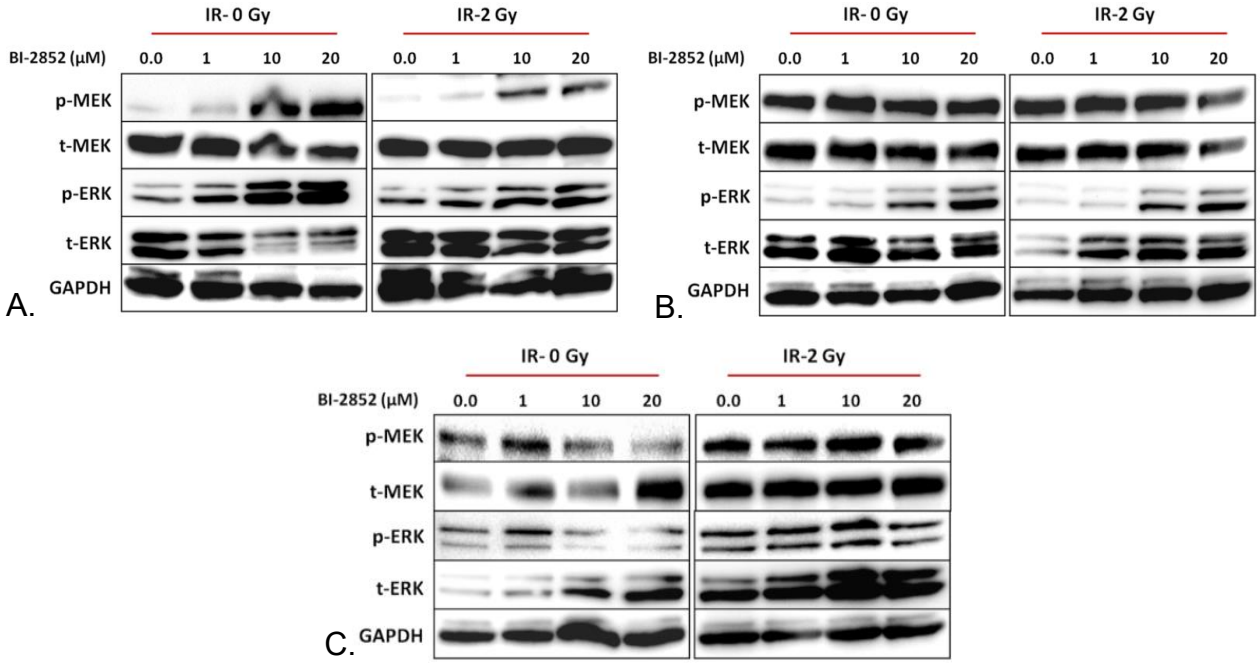

Figure 13: Western blot analysis of MEK and ERK pathway activity in MiaPaCa-2 (A), Panc-1 (B), and BxPC-3 (C) treated with BI-2852 with or without concomitant irradiation at a dose of 2 Gy.

3.2 Combinatorial pathway blockade

3.2.1 Combination of AMG-510 and binimetinib inhibits growth and clonogenecitiy of KRAS G12C mutant pancreatic cancer cells

MiaPaCa-2 cells were treated with AMG-510 in combination with binimetinib both at a dose of 10 nM and concomitant irradiation at a dose of 2 Gy. Again, relative cell viability and colony formation were determined using MTS (Fig. 14A) and clonogenitic replating (Fig. 14B). Of note, MiaPaCa-2 cells treated with AMG-510 plus binimetinib combination showed significantly reduced cell viability with increasing drug doses, suggesting that therapeutic synergism conferred by MEK inhibition with binimetinib to AMG-510-mediated inhibition of oncogenic KRAS signaling in pancreatic cancer cells with KRAS G12C mutation, and this effect was more pronounced upon additional irradiation therapy as indicated.

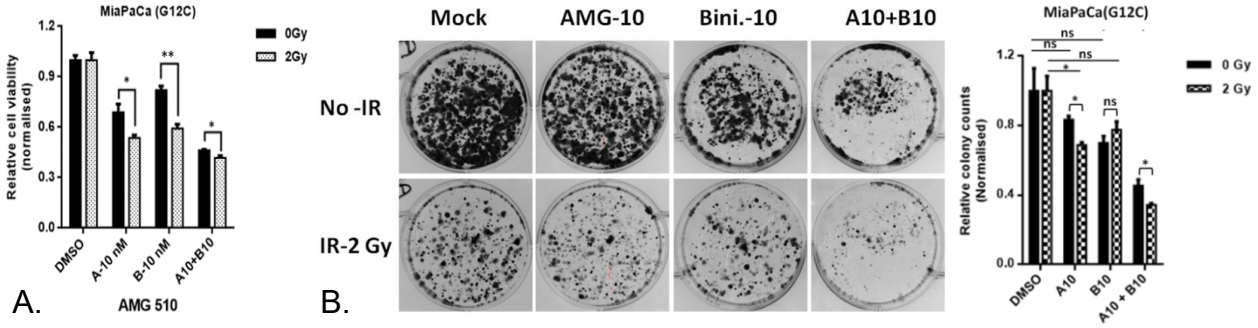

Figure 14: Relative cell viability (A) and colony formation assays (B) were performed in KRAS G12C mutant MiaPaCa-2 pancreatic cancer cells treated with 10 nM of AMG-510, binimetinib or combination, respectively, with or without 2 Gy of concomitant irradiation. 10 nM AMG-510 monotherapy showed a significant reduction of cell viability, the effect became more pronounced with 2 Gy irradiation, and when combined with 10 nM binimetinib, the relative cell viability decreased further, 2 Gy irradiation synergistic effect was statistically significant. Colony formation of MiaPaCa-2 treated by AMG-510 combined with binimetinib showed significant and additive reduction of clonogenecity of the MiaPaCa-2 cells. The graph on the right shows a representation of three independent experiments, along with their combined colony counts (* prompts $p<0.05$, ** prompts $p<0.01$, *** prompts $p<0.001$ as compared to mock treated controls respectively).

In line with growth inhibition as detected using MTS assays, there was similarly a marked reduction in steady state ATP levels (Fig. 15A) conferred by KRAS inhibition by AMG-510 that was further enhanced by combination of KRAS and MEK inhibition by treatment with AMG-510 plus binimetinib. Maximum reduction in ATP levels was achieved by combinatorial KRAS plus MEK inhibition in combination with radiation therapy, suggesting a possible therapeutic synergism.

Western blot assays were performed (Fig. 15B) and demonstrated downregulation of phospho-ERK by KRAS plus MEK inhibition as well as by the respective monotherapies, while expectedly MEK-phosphorylation was enhanced by binimetinib treatment in a positive feedback.

3.2.2 AMG-510 and binimetinib combination therapy supported by therapeutic irradiation blocks cell cycle progression and induces apoptosis in locking KRAS G12C mutant cells

During cell cycle progression, p27 protein levels are highest in quiescent cells and start to decrease after stimulated by mitogenic sources. At the peak of DNA synthesis, p27 protein expression decreases to its lowest level, which leads to cell cycle progression in G1 phase. After co-treatment of MiaPaCa-2 cells with 10 nM AMG-510 and 10 nM binimetinib, the combination of AMG-510 with binimetinib significantly increased the fraction of cells in G1 phase, mirrored by marked upregulation of p27 Kip1. Irradiation at a dose of 2 Gy leads to significantly stronger upregulation of p27 Kip1 both in AMG-510 monotherapy and in AMG-510 plus binimetinib combination therapy (Fig. 16A), suggesting that AMG-510 monotherapy and its combination with binimetinib supported by therapeutic irradiation can inhibit cancer growth by locking KRAS G12C mutant cells by inducing G1 cell cycle arrest. Caspase 3 represents one of the pivotal mediators of apoptosis and is activated and transformed into its activated form cleaved caspase 3, which plays a partial or total cleavage role for many key proteins, such as poly ADP-ribose polymerase (PARP). Western blot showed strong induction of cleaved caspase 3 and PARP in MiaPaCa-2 cells upon 2 Gy of irradiation (Fig. 16A). Moreover, AMG-510 monotherapy and AMG-510 plus binimetinib combination showed markedly enhanced induction of apoptosis-related markers cleaved PARP and cleaved caspase 3 upon combinatorial irradiation, suggesting that radiotherapy might promote synergistic effects of the combination in inducing apoptosis.

To further elaborate these observations, luminescence assays were performed as an alternative means to quantify induction of apoptosis (Fig. 16B). Of note, apoptosis of Mia-PaCa-2 treated by AMG-510 combined with binimetinib with or without 2 Gy of irradiation was obtained, showing that radiotherapy significantly increased the relative luminescence, which served as quantifier for induction of apoptosis. These results further support the hypothesis that radiotherapy augments induction of apoptosis in KRAS G12C mutant MiaPaCa-2 pancreatic cancer cells by combined KRAS and MEK inhibition with AGM-510 plus binimetinib combination therapy.

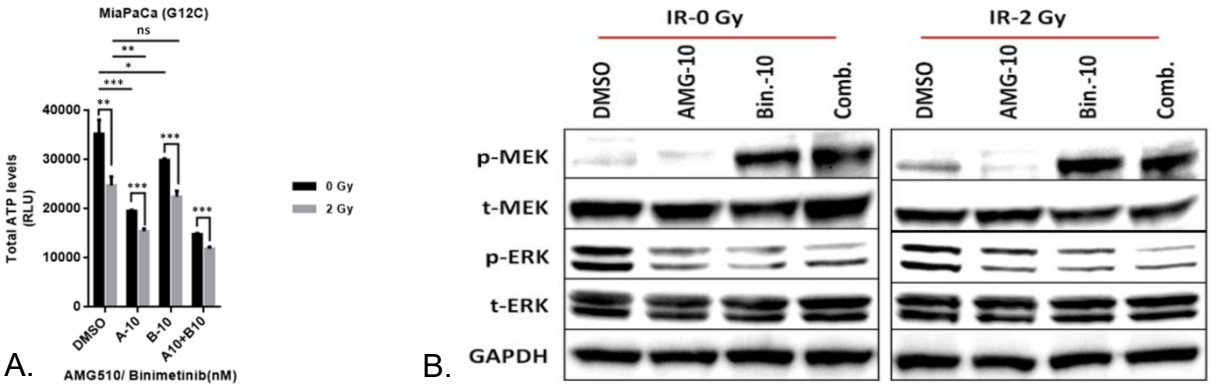

Figure 15: Considerable reduction of steady state ATP levels were found upon AMG-510 plus binimetinib treatment plus irradiation (A). Western blot analysis of MiaPaCa-2 treated by AMG-510 combined with binimetinib (B) with or without 2 Gy of irradiation showed a pattern of ERK phosphorylation consistent with the results of MTS, ATP and clonogenitic assays. The graph on the right shows a representation of three independent experiments, along with their combined colony counts (* prompts p<0.05, ** prompts p<0.01, *** prompts p<0.001 as compared to mock treated controls respectively).

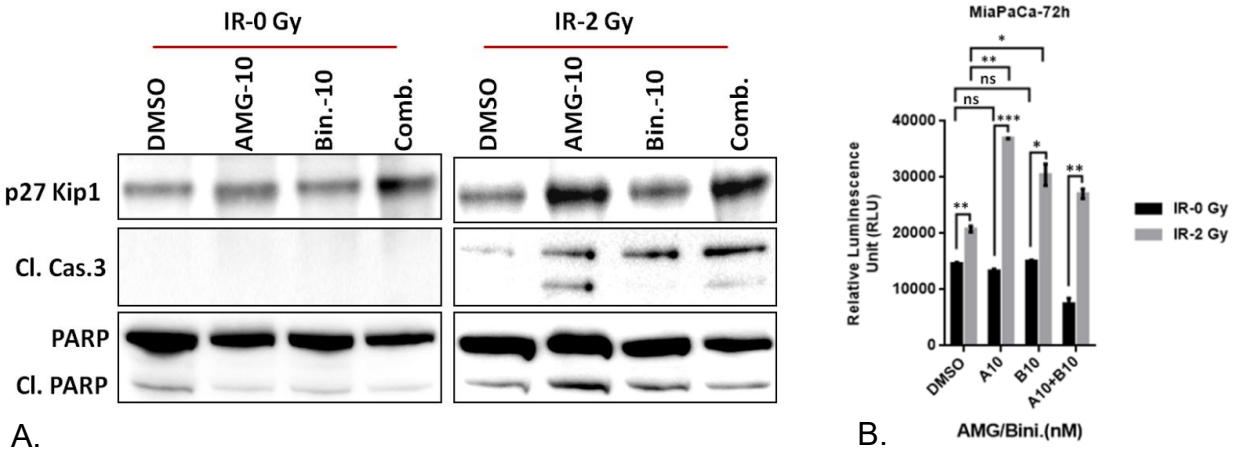

Figure 16: Western blot analysis of p27 Kip1, cleaved caspase 3 and cleaved PARP in MiaPaCa-2 treated by AMG-510 combined with binimetinib with or without 2 Gy dose of radiation (A). Cell Titer-Glo assay of MiaPaCa-2 cells treated with AMG-510, binimetinib and 2 Gy radiation (B).

Taken together, these observations thus suggest that AMG-510 in combination with binimetinib could effectively inhibit the growth and clonogenecitiy of KRAS G12C mutant pancreatic cancer cells by inhibiting the MEK/ERK pathway and enhance their sensitivity to radiation therapy.

3.2.3 Combination of AMG-510 and binimetinib shows no therapeutic activity KRAS G12D mutant pancreatic cancer cells

Next, in order to evaluate genotype-specificity of AMG-510 used as KRAS G12C inhibitor, the experiments previously performed in KRAS G12C mutant MiaPaCa-2 pancreatic cancer cells were now performed using KRAS G12D mutant Panc-1 pancreatic cancer cells.

Panc-1 cells were treated with 10 nM AMG-510 and 10 nM binimetinib under the application of 2 Gy dose of irradiation. Of interest, and as opposed to what had previously been found for MiaPaCa-2, viability and clonogenecity of Panc-1 were not affected by AMG-510 administration alone, or concomitant binimetinib plus irradiation combinations as assessed using MTS (Fig. 17A) or clonogenic replating assays (Fig. 17B), respectively. Which only slightly reduced when being exposed in 2 Gy radiotherapy.

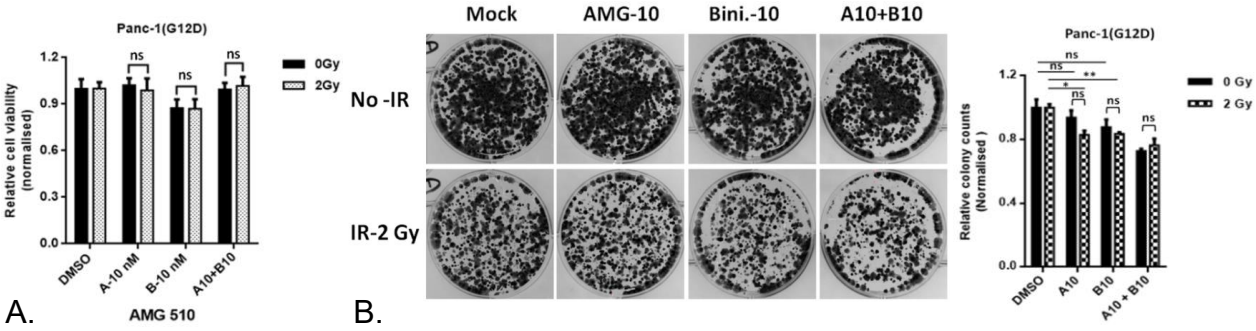

Figure 17: MTS (A) assays were used to determine the relative cell viability of Panc-1 cells treated with combination of AMG-510 and binimetinib with or without 2 Gy dose of radiotherapy. (B) Colony formation of Panc-1 treated with AMG-510 combined with binimetinib was not significantly altered, while it was slightly reduced by 2 Gy radiotherapy. The graph on the right shows a representation of three independent experiments, along with their combined colony counts (* prompts $p<0.05$, ** prompts $p<0.01$, *** prompts $p<0.001$ as compared to mock treated controls respectively).

Total ATP levels of Panc-1 cells were only marginally reduced using irradiation, but did not respond to either AMG-510 nor binimetinib treatment or combination inhibitor therapy (Fig. 18A). In line with the findings above, Western blot assays (Fig. 18B) showed that there was no change in ERK or MEK phosphorylation due to administration of AMG-510, but only binimetinib expectedly caused reduction of ERK-phosphorylation and increase of

MEK-phosphorylation, that was only marginally further altered by addition of irradiation.

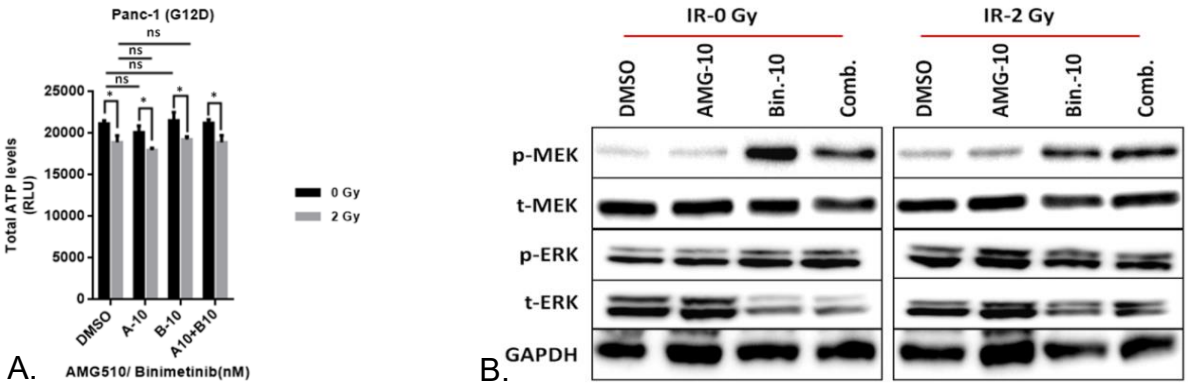

Figure 18: (A) ATP steady state levels were assessed in Panc-1 cells treated by AMG-510, binimetinib or combination with or without concomitant irradiation. (B) Shows western blot analyses of MEK and ERK phosphorylation detected in Panc-1 cells treated with AMG-510, binimetinib or combination with or without irradiation.

Taken together, these results did not indicate significant sign of therapeutic activity of AMG-510 monotherapy or combination regimens as indicated in KRAS G12D mutant pancreatic cancer cells.

3.2.4 AMG-510 and binimetinib synergistically inhibit colony formation and anchorage-independent growth of KRAS-mutated pancreatic cancer cells in vitro

Soft agar colony formation of single cell suspensions was carried out to access the effect of RAS inhibition by AMG-510 treatment of colony formation and anchorage independent growth of MiaPaCa-2 cells (Fig. 19A) and Panc-1 (Fig. 19B). Of interest, at the relatively low indicated drug concentrations chosen for this series of experiments, neither AMG-510 nor binimetinib alone had any major tangible effect, while combined KRAS plus MEK inhibition with combinatorial AMG-510 plus binimetinib lead to significant inhibition of colony formation in this three dimensional cell culture assay, especially in KRAS G12C mutant cells, which caused near complete inhibition on MiaPaCa-2 cell line.

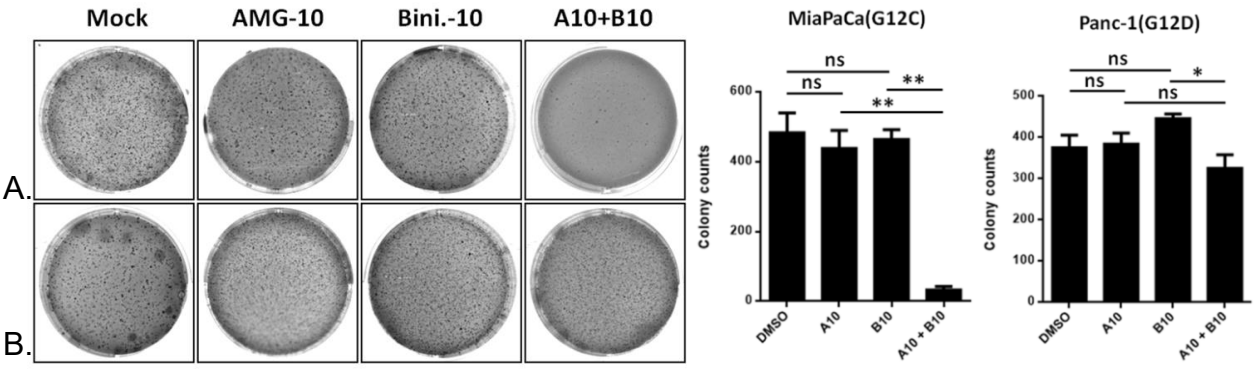

Figure 19: In soft agar colony formation assays combination of AMG-510 at 10 nM with binimetinib at 10 nM significantly reduced colony formation and anchorage independent growth of MiaPaCa-2 cells (A), while the combination of these compounds somewhat reduced the number of Panc-1 cell colonies in soft agar and attenuated anchorage-dependent growth. The graph on the right shows a representation of three independent experiments, along with their combined colony counts (* prompts $p<0.05$, ** prompts $p<0.01$, *** prompts $p<0.001$ as compared to mock treated controls respectively).

3.2.5 Coadministration of AMG-510 and binimetinib blocks Ral A activation in KRAS G12C mutant pancreatic cancer cells

Ral pathway is activated by interacting with the active form of Ras and signaling to downstream effectors such as Ral A, which is subsequently converted to the GTP-bound form. To investigate the biological role of Ral signaling in KRAS mutant cell lines after coadministration, the levels of GTP-related forms of Ral A as well as Total Ral A by affinity precipitation assays were assessed (Fig. 20). It was found that Ral A was normally activated in cells treated by AMG-510 or binimetinib monotherapy, while Ral A-GTP level in MiaPaCa-2 (KRAS G12C mutant) cell line was significantly reduced after the combination of these two compounds, suggesting that combination of AMG-510 and binimetinib could effectively suppress proliferation and differentiation of KRAS G12C mutant pancreatic cancer cell lines by inhibiting the Ral signaling pathway.

3.2.6 BI-3406 in combination with binimetinib significantly inhibits the proliferation of KRAS-G12C mutant pancreatic cancer cells in vitro

BI-3406 represents another compound developed to inhibit oncogenic KRAS signaling,

which could not only effectively reduce the formation of GTP-bound KRAS but also inhibit the MAPK pathway signaling (Hofmann et al., 2021). Since the combination of KRAS G12C inhibitors and MEK showed therapeutic efficacy only in KRAS G12C mutated pancreatic cancer cells, which showed slight effect on the growth of KRAS G12D mutated cell lines, the combination effect of other compounds on these cell lines were also explored. MiaPaCa-2 cells were treated by 100 nM BI-3406 in combination with 10 nM binimetinib, combinatorial irradiation at a dose of 2 Gy was compared to drug treatment alone. Of interest, MTS assays revealed only limited reduction of MiaPaCa-2 viability upon treatment with BI-3406, and unlike to what was found for AMG-510 as described above, there was no additive growth inhibition upon combination with the MEK inhibitor binimetinib, therapeutic irradiation, or both treatment modalities (Fig. 21A). However, in clonogenic replating assays, combination of BI-3406 plus binimetinib was more effective in reducing clonogenecity than either compound alone, irradiation did not add therapeutic efficacy in this setup (Fig. 21B).

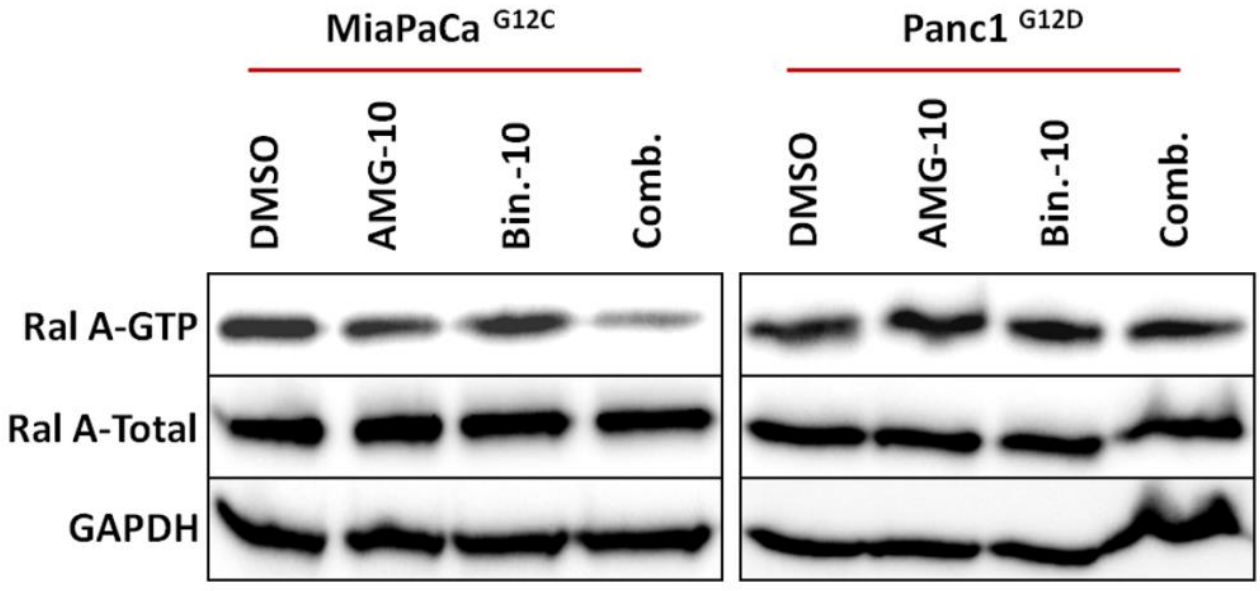

Figure 20: Activation levels of Ral A signaling elements in MiaPaCa-2 (KRAS G12C mutant) and Panc-1 (KRAS G12D mutant) cells when coadministered with AMG-510 and binimetinib.

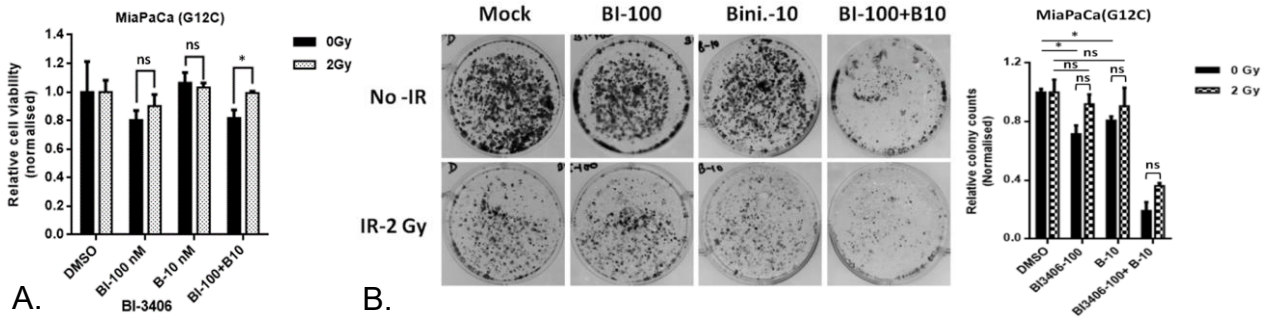

Figure 21: MTS (A) assays were used to determine the relative cell viability of MiaPaCa-2 cells treated with combination of BI-3406 and binimetinib with or without 2 Gy dose of radiotherapy. 100 nM BI-3406 combined with 10 nM binimetinib showed no significant change in relative cell viability of MiaPaCa-2 cells based on MTS assay with or without radiotherapy. Colony formation of MiaPaCa-2 treated by BI-3406 combined with binimetinib (B) showed that the combination of BI-3406 with binimetinib significantly inhibited clonogenecity of MiaPaCa-2, which was enhanced by 2 Gy radiotherapy. The graph on the right shows a representation of three independent experiments, along with their combined colony counts (* prompts $p<0.05$, ** prompts $p<0.01$, *** prompts $p<0.001$ as compared to mock treated controls respectively).

However, BI-3406 plus binimetinib more potently reduced steady state ATP levels than any of the two compounds alone, and this effect was more pronounce upon concomitant irradiation (Fig. 22A). This was in line with changes in phosphorylation of MEK and ERK and mirrored what had previously been found for AMG-510 combination regimens (Fig. 22B).

3.2.7 BI-3406 in combination with binimetinib inhibits clonogenecity and anchorage-independent growth of KRAS G12D mutant pancreatic cancer cells

Panc-1 cells were treated with 100 nM BI-3406 and 10 nM binimetinib under the application of 2 Gy dose of irradiation. Of note, BI-3406 treatment, applied either as single agent therapy or in combination with binimetinib, this dose did not lead to any tangible growth inhibition and reduction of cell viability in MTS assays (Fig. 23A). BI-3406 monotherapy caused reduction in clonogenecity in colony formation assays (Fig. 23B).

Of interest, however, irradiation in combination with BI-3406 plus binimetinib led to significantly reduced clonogenecity, suggesting radiosensitation conferred by KRAS and

MEK inhibition conferred by treatment with these two compounds in Panc-1 cells.

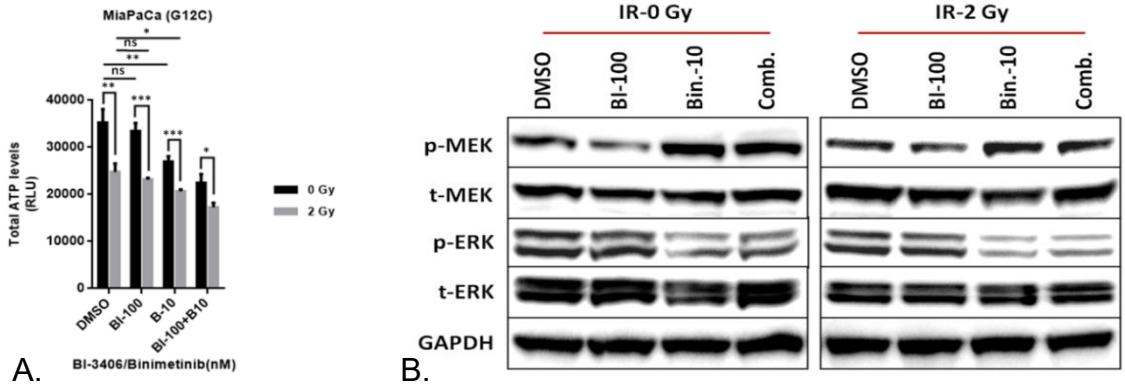

Figure 22: (A) ATP steady state levels were significantly decreased by treatment with either BI-3406 or binimetinib. Combination therapy showed more pronounced ATP reduction, and the synergistic effect with 2 Gy irradiation was statistically significant. Western blot of MiaPaCa-2 treated with BI-3406 combined with binimetinib with or without 2 Gy of irradiation (B) showed a tendency of ERK phosphorylation consistent with the results of ATP and clonogenitic assays.

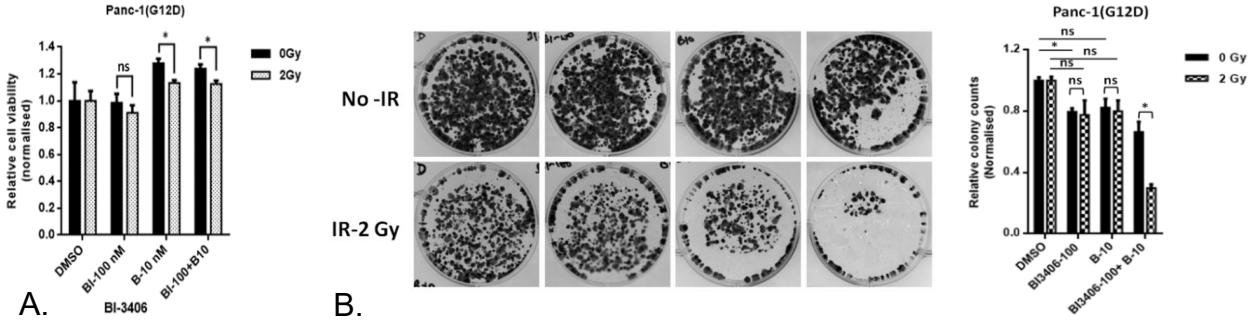

Figure 23: MTS (A) assays were used to determine the relative cell viability of Panc-1 cells treated with combination of BI-3406 and binimetinib with or without 2 Gy dose of radiotherapy. (B) Colony formation of Panc-1 treated with BI-3406 combined with binimetinib was reduced, while it was vastly inhibited by 2 Gy combination radiotherapy. The graph on the right shows a representation of three independent experiments, along with their combined colony counts (* prompts $p<0.05$, ** prompts $p<0.01$, *** prompts $p<0.001$ as compared to mock treated controls respectively).

Furthermore, irradiation was mirrored by marked reduction of ATP levels in this cell line at the dose levels indicated (Fig. 24A). Not unexpectedly BI-3406 treatment resulted in phospho-ERK and phospho-MEK downregulation as surrogate for inhibition of KRAS downstream effector signaling axes, and these alterations were enhanced upon concomitant irradiation (Fig. 24B). Again and as expected as well, MEK inhibition by bini-

metinib treatment caused feedback up-regulation of phospho-MEK as determined using Western blot analysis.

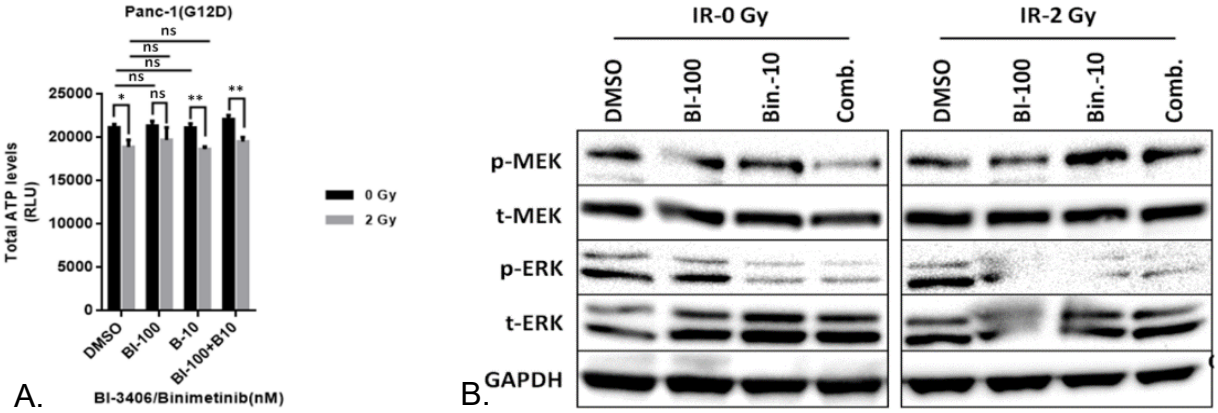

Figure 24: (A) ATP steady state levels were assessed in Panc-1 cells treated with BI-3406, binimetinib or combination with or without concomitant irradiation. (B) Shows western blot analyses of MEK and ERK phosphorylation detected in Panc-1 cells treated with BI-3406, binimetinib or combination with or without irradiation.

3.2.8 Combination therapy of BI-3406 plus binimetinib shows marked therapeutic synergy in KRAS G12D mutant pancreatic cancer

Soft agar colony formation assays from single cell suspensions were also carried out to determine the effect of BI-3406 in combination with binimetinib on the ability of KRAS G12C mutant MiaPaCa-2 cells (Fig. 25A) and G12D mutant Panc-1 cells (Fig. 25B) to form colonies and growth anchorage-independently in this three-dimensional culture system. BI-3406 appeared to be slightly less potent to inhibit MiaPaCa-2 colony formation and anchorage independent growth in soft agar assays, which is in line with previous MTS and replating data presented above. Of note, AMG-510 treatment did not cause any alteration in colony formation and anchorage independent growth, while both BI-3406 as well as binimetinib monotherapies did cause reduced colony formation as indicated. Interestingly, there was marked therapeutic synergy of combination therapy of Panc-1 cells with BI-3406 plus binimetinib.

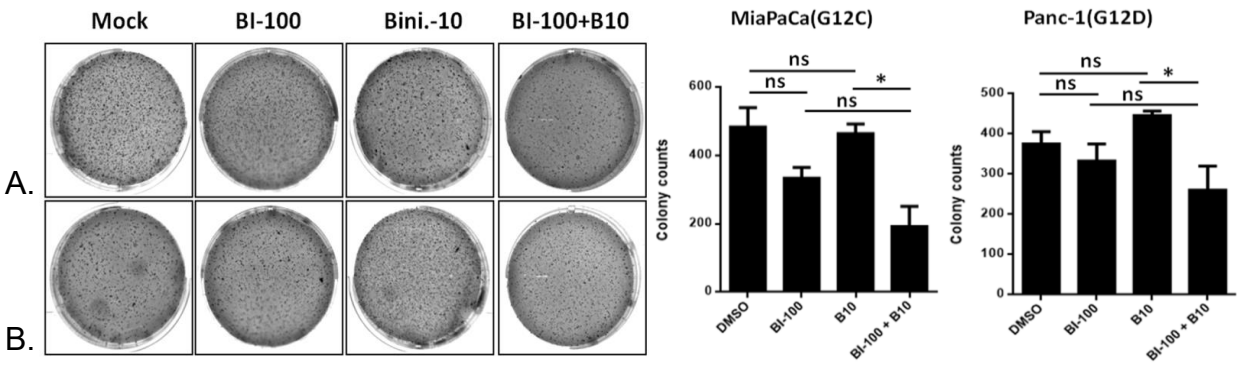

Figure 25: 100 nM BI-3406 in combination with 10 nM binimetinib compound somewhat reduced the number of MiaPaCa-2 cell colonies (A) in soft agar and attenuated anchorage-dependent growth. Likewise, the same setting showed a similar effect on Panc-1 cells (B). The graph on the right shows a representation of three independent experiments, along with their combined colony counts (* prompts $p<0.05$, ** prompts $p<0.01$, *** prompts $p<0.001$ as compared to mock treated controls respectively).

3.2.9 Combination of BI-3406 and binimetinib inhibits colony formation and anchorage-independent growth of KRAS mutant pancreatic cancer cell

The combination of BI-3406 with binimetinib was more effective than AMG-510 plus binimetinib on Panc-1 cells, suggesting that the combination of BI-3406 and binimetinib is more therapeutic in pancreatic cancer with KRAS G12D mutation than the combination of AMG510 and binimetinib.

Levels of GTP-related forms of Ral A as well as Total Ral A by affinity precipitation assays were assessed on KRAS mutant cell lines treated with BI-3406 and binimetinib (Fig. 26). It was found that Ral A was normally activated in cells treated by BI-3406 or binimetinib monotherapy, while Ral A-GTP level in MiaPaCa-2 (KRAS G12C mutant) cell line was slightly reduced after the combination of these two compounds. This level was even increased in Panc-1 (KRAS G12D mutant) cells.

3.2.10 Growth and clonogenecity of KRAS G12C mutant pancreatic cancer cells is significantly reduced upon dual pathway blockade by BI-2852 plus binimetinib combination therapy

BI-2852 was evaluated as another means to inhibit oncogenic KRAS signaling in

pancreatic cancer cells. BI-2852 is a structurally designed switch I/II pocket-based KRAS inhibitor with nanomolar affinity. Which could block the interaction of GEF, GAP and effectors with KRAS, leading to inhibition of downstream signaling and anti-proliferative effects in KRAS mutant cells. Notably, this compound is more effective in combination with KRAS G12D mutations (Tran et al., 2020).

MiaPaCa-2 cells were cultured in the presence of BI-2852 combined with binimetinib under the application of 2 Gy of irradiation. Again, relative cell viability was measured using MTS assays (Fig. 27A). Similar to what was found for BI-3406 as described above, MiaPaCa-2 cells treated with BI-2852 showed only marginally reduced viability, and additional application of binimetinib or concomitant irradiation conferred little additional therapeutic efficacy in this setting. Of interest, clonogenecity was significantly reduced upon dual pathway blockade by BI-2852 plus binimetinib combination therapy, and there was significant therapeutic synergism with irradiation (Fig. 27B).

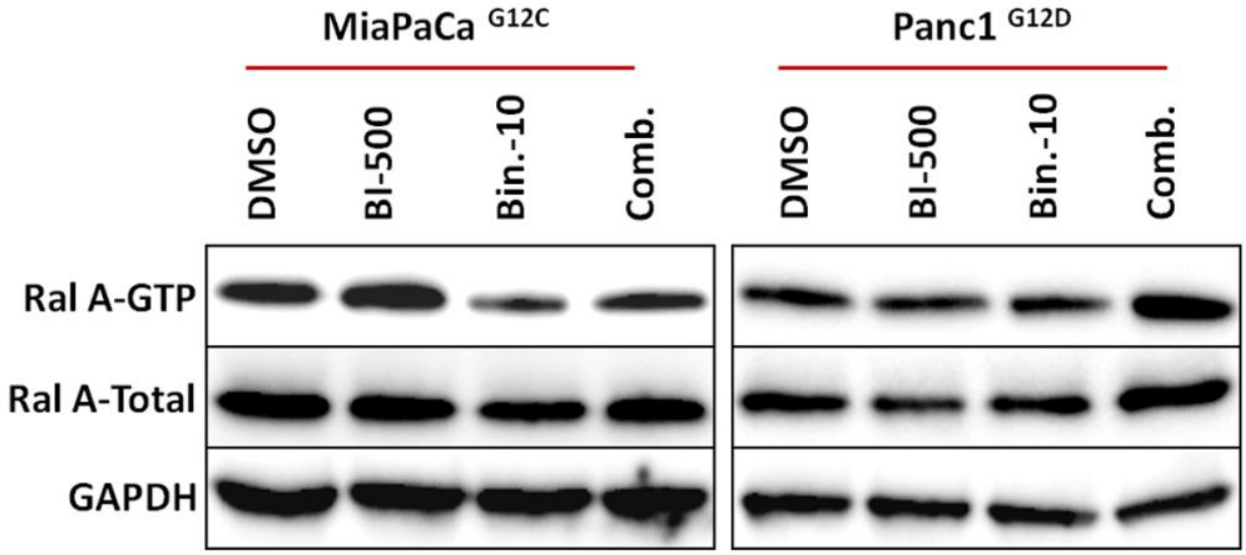

Figure 26: Activation levels of Ral A signaling elements in MiaPaCa-2 (KRAS G12C mutant) and Panc-1 (KRAS G12D mutant) cells when coadministered with BI-3406 and binimetinib.

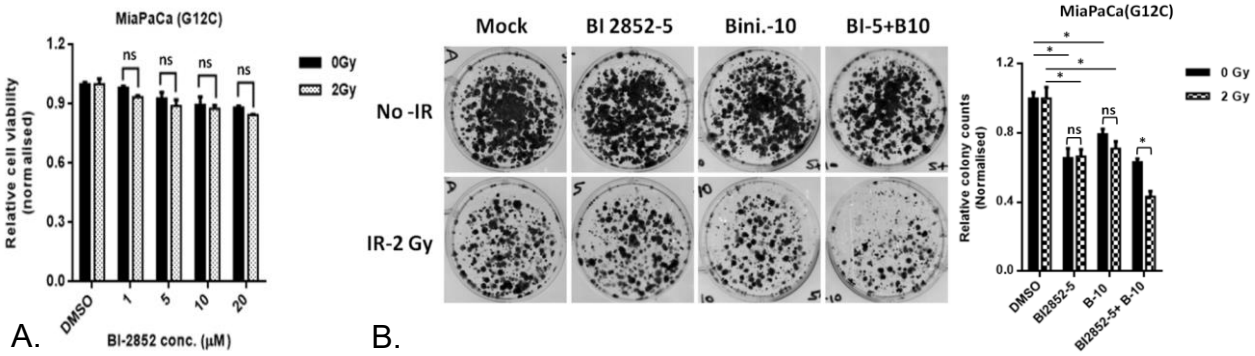

Figure 27: MTS (A) assays were used to determine the relative cell viability of MiaPaCa-2 cells treated with combination of BI-2852 and binimetinib with or without 2 Gy dose of radiotherapy. 10 nM BI-2852 combined with 10 nM binimetinib showed no significant change in relative cell viability of MiaPaCa-2 cells based on MTS assay with or without radiotherapy as compared to BI-2852 monotherapy. Colony formation of MiaPaCa-2 treated with BI-2852 combined with binimetinib (B) showed that the combination of BI-2852 with binimetinib significantly inhibited clonogenecity of MiaPaCa-2, which was enhanced by 2 Gy radiotherapy. The graph on the right shows a representation of three independent experiments, along with their combined colony counts (* prompts $p<0.05$, ** prompts $p<0.01$, *** prompts $p<0.001$ as compared to mock treated controls respectively).

Further, the above observation in MiaPCa-2 treated by BI-2852 and binimetinib were directly mirrored by significantly enhanced reduction of ATP levels (Fig. 28A) and reduced ERK phosphorylation (Fig. 28B) upon combination inhibitor therapy augmented by therapeutic irradiation. Again, similar what had previously been found for other KRAS inhibitor combinations, addition of binimetinib caused a feedback upregulation of MEK phosphorylation.

3.2.11 BI-2852 and binimetinib combination therapy in KRAS G12D mutant pancreatic cancer cells

Panc-1 cells were treated with BI-2852 and binimetinib under the application of 2 Gy dose of irradiation, the relative cell viability, proliferation ability and colony formation capacity were measured using MTS assay (Fig. 29A) and clonogenitic assay (Fig. 29B). Viability of Panc-1 cells treated with BI-2852 at 100 nM combined with binimetinib at 10 nM did not change significantly. However, the promotion of compound efficacy by radiotherapy was

statistically significant, suggesting a slight additive therapeutic efficacy.

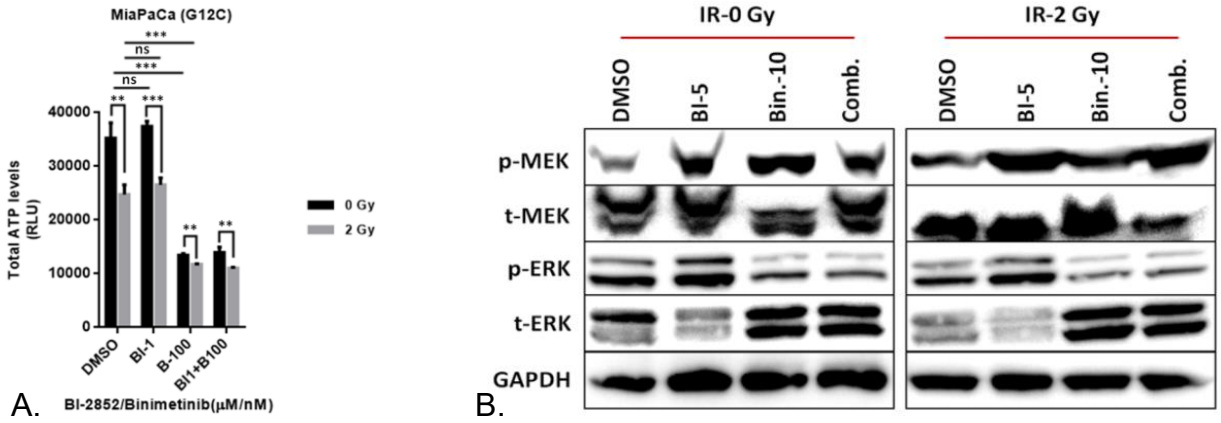

Figure 28: (A) ATP steady state levels were significantly decreased by treatment with either BI-2852 or binimetinib. Combination therapy showed more pronounced ATP reduction, and the synergistic effect with 2 Gy irradiation was statistically significant. Western blot of MiaPaCa-2 treated with BI-2852 combined with binimetinib with or without 2 Gy of irradiation (B) showed a tendency of ERK phosphorylation consistent with the results of ATP and clonogenitic assays.

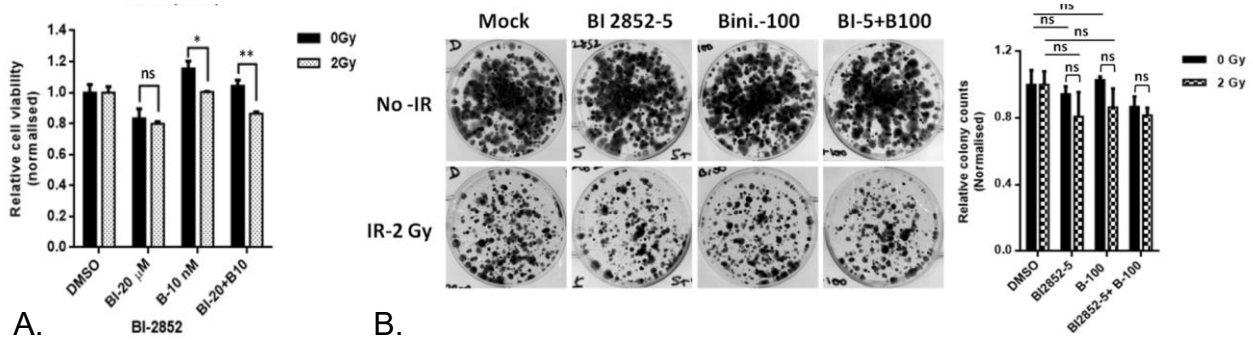

Figure 29: MTS (A) assays were used to determine the relative cell viability of Panc-1 cells treated with combination of BI-2852 and binimetinib with or without 2 Gy dose of radiotherapy. (B) Colony formation of Panc-1 treated by BI-2852 combined with binimetinib was reduced, while it was vastly inhibited by 2 Gy combination radiotherapy. The graph on the right shows a representation of three independent experiments, along with their combined colony counts (* prompts $p<0.05$, ** prompts $p<0.01$, *** prompts $p<0.001$ as compared to mock treated controls respectively).

ATP levels (Fig. 30A) of Panc-1 cells treated with this combination showed the similar changes of whose relative cell viabilities. Western blot assays were performed (Figure 30B) for demonstrating mechanism of the action, whose results showed that the ERK

phosphorylation tendency was generally consistent with the results of the clonogenitic assay, supporting that the ability of BI-2852 in combination with binimetinib could inhibit the proliferative capacity of KRAS G12D mutated pancreatic cancer cells by inhibiting the MEK/ERK pathway under 2 Gy radiotherapy conditions.

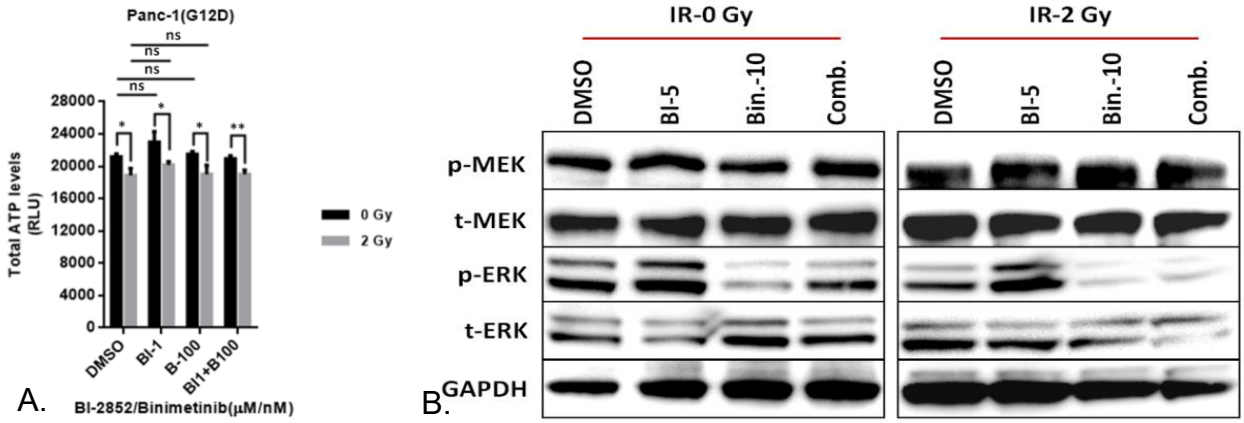

Figure 30: (A) ATP steady state levels were assessed in Panc-1 cells treated with BI-2852, binimetinib or combination with or without concomitant irradiation. (B) Shows western blot analyses of MEK and ERK phosphorylation detected in Panc-1 cells treated with BI-2852, binimetinib or combination with or without irradiation.

3.2.12 BI-2852 in combination with binimetinib reduces colony formation and anchorage-independent growth of KRAS mutant pancreatic cancer cells

Soft agar colony formation of single cell suspensions was again carried out to assess the effect of BI-2852 in combination with binimetinib on the ability of KRAS G12C mutant MiaPaCa-2 (Fig. 31A) and KRAS G12D mutant Panc-1 cells (Fig. 31B) to form colonies and grow anchorage-independently in this three-dimensional culture system. It is noteworthy that at the relatively low indicated drug concentrations chosen for this series of experiments, the combination of BI-2852 plus binimetinib caused reduced colony formation of both MiaPaCa-2 and Panc-1 cells, respectively.

3.2.13 BI-2852 and binimetinib do not affect Ral A activation

Levels of GTP-bound forms of Ral A as well as Total Ral A by affinity precipitation assays were assessed in KRAS mutant cell lines treated with BI-2852 and binimetinib (Fig. 32).

It was found that Ral A was normally activated in both cell lines treated with this setting, suggesting that combination of BI-2852 and binimetinib has no effect on the Ral pathway of KRAS mutant cell lines.

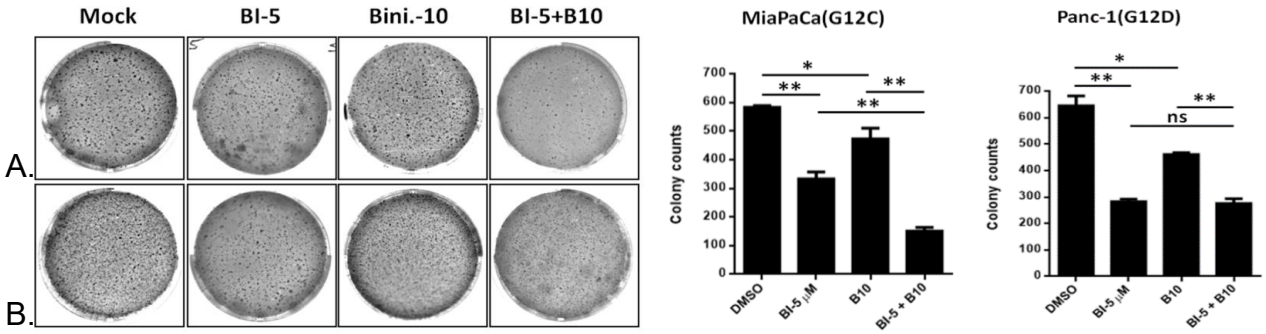

Figure 31: In soft agar and attenuated anchorage-dependent assays, combination of BI-2852 at 5 μM with binimetinib at 10 nM significantly reduced colony formation and anchorage independent growth both of MiaPaCa-2 cells (A) and Panc-1 cells (B). The graph on the right shows a representation of three independent experiments, along with their combined colony counts (* prompts p<0.05, ** prompts p<0.01, *** prompts p<0.001 as compared to mock treated controls respectively).

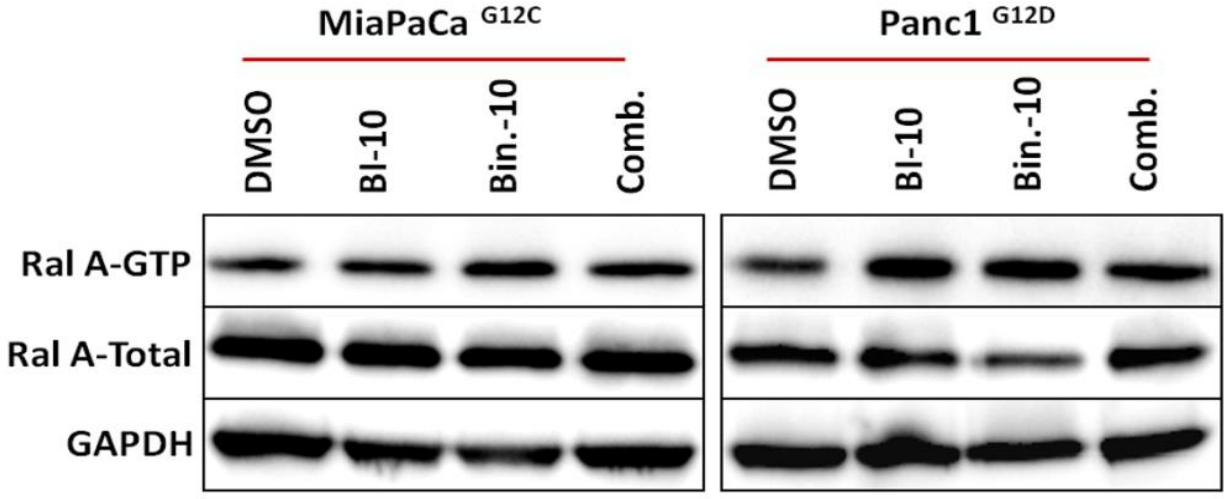

Figure 32: Activation levels of Ral A signaling elements in MiaPaCa-2 (KRAS G12C mutant) and Panc-1 (KRAS G12D mutant) cells when coadministered with BI-2852 and binimetinib.

3.2.14 Combination of BI-2852 and binimetinib in wild type pancreatic cancer cells

For complementary comparison we next treated KRAS wild type BxPC-3 pancreatic cancer cells with AMG-510, BI-3406, BI-2852, respectively, again applied as either single

agent monotherapy, in combination with the MEK inhibitor binimetinib, or with augmentation by concomitant irradiation of 2 Gy.

In MTS assays, no change in BxPC-3 cell viability was found upon treatment with any of these compounds, and no radiosensitation by concomitant irradiation was seen (Fig. 33), underscoring on-target efficacy and vice versa absence of unspecific off-target toxicity conferred by either of these compounds applied at the doses indicated.

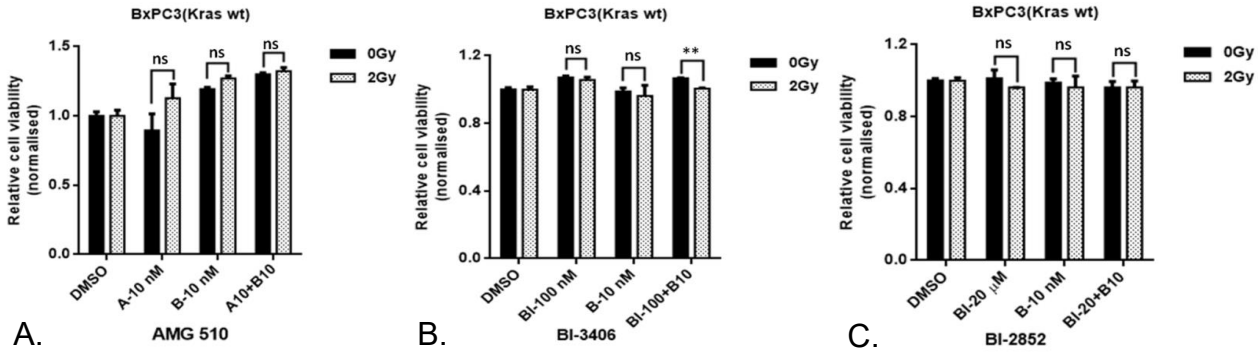

Figure 33: Treatment of BxPC-3 with binimetinib combined with AMG-510 (A), BI-3406 (B), and BI-2852 (C) separately, assessed by cell viability (MTS) assays in dose-independent manner, showing that the combination of these compounds had no effect on BxPC-3 cell line relative cell viability, regardless of whether or not they were exposed to 2 Gy irradiation therapy. All of the experiments were repeated three times (* prompts $p<0.05$, ** prompts $p<0.01$, *** prompts $p<0.001$ as compared to mock treated controls respectively).

There was also no significant change in proliferative capacity of the cell line after treated by compounds combination, suggesting that binimetinib has no synergistic effect on AMG-510 (Fig. 34A), BI-3406 (Fig. 34B) or BI-2852 (Fig. 34C) in the treatment of wild-type pancreatic cancer cells, nor did radiotherapy promote growth inhibition of this cell line under the combination.

Western blot assays were performed (Fig. 35) for demonstrating mechanism of the action, whose results showed that ERK phosphorylation tendency was generally consistent with the results of MTS and clonogenitic assays, suggesting that binimetinib combined with AMG-510, BI-3406 or BI-2852 were unable to effectively inhibit MEK/ERK pathway and failed to inhibit wild-type pancreatic cancer cell viability or proliferative capacity, even

under the 2 Gy radiotherapy condition.

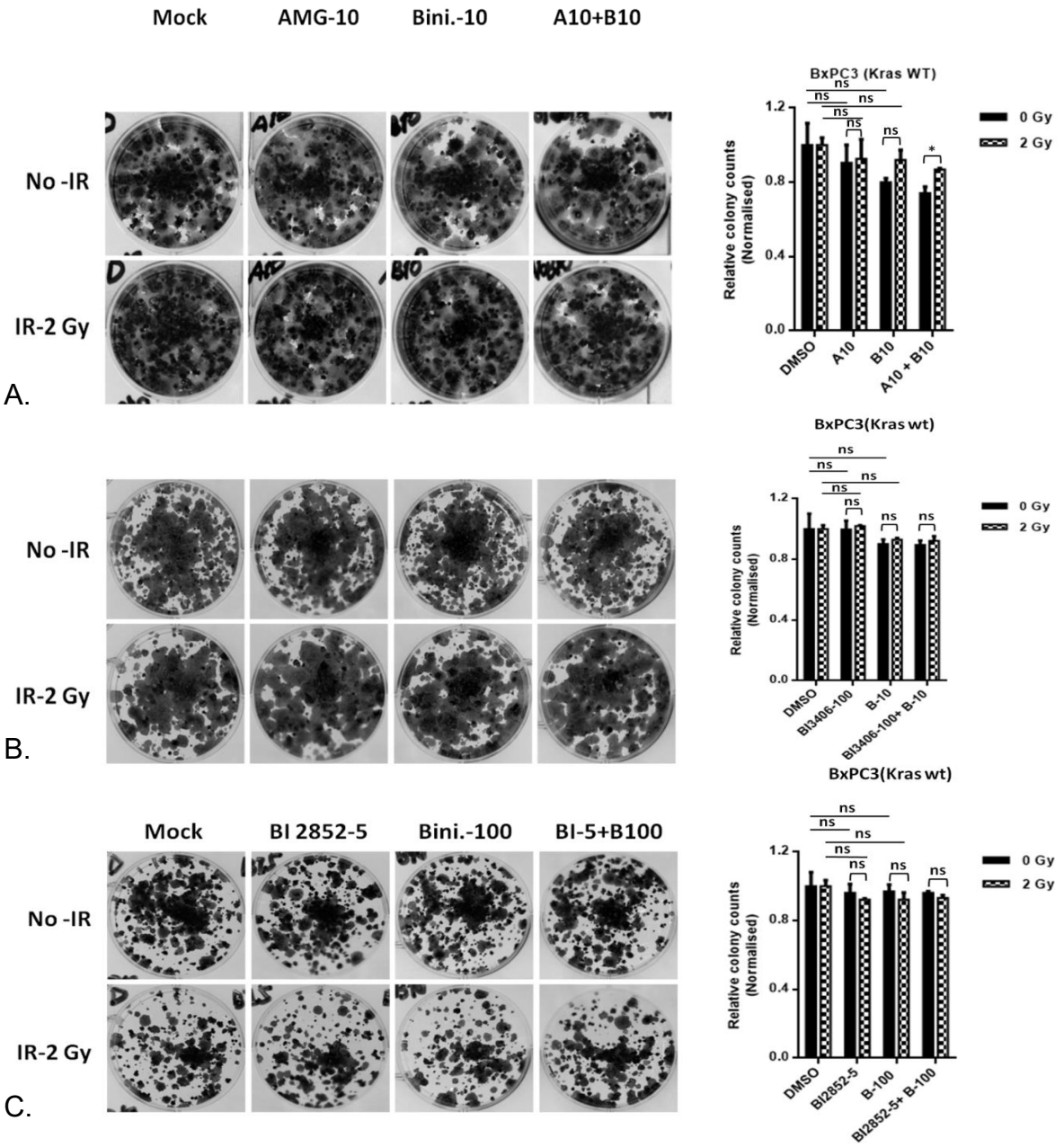

Figure 34: Colony formation of BxPC-3 treated by binimetinib combined with AMG-510 (A), BI-3406 (B), and BI-2852 (C) separately. The combination of these compounds had no effect on BxPC-3 cell line proliferative capacity, regardless of whether or not they were exposed to 2 Gy irradiation therapy. All of the experiments were repeated three times (* prompts $p<0.05$, ** prompts $p<0.01$, *** prompts $p<0.001$ as compared to mock treated controls respectively).

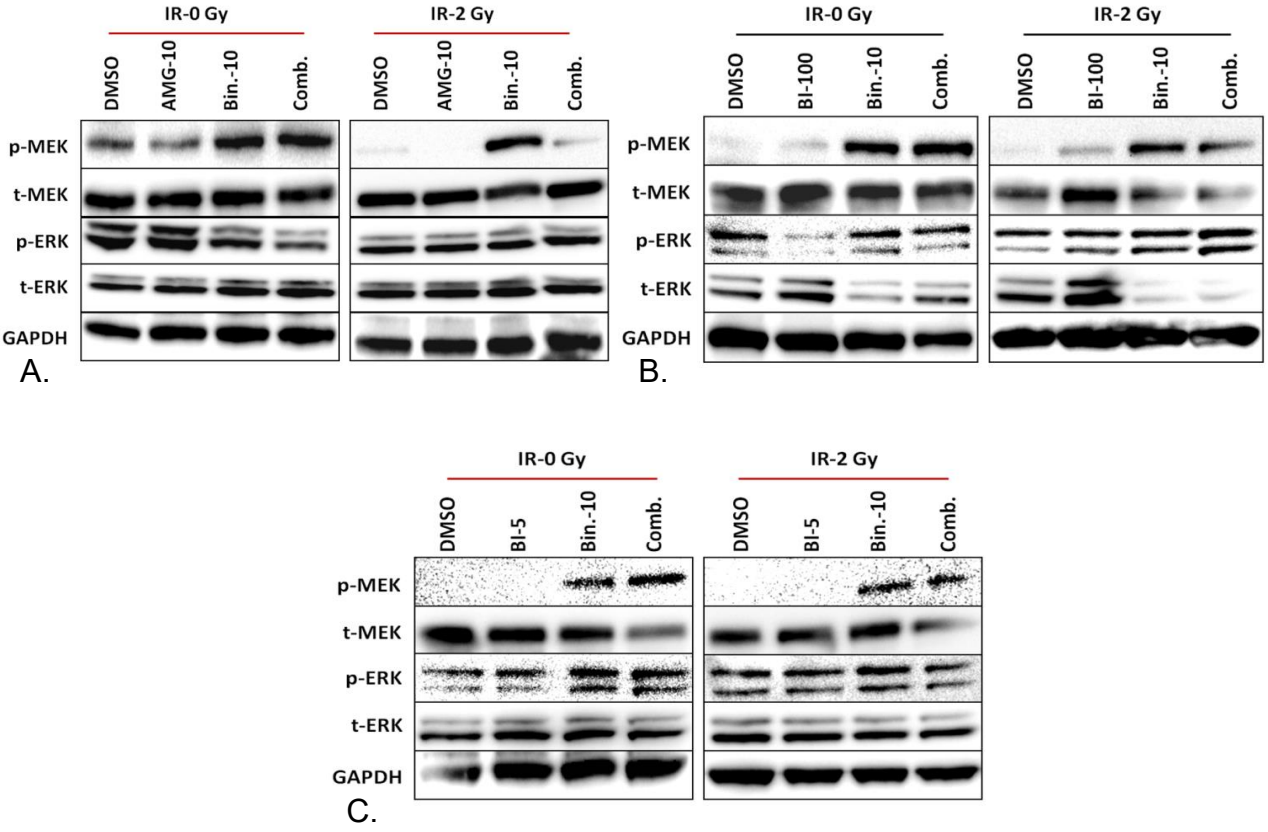

Figure 35: Western blot of BxPC-3 treated by binimetinib combined with AMG-510 (A), BI-3406 (B), and BI-2852 (C) separately with or without 2 Gy irradiation therapy, showing a tendency of MEK/ERK phosphorylation that was generally consistent with the results of MTS and clonogenitic assays.

4. Conclusion and Perspective

4.1 KRAS inhibition with sotorasib shows therapeutic synergism with MEK inhibition by binimetinib in KRAS G12C mutant pancreatic cancer cells

While molecularly targeting oncogenic KRAS driven malignancies has long been deemed impossible, the introduction of sotorasib (AMG-510) as first-in-class small molecule KRAS G12C inhibitor has dramatically changed this paradigm and in fact now represents a standard therapeutic option for KRAS G12C-mutant NSCLC patients (Kim et al., 2020). While unlike in NSCLC G12C mutations represent only a minor fraction of KRAS driver mutations detected in PDAC, this therapeutic approach has nevertheless been evaluated in gastrointestinal carcinomas, including pancreatic cancer, as well, albeit with limited success. sotorasib monotherapy showed modest clinical activity in KRAS G12C mutant colorectal cancer with objective response in 6/62 (9.7%) cases in the phase 2 CodeBreaK 100 trial (Fakih et al., 2022).

Therefore, identification of co-vulnerabilities and development of suitable combination therapy approaches to achieve long-lasting remissions in a majority of patients and to overcome adaptive resistance is currently an important field of active investigation (Brown et al., 2020). Increasing evidence suggests that identification of such combinatorial strategies aiming at synthetic lethality with oncogenic KRAS inhibition might be highly tissue-specific and vary with individual sites of tumor origin and with individual patterns of accompanying oncogenic genomic variants (Manchado et al., 2016).

In our current study presented here, treatment with sotorasib monotherapy significantly but sub totally reduced in vitro net cell viability and clonogenecity of KRAS G12C mutant MiaPaCa-2 pancreatic cancer cells in a dose-dependent manner. This effect was mirrored by marked down-regulation of MEK- as well as ERK-phosphorylation indication robust inhibition of signaling through these KRAS downstream effector axes. Of note, KRAS G12D Panc-1 or KRAS wild type BxPC-3 pancreatic cancer cells were not affected, sug-

gesting specific on-target efficacy of sotorasib under the experimental conditions applied here.

While binimetinib monotherapy similarly showed modest but reproducible, dose-dependent reduction of in vitro net cell viability and clonogenecity, mirrored by ERK-dephosphorylation, in both KRAS mutant pancreatic cancer cell lines tested here (MiaPaCa-2 and Panc-1), these effects were not observed in KRAS wild type pancreatic cancer cells (BxPC-3). These results are in line with modest therapeutic in vitro and in vivo efficacy of MEK inhibitors in KRAS mutant pancreatic cancer previously described by others (Pedersen et al., 2017, Hamidi et al., 2014).

Of interest, combinatorial inhibition of oncogenic KRAS and MEK signaling axes by sotorasib plus binimetinib combination therapy administered at low concentrations of 10 nM showed strong additive of synergistic efficacy in reducing net viability and clono-genecity of MIAPaCa-2, but not Panc-1 or BxPC-3 cells, respectively, suggesting synthetic lethality by double pathway blockade specifically in KRAS G12C mutant PDAC cells. Enhanced ERK-dephosphorylation as well as ATP depletion were documented as sur-rogates of putative underlying mechanism. We further found expression of p27 Kip1 to be upregulated particularly by sotorasib plus binimetinib combination therapy hinting at enhanced induction of apoptosis by this approach.

These observations are in line with previous reports by others. Combined pathway blockade by means of MEK and PI3K inhibitor combination therapy showed promising therapeutic efficacy in preclinical in vitro and in vivo model systems but were unsuccessful in clinical trials with marked adverse toxicity (Grilley-Olson et al., 2016, Bedard et al., 2015, Weisner et al., 2019).

Brown et al. (2020) reported therapeutic synergism of combined KRAS and MEK inhibition in pancreatic cancer and found sustained suppression of PDAC tumor progression upon additional mTORC1/2 inhibition.

Induction of autophagy and positive feedback loops leading to activation of upstream targets have more recently been suggested as potentially underlying therapeutic

synergism of KRAS and MEK/ERK pathway blockade (Bryant et al., 2019, Hallin et al., 2020, Xue et al., 2020, Fedele et al., 2018). Combination of KRAS inhibition and inhibitors of SHP2 have recently been found to diminish NSCLC and PDAC growth in respective tumor models (Fedele et al., 2018, Ruess et al., 2018).

Finally, strong therapeutic synergism of sotorasib plus binimetinib combination therapy was observed using a three-dimensional cell culture model system. In soft agar assays, sotorasib (c=10nM) and binimetinib (c=10nM) combination treatment caused near complete abrogation of colony formation and anchorage independent growth of KRAS G12C mutant MiaPaCa-2 cells. Of note, colony formation and growth of Panc-1 cells that are driven by KRAS G12D was not affected ruling out unspecific cytotoxicity. Three dimensional colony formation has previously been linked to signaling through the RALGDS-RAL axis downstream of oncogenic KRAS (Feldmann et al., 2010, Lim et al., 2005, 2006). Indeed, in our hands sotorasib plus binimetinib combination treatment specifically led to markedly enhanced downregulation of Ral A-GTP, the active form of Ral A, as compared to the respective monotherapies in MiaPaCa-2, but not in Panc-1 cells, suggesting the importance of this often disregarded KRAS effector signaling axis.

4.2 Synergism of KRAS and MEK inhibition with irradiation

The role of radiotherapy in pancreatic cancer is currently not well established and is a matter of ongoing investigation (Versteijne et al., 2022, Lo and Zureikat, 2022). Nevertheless, pancreatic cancer has so far proven to be difficult to treat by radiotherapy (Colbert et al., 2014). Early reports of therapeutic KRAS inhibition with sotorasib hinted at potential synergisms with various tyrosine kinase inhibitors and suggested an effect on antitumor immune response (Canon et al., 2019). Oncogenic KRAS signaling has been linked to resistance of tumor cells to radiotherapy, and therefore there is room to hypothesize that KRAS inhibitors might act as radiosensitizers in RAS-driven malignancies (Cáceres-Gutiérrez et al., 2022, Toulany, 2022).

In fact, our present data presented here indicate enhanced reduction of net cell growth and clonogenecity of AMG-510 monotherapy on KRAS G12C mutant MiaPaCa-2 cells upon concomitant irradiation at a dose of 2Gy. Curiously, this effect was mirrored by similarly enhanced dephosphorylation of ERK and MEK, as demonstrated using Western blot analysis. Again, this observation was not made with KRAS G12D mutant Panc-1 or wild type BxPC-3 pancreatic cancer cells used as controls.

More importantly, combinatorial pathway blockade by sotorasib plus binimetinib combination therapy led to even more pronounced reduction in cell viability and almost completely abolished clonogenecity of MiaPaCa-2 cells when combined with 2 Gy of irradiation. Irradiation alone strongly induced apoptosis in MiaPaCa-2 cells as determined using luminescence assays and led to induction of apoptosis-related protein expression of p27 Kip1 and Cleaved Caspase 3. Again, these effects were further boostered by combinatorial pathway inhibition by sotorasib and binimetinib combination. Of note, this observation was not made upon combination of radiotherapy plus binimetinib without sotorasib treatment, demonstrating that specific inhibition of oncogenic KRAS G12C with sotorasib is required for radiosensitation as observed here.

To the best of our knowledge, these findings represent a novel observation and warrant further evaluation of combinatorial KRAS and MEK inhibition by sotorasib and binimetinib plus radiation therapy as a novel approach to treat pancreatic cancer.

4.3 BI-3406 and BI-2852 synergize with binimetinib in the treatment KRAS mutant pancreatic cancer cells

While pancreatic cancers are driven by oncogenic KRAS mutations in the majority (approx. 60-95%) of cases, the majority of these mutations are non-G12C and are thus not amenable to treatment with sotorasib (Singhi et al., 2019) (Huang L et al., 2021). More recently, novel modulators of KRAS regulators such as SOS1, SOS1 or CRAF have been evaluated as potential "pan-KRAS" inhibitors and are currently undergoing active

preclinical and early clinical investigation as potential anticancer agents (Coley et al., 2022).

In our study presented here, BI-3406 as well as BI-2852, respectively, showed limited single agent in vitro therapeutic efficacy in terms of net cell growth and clonogenicity inhibition. However, either compound showed clear therapeutic synergism with combinatorial MEK inhibition by mean of binimetinib combination therapy in KRAS mutant MiaPaCa-2 and Panc-1, but not in wild type BxPC-3 pancreatic cancer cells. Thus, therapeutic efficacy of either BI-3406 plus binimetinib or BI-2852 plus binimetinib combination was irrespective of the specific subtype of oncogenic KRAS mutation under the conditions presented here and were accompanied by robust pathway blockade as illustrated by downregulation of MEK and ERK phosphorylation in Western blot analyses.

These results are in line with similar observations previously reported by others. Hofmann et al. (2021) found therapeutic efficacy upon combination therapy with BI-3406 and the MEK inhibitor trametinib in KRAS driven malignant cancer cells, including pancreatic cancer. This approach was described to be active in a range of KRAS mutations including G12D, G12V, G12C and G13D and was also validated in vivo.

Curiously, as opposed to results with sotorasib discussed above, our data presented here showed limited additional therapeutic in vitro efficacy of concomitant radiotherapy with either BI-3406 or BI-2852 combination regimens. An exception was combination treatment of Panc-1 cells, in which combination of BI-3406 and binimetinib lead to marked radiosensitesation and near-complete abrogation of clonogenecity upon concomitant irradiation. These observations suggest that potential additional benefit of combinatorial radiotherapy with BI-3406 plus binimetinib might be dependent on specific subtypes of KRAS mutations as well as co-mutational patterns.

It is an obvious limitation of this current work presented here that while various measures were taken to corroborate the validity of our findings using different complementary experimental approaches wherever possible, prediction of clinical efficacy solely based on in vitro model systems is not sufficient. While the cancer cell line models mostly

represent the spectrum of oncogenic driver alterations including the full range of co-variants and potential resistance-conferring alterations, other pathophysiologically relevant key factors are not adequately represented. A key feature of pancreatic cancer is the presence of an extensive desmoplasmic reaction and tumor stroma, that is thought to confer therapy resistance in many cases and is insufficiently addressed in this current work. Moreover, effects conferred by the host's immune system can not be taken into account using the in vitro models as presented here. Moreover, the complex process tumor progression and metastatic spread are to a wide extend determined by local human anatomy, that is necessarily insufficiently simulated using in vitro model systems.

On the other hand, given our exponentially growing understanding of inter-individually often highly variable cancer genomes, and the increasing availability of clinically suited inhibitors, the amount of potentially promising combinations exceeds the possibility to thoroughly study all of these using in vivo model systems by far. Exploitation of animal models in this context is limited, among other factors, by high cost- and labor-intensity as well as ethical considerations regarding animal welfare. Moreover, clinical response of a certain cancer therapy regimen is usually still poorly predicted by one single in vivo model system alone, but instead often require the evaluation in several complementary model systems to justify subsequent evaluation in human patients.

4.4 Outlook

Taken together, our results suggest that combination therapy of KRAS and MEK inhibition plus radiotherapy might be a valuable therapeutic approach for pancreatic cancers that should be further evaluated in vivo. Concomitant radiotherapy appears to be particularly promising with sotorasib plus binimetinib combination therapy in KRAS G12C driven pancreatic cancers.

5. Abstract

Pancreatic ductal adenocarcinomas account for 80−90% of all pancreatic malignancies and are among the most lethal of cancers known to date. They are driven by oncogenic KRAS mutations in over 90% of cases, which have been linked to early metastasis and overall poor prognosis and which confer relative resistance to classical cytostatic chemotherapy as well as other forms of systemic therapeutic approaches. The spectrum of oncogenic KRAS variants observed in pancreatic cancers differ significantly from those observed in non-small cell lung, colorectal or other forms of cancer. Pathological KRAS mutations have long been deemed to be "undruggable". Only recently first examples of specific KRAS inhibitors entered the clinical arena, but therapeutic efficacy found in pancreatic cancer is limited and usually not long lasting. In this current work presented here, combinatorial regimens of KRAS and MEK inhibitors are evaluated under the addition of radiotherapy. Pancreatic cancer cell lines with oncogenic KRAS G12C, G12D or wild type KRAS were treated with specific KRAS or SOS1/2 Inhibitors and therapeutic synergisms with concomitant MEK inhibition and irradiation were systematically evaluated by means of MTS, colony formation-, migration-, soft agar-, and apoptosis assays. Underlying pathophysiological mechanisms were examined by using Western blot analyses, ATP- formation-, RealTime-Glo™ and Ral A activation assays. KRAS inhibition with the small molecule inhibitor sotorasib showed therapeutic synergism with the MEK inhibitor binimetinib in KRAS G12C-driven pancreatic cancer cells. This observation was also made with two additional substances that were evaluated as "pan KRAS" inhibitors, BI-3406 and BI-2852. Moreover, markedly enhanced sensitivity of therapeutic irradiation was documented upon combined inhibition of KRAS and MEK. These observations represent a therapeutic approach for pancreatic cancer that should further evaluated using in vivo model systems in the future.

6. List of figures

7. List of tables

8. References

Adrianus JL, Melissa LJ, Julien M. Sotorasib versus docetaxel for previously treated non-small-cell lung cancer with KRASG12C mutation: a randomised, open-label, phase 3 trial. Lancet. 2023; 401: 617-704

Ahearn IM, Haigis K, Bar-Sagi D, Philips MR. Regulating the regulator: post-translational modification of RAS. Nature reviews Molecular cell biology. 2011; 13: 39-51

Andreyev HJ, Norman AR, Cunningham D, Oates J, Dix BR, Iacopetta BJ, Young J, Walsh T, Ward R, Hawkins N, Beranek M. Kirsten ras mutations in patients with colorectal cancer: the 'RASCAL II'study. British journal of cancer. 2001; 85: 692-696

Ardito CM, Grüner BM, Takeuchi KK, Lubeseder-Martellato C, Teichmann N, Mazur PK, DelGiorno KE, Carpenter ES, Halbrook CJ, Hall JC, Pal D. EGF receptor is required for KRAS-induced pancreatic tumorigenesis. Cancer cell. 2012; 22: 304-317

Auclin E, Marthey L, Abdallah R, Mas L, Francois E, Saint A, Cunha AS, Vienot A, Lecomte T, Hautefeuille V, de La Fouchardière C. Role of FOLFIRINOX and chemoradiotherapy in locally advanced and borderline resectable pancreatic adenocarcinoma: update of the AGEO cohort. British journal of cancer. 2021; 124: 1941-1948

Baker R, Wilkerson EM, Sumita K, Isom DG, Sasaki AT, Dohlman HG, Campbell SL. Differences in the regulation of K-Ras and H-Ras isoforms by monoubiquitination. Journal of Biological Chemistry. 2013; 288: 36856-36862

Barltrop JA, Owen TC, Cory AH, Cory JG. 5-(3-carboxymethoxyphenyl)-2-(4, 5-dimethylthiazolyl)-3-(4-sulfophenyl) tetrazolium, inner salt (MTS) and related analogs of 3-(4, 5-dimethylthiazolyl)-2, 5-diphenyltetrazolium bromide (MTT) reducing to purple

water-soluble formazans as cell-viability indicators. Bioorganic & Medicinal Chemistry Letters. 1991; 1: 611-614

Bedard PL, Tabernero J, Janku F, Wainberg ZA, Paz-Ares L, Vansteenkiste J, Van Cutsem E, Pérez-García J, Stathis A, Britten CD, Le N. A Phase Ib Dose-Escalation Study of the Oral Pan-PI3K Inhibitor Buparlisib (BKM120) in Combination with the Oral MEK1/2 Inhibitor Trametinib (GSK1120212) in Patients with Selected Advanced Solid TumorsPI3K Inhibitor Buparlisib with MEK Inhibitor Trametinib. Clinical Cancer Research. 2015; 21: 730-738

Bisht S, Feldmann G. Novel targets in pancreatic cancer therapy-current status and ongoing translational efforts. Oncology Research and Treatment. 2018; 41: 596-602

Bokemeyer C, Bondarenko I, Hartmann JT, De Braud F, Schuch G, Zubel A, Celik I, Schlichting M, Koralewski P. Efficacy according to biomarker status of cetuximab plus FOLFOX-4 as first-line treatment for metastatic colorectal cancer: the OPUS study. Annals of oncology. 2011; 22: 1535-1546

Brose MS, Volpe P, Feldman M, Kumar M, Rishi I, Gerrero R, Einhorn E, Herlyn M, Minna J, Nicholson A, Roth JA. BRAF and RAS mutations in human lung cancer and melanoma. Cancer research. 2002; 62: 6997-7000

Brown WS, McDonald PC, Nemirovsky O, Awrey S, Chafe SC, Schaeffer DF, Li J, Renouf DJ, Stanger BZ, Dedhar S. Overcoming adaptive resistance to KRAS and MEK inhibitors by co-targeting mTORC1/2 complexes in pancreatic cancer. Cell Reports Medicine. 2020; 1: 100131-100131

Bryant KL, Stalnecker CA, Zeitouni D, Klomp JE, Peng S, Tikunov AP, Gunda V, Pierobon M, Waters AM, George SD, Tomar G. Combination of ERK and autophagy inhibition as a treatment approach for pancreatic cancer. Nature medicine. 2019; 25: 628-640

Buttke TM, McCubrey JA, Owen TC. Use of an aqueous soluble tetrazolium/formazan assay to measure viability and proliferation of lymphokine-dependent cell lines. Journal of immunological methods. 1993; 157: 233-240

Cáceres-Gutiérrez RE, Alfaro-Mora Y, Andonegui MA, Díaz-Chávez J, Herrera LA. The Influence of Oncogenic RAS on Chemotherapy and Radiotherapy Resistance Through DNA Repair Pathways. Frontiers in Cell and Developmental Biology. 2022; 10: 751367-751367

Canon J, Rex K, Saiki AY, Mohr C, Cooke K, Bagal D, Gaida K, Holt T, Knutson CG, Koppada N, Lanman BA. The clinical KRAS (G12C) inhibitor AMG 510 drives anti-tumour immunity. Nature. 2019; 575: 217-223

Cataldo VD, Gibbons DL, Pérez-Soler R, Quintás-Cardama A. Treatment of non–small-cell lung cancer with erlotinib or gefitinib. New England Journal of Medicine. 2011; 364: 947-955

Chen X, Guo X, Zhang H, Xiang Y, Chen J, Yin Y, Cai X, Wang K, Wang G, Ba Y, Zhu L. Role of miR-143 targeting KRAS in colorectal tumorigenesis. Oncogene. 2009; 28: 1385-1392

Colbert LE, Petrova AV, Fisher SB, Pantazides BG, Madden MZ, Hardy CW, Warren MD, Pan Y, Nagaraju GP, Liu EA, Saka B. CHD7 Expression Predicts Survival Outcomes in Patients with Resected Pancreatic CancerLow CHD7 Expression Predicts Improved Outcome in PAC. Cancer research. 2014; 74: 2677-2687

Coley AB, Ward A, Keeton AB, Chen X, Maxuitenko Y, Prakash A, Li F, Foote JB, Buchsbaum DJ, Piazza GA. Pan-RAS inhibitors: Hitting multiple RAS isozymes with one stone. RAS: Past, Present, and Future. 2022: 131-168

Collins MA, Bednar F, Zhang Y, Brisset JC, Galbán S, Galbán CJ, Rakshit S, Flannagan KS, Adsay NV, Di Magliano MP. Oncogenic Kras is required for both the initiation and maintenance of pancreatic cancer in mice. The Journal of clinical investigation. 2012; 122: 639-653

Collisson EA, Trejo CL, Silva JM, Gu S, Korkola JE, Heiser LM, Charles RP, Rabinovich BA, Hann B, Dankort D, Spellman PT. A Central Role for RAF→ MEK→ ERK Signaling in the Genesis of Pancreatic Ductal AdenocarcinomaA Central Role for RAF→ MEK→ ERK Signaling in the Genesis of Pancreatic Ductal Adenocarcinoma. Cancer discovery. 2012; 2: 685-693

Cory AH, Owen TC, Barltrop JA, Cory JG. Use of an aqueous soluble tetrazolium/formazan assay for cell growth assays in culture. Cancer communications. 1991; 3: 207-212

Di Magliano MP, Logsdon CD. Roles for KRAS in pancreatic tumor development and progression. Gastroenterology. 2013; 144: 1220-1229

Di Nicolantonio F, Martini M, Molinari F, et al. Wild-type BRAF is required for response to panitumumab or cetuximab in metastatic colorectal cancer. Journal of clinical oncology. 2008; 26: 5705-5712

Dixon AS, Schwinn MK, Hall MP, Zimmerman K, Otto P, Lubben TH, Butler BL, Binkowski BF, Machleidt T, Kirkland TA, Wood MG. NanoLuc complementation reporter optimized for accurate measurement of protein interactions in cells. ACS chemical biology. 2016; 11: 400-408

Dogan S, Shen R, Ang DC, Johnson ML, D'Angelo SP, Paik PK, Brzostowski EB, Riely GJ, Kris MG, Zakowski MF, Ladanyi M. Molecular Epidemiology of EGFR and KRAS Mutations in 3,026 Lung Adenocarcinomas: Higher Susceptibility of Women to Smoking-

Related KRAS-Mutant CancersMolecular Epidemiology of Lung Cancer Driver Mutations. Clinical cancer research. 2012; 18: 6169-77

Ducreux M, Cuhna AS, Caramella C, Hollebecque A, Burtin P, Goéré D, Seufferlein T, Haustermans K, Van Laethem JL, Conroy T, Arnold D. Cancer of the pancreas: ESMO Clinical Practice Guidelines for diagnosis, treatment and follow-up. Annals of Oncology. 2015; 26: v56-v68

Dunnett-Kane V, Nicola P, Blackhall F, Lindsay C. Mechanisms of resistance to KRASG12C inhibitors. Cancers. 2021; 13: 151-151

E Poruk K, Z Gay D, Brown K, D Mulvihill J, M Boucher K, L Scaife C, A Firpo M, J Mulvihill S. The clinical utility of CA 19-9 in pancreatic adenocarcinoma: diagnostic and prognostic updates. Current molecular medicine. 2013; 13: 340-351

Fakih MG, Kopetz S, Kuboki Y, Kim TW, Munster PN, Krauss JC, Falchook GS, Han SW, Heinemann V, Muro K, Strickler JH. Sotorasib for previously treated colorectal cancers with KRASG12C mutation (CodeBreaK100): a prespecified analysis of a single-arm, phase 2 trial. The Lancet Oncology. 2022; 23: 115-124

Fedele C, Ran H, Diskin B, Wei W, Jen J, Geer MJ, Araki K, Ozerdem U, Simeone DM, Miller G, Neel BG. SHP2 Inhibition Prevents Adaptive Resistance to MEK Inhibitors in Multiple Cancer ModelsSHP2/MEK Inhibitor Combination Therapy. Cancer discovery. 2018; 8: 1237-1249

Feldmann G, Mishra A, Hong SM, Bisht S, Strock CJ, Ball DW, Goggins M, Maitra A, Nelkin BD. Inhibiting the cyclin-dependent kinase CDK5 blocks pancreatic cancer formation and progression through the suppression of Ras-Ral signaling. Cancer research. 2010; 70: 4460-4469

Fell JB, Fischer JP, Baer BR, Blake JF, Bouhana K, Briere DM, Brown KD, Burgess LE, Burns AC, Burkard MR, Chiang H. Identification of the clinical development candidate MRTX849, a covalent KRASG12C inhibitor for the treatment of cancer. Journal of medicinal chemistry. 2020; 63: 6679-6093

Ferlay J, Soerjomataram I, Dikshit R, Eser S, Mathers C, Rebelo M, Parkin DM, Forman D, Bray F. Cancer incidence and mortality worldwide: sources, methods and major patterns in GLOBOCAN 2012. International journal of cancer. 2015; 136: E359-E386

Gerboth S, Frittoli E, Palamidessi A, Baltanas FC, Salek M, Rappsilber J, Giuliani C, Troglio F, Rolland Y, Pruneri G, Kreutmair S. Phosphorylation of SOS1 on tyrosine 1196 promotes its RAC GEF activity and contributes to BCR-ABL leukemogenesis. Leukemia. 2018; 32: 820-827

Gimple RC, Wang X. RAS: Striking at the Core of the Oncogenic Circuitry. Frontiers in oncology. 2019; 9: 965-965

Grilley-Olson JE, Bedard PL, Fasolo A, Cornfeld M, Cartee L, Razak AR, Stayner LA, Wu Y, Greenwood R, Singh R, Lee CB. A phase Ib dose-escalation study of the MEK inhibitor trametinib in combination with the PI3K/mTOR inhibitor GSK2126458 in patients with advanced solid tumors. Investigational new drugs. 2016; 34: 740-749

Haan C, Behrmann I. A cost effective non-commercial ECL-solution for Western blot detections yielding strong signals and low background. Journal of immunological methods. 2007; 318: 11-19

Haigis KM. KRAS Alleles: The Devil Is in the Detail. Trends Cancer. 2017; 3: 686-697

Hallin J, Engstrom LD, Hargis L, Calinisan A, Aranda R, Briere DM, Sudhakar N, Bowcut V, Baer BR, Ballard JA, Burkard MR. The KRASG12C Inhibitor MRTX849 Provides Insight toward Therapeutic Susceptibility of KRAS-Mutant Cancers in Mouse Models and

PatientsTherapeutic Insight from the KRASG12C Inhibitor MRTX849. Cancer discovery. 2020; 10: 54-71

Hamidi H, Lu M, Chau K, Anderson L, Fejzo M, Ginther C, Linnartz R, Zubel A, Slamon DJ, Finn RS. KRAS mutational subtype and copy number predict in vitro response of human pancreatic cancer cell lines to MEK inhibition. British journal of cancer. 2014; 111: 1788-1801

Han K, Kim MH, Seeburg D, Seo J, Verpelli C, Han S, Chung HS, Ko J, Lee HW, Kim K, Heo WD. Regulated RalBP1 binding to RalA and PSD-95 controls AMPA receptor endocytosis and LTD. PLoS biology. 2009; 7: e1000187-e1000187

Hobbs GA, Der CJ, Rossman KL. RAS isoforms and mutations in cancer at a glance. Journal of cell science. 2016; 129 :1287-1292

Hofmann MH, Gmachl M, Ramharter J, Savarese F, Gerlach D, Marszalek JR, Sanderson MP, Kessler D, Trapani F, Arnhof H, Rumpel K. BI-3406, a Potent and Selective SOS1–KRAS Interaction Inhibitor, Is Effective in KRAS-Driven Cancers through Combined MEK InhibitionPan-KRAS SOS1 Protein–Protein Interaction Inhibitor BI-3406. Cancer discovery. 2021; 11: 142-157

Huang L, Guo ZX, Wang F. KRAS mutation: from undruggable to druggable in cancer. Signal Transduct Target Ther. 2021; 6: 386-405

Jančík S, Drábek J, Radzioch D, Hajdúch M. Clinical relevance of KRAS in human cancers. Journal of Biomedicine and Biotechnology. 2010; 2010:150960-150960

Jiao D, Yang S. Overcoming resistance to drugs targeting KRASG12C mutation. The Innovation. 2020; 1: 100035-100035

Johnson SM, Grosshans H, Shingara J, Byrom M, Jarvis R, Cheng A, Labourier E, Reinert KL, Brown D, Slack FJ. RAS is regulated by the let-7 microRNA family. Cell. 2005; 120: 635-647

Kaiser MH, Ellenberg SS. Pancreatic cancer: adjuvant combined radiation and chemotherapy following curative resection. Archives of surgery. 1985; 120: 899-903

Mizrahi JD, Surana R, Valle JW, Shroff RT. Pancreatic cancer. The Lancet. 2020; 395: 2008-2020

Kim D, Xue JY, Lito P. Targeting KRAS (G12C): from inhibitory mechanism to modulation of antitumor effects in patients. Cell. 2020; 183: 850-859

Kortlever RM, Sodir NM, Wilson CH, Burkhart DL, Pellegrinet L, Swigart LB, Littlewood TD, Evan GI. Myc cooperates with Ras by programming inflammation and immune suppression. Cell. 2017; 171: 1301-1315

Kosaka T, Yatabe Y, Endoh H, Kuwano H, Takahashi T, Mitsudomi T. Mutations of the epidermal growth factor receptor gene in lung cancer: biological and clinical implications. Cancer research. 2004; 64: 8919-8923

Kupcho K, Peters C, Niles A, 2017: Real-time assessment of apoptosis and necrosis. https://www.bmglabtech.com/en/application-notes/real-time-assessment-of-apoptosis-and-necrosis (data accesses: 27.11.2022)

Lambert JM, Lambert QT, Reuther GW, Malliri A, Siderovski DP, Sondek J, Collard JG, Der CJ. Tiam1 mediates Ras activation of Rac by a PI (3) K-independent mechanism. Nature cell biology. 2002: 4: 621-625

Lim KH, Baines AT, Fiordalisi JJ, Shipitsin M, Feig LA, Cox AD, Der CJ, Counter CM. Activation of RalA is critical for Ras-induced tumorigenesis of human cells. Cancer cell. 2005; 7: 533-545

Lim KH, O'Hayer K, Adam SJ, Kendall SD, Campbell PM, Der CJ, Counter CM. Divergent roles for RalA and RalB in malignant growth of human pancreatic carcinoma cells. Current Biology. 2006; 16: 2385-2394

Lito P, Solomon M, Li LS, Hansen R, Rosen N. Allele-specific inhibitors inactivate mutant KRAS G12C by a trapping mechanism. Science. 2016; 351: 604-608

Liu P, Wang Y, Li X. Targeting the untargetable KRAS in cancer therapy. Acta Pharmaceutica Sinica B. 2019; 9: 871-879

Lo W, Zureikat A. Neoadjuvant therapy in pancreatic cancer: A review and update on recent trials. Current Opinion in Gastroenterology. 2022; 38: 521-531

Ma CM, Coffey CW, DeWerd LA, Liu C, Nath R, Seltzer SM, Seuntjens JP. AAPM protocol for 40–300 kV x-ray beam dosimetry in radiotherapy and radiobiology. Medical physics. 2001; 28: 868-893

Manchado E, Weissmueller S, Morris JP, Chen CC, Wullenkord R, Lujambio A, de Stanchina E, Poirier JT, Gainor JF, Corcoran RB, Engelman JA. A combinatorial strategy for treating KRAS-mutant lung cancer. Nature. 2016; 534: 647-651

Martin S, Reutelingsperger CP, McGahon AJ, Rader JA, Van Schie RC, LaFace DM, Green DR. Early redistribution of plasma membrane phosphatidylserine is a general feature of apoptosis regardless of the initiating stimulus: inhibition by overexpression of Bcl-2 and Abl. The Journal of experimental medicine. 1995; 182: 1545-1556

Martinelli E, Morgillo F, Troiani T, Ciardiello F. Cancer resistance to therapies against the EGFR-RAS-RAF pathway: the role of MEK. Cancer treatment reviews. 2017; 53: 61-69

Morris EJ, Jha S, Restaino CR, Dayananth P, Zhu H, Cooper A, Carr D, Deng Y, Jin W, Black S, Long B. Discovery of a novel ERK inhibitor with activity in models of acquired resistance to BRAF and MEK inhibitors. Cancer discovery. 2013; 3: 742-750

Mukhopadhyay S, Vander Heiden MG, McCormick F. The metabolic landscape of RAS-driven cancers from biology to therapy. Nature cancer. 2021; 2: 271-283

Muzumdar MD, Chen PY, Dorans KJ, Chung KM, Bhutkar A, Hong E, Noll EM, Sprick MR, Trumpp A, Jacks T. Survival of pancreatic cancer cells lacking KRAS function. Nature communications. 2017; 8: 1-9

Neel NF, Rossman KL, Martin TD, Hayes TK, Yeh JJ, Der CJ. The RalB small GTPase mediates formation of invadopodia through a GTPase-activating protein-independent function of the RalBP1/RLIP76 effector. Molecular and cellular biology. 2012; 32: 1374-1386

Ostrem JM, Peters U, Sos ML, Wells JA, Shokat KM. K-Ras (G12C) inhibitors allosterically control GTP affinity and effector interactions. Nature. 2013; 503: 548-551

Ostrem JM, Shokat KM. Direct small-molecule inhibitors of KRAS: from structural insights to mechanism-based design. Nature reviews Drug discovery. 2016; 15: 771-785

Pai EF, Kabsch W, Krengel U, Holmes KC, John J, Wittinghofer A. Structure of the guanine-nucleotide-binding domain of the Ha-ras oncogene product p21 in the triphosphate conformation. Nature. 1989; 341: 209-214

Patricelli MP, Janes MR, Li LS, Hansen R, Peters U, Kessler LV, Chen Y, Kucharski JM, Feng J, Ely T, Chen JH. Selective Inhibition of Oncogenic KRAS Output with Small

Molecules Targeting the Inactive StateTargeting Inactive KRASG12C Suppresses Oncogenic Signaling. Cancer discovery. 2016; 6: 316-329

Pedersen K, Bilal F, Bernado Morales C, Salcedo MT, Macarulla T, Massó-Vallés D, Mohan V, Vivancos A, Carreras MJ, Serres X, Abu-Suboh M. Pancreatic cancer heterogeneity and response to Mek inhibition. Oncogene. 2017; 36: 5639-5647

Pierre S, Coumoul X. Understanding SOS (son of sevenless). Biochemical pharmacology. 2011; 82: 1049-1056

Pylayeva-Gupta Y, Grabocka E, Bar-Sagi D. RAS oncogenes: weaving a tumorigenic web. Nature Reviews Cancer. 2011; 11: 761-774

Riely GJ, Marks J, Pao W. KRAS mutations in non–small cell lung cancer. Proceedings of the American Thoracic Society. 2009; 6: 201-205

Ruess DA, Heynen GJ, Ciecielski KJ, Ai J, Berninger A, Kabacaoglu D, Görgülü K, Dantes Z, Wörmann SM, Diakopoulos KN, Karpathaki AF. Mutant KRAS-driven cancers depend on PTPN11/SHP2 phosphatase. Nature medicine. 2018; 24: 954-960

Ryan MB, Corcoran RB. Therapeutic strategies to target RAS-mutant cancers. Nature reviews Clinical oncology. 2018; 15: 709-720

Salojin KV, Zhang J, Meagher C, Delovitch TL. ZAP-70 is essential for the T cell antigen receptor-induced plasma membrane targeting of SOS and Vav in T cells. Journal of Biological Chemistry. 2000; 275: 5966-5975

Schreiber RD, Old LJ, Smyth MJ. Cancer immunoediting: integrating immunity's roles in cancer suppression and promotion. Science. 2011; 331: 1565-1570

Schwartz MA. Integrins, oncogenes, and anchorage independence. The Journal of cell biology. 1997; 139: 575-578

Shen Y, Zhu X, Cao F, Xie H, Ju X, Cao Y, Qing S, Jia Z, Gu L, Fang F, Zhang H. Re-irradiation with Stereotactic Body Radiotherapy (SBRT) for In-field Recurrence of Pancreatic Cancer After Prior SBRT: Analysis of 24 Consecutive Cases. Frontiers in Oncology. 2021: 4396-4396

Shields JM, Pruitt K, McFall A, Shaub A, Der CJ. Understanding Ras:'it ain't over'til it's over'. Trends in cell biology. 2000; 10: 147-154

Shimizu T, Tolcher AW, Papadopoulos KP, Beeram M, Rasco DW, Smith LS, Gunn S, Smetzer L, Mays TA, Kaiser B, Wick MJ. The Clinical Effect of the Dual-Targeting Strategy Involving PI3K/AKT/mTOR and RAS/MEK/ERK Pathways in Patients with Advanced CancerClinical Effect of Dual PI3K and MAPK Pathways Inhibitions. Clinical Cancer Research. 2012; 18: 2316-2325

Shipman L. Putting the brakes on KRAS-G12C nucleotide cycling. Nature Reviews Drug Discovery. 2016; 15: 159-159

Siegel RL, Miller KD, Fedewa SA, Ahnen DJ, Meester RG, Barzi A, Jemal A. Colorectal cancer statistics. CA: A Cancer Journal for Clinicians. 2017; 67: 177-193

Siegel RL, Miller, KD, Jemal, A. Cancer statistics, 2018. CA: A Cancer Journal for Clinicians. 2018; 68: 7-30

Siegel RL, Miller KD, Jemal A. Cancer statistics, 2019. CA: A Cancer Journal for Clinicians. 2019; 69: 7-34

Simanshu DK, Nissley DV, McCormick F. RAS proteins and their regulators in human disease. Cell. 2017; 170: 17-33

Singhi AD, George B, Greenbowe JR, Chung J, Suh J, Maitra A, Klempner SJ, Hendifar A, Milind JM, Golan T, Brand RE. Real-time targeted genome profile analysis of pancreatic

ductal adenocarcinomas identifies genetic alterations that might be targeted with existing drugs or used as biomarkers. Gastroenterology. 2019; 156: 2242-2253

Slebos RJ, Kibbelaar RE, Dalesio O, Kooistra A, Stam J, Meijer CJ, Wagenaar SS, Vanderschueren RG, van Zandwijk N, Mooi WJ, Bos JL. K-ras oncogene activation as a prognostic marker in adenocarcinoma of the lung. New England Journal of Medicine. 1990; 323: 561-565

Song S, Cong W, Zhou S, Shi Y, Dai W, Zhang H, Wang X, He B, Zhang Q. Small GTPases: Structure, biological function and its interaction with nanoparticles. Asian journal of pharmaceutical sciences. 2019; 14: 30-39

Statements FL. Amgen Announces New Clinical Data Evaluating Novel Investigational KRAS (G12C) Inhibitor in Larger Patient Group. World Conference on Lung Cancer. 2019

Strickler JH, Satake H, George TJ. Sotorasib in KRAS p.G12C–Mutated Advanced Pancreatic Cancer. N Engl J Med. 2023; 388: 33-43

Takahashi K, Nakagawa M, Young SG, Yamanaka S. Differential membrane localization of ERas and Rheb, two Ras-related proteins involved in the phosphatidylinositol 3-kinase/mTOR pathway. Journal of Biological Chemistry. 2005; 280: 32768-32774

Tan L, Cho KJ, Kattan WE, Garrido CM, Zhou Y, Neupane P, Capon RJ, Hancock JF. Acylpeptide hydrolase is a novel regulator of KRAS plasma membrane localization and function. Journal of cell science. 2019; 132: jcs232132

Toulany M. Targeting K-Ras-mediated DNA damage response in radiation oncology: Current status, challenges and future perspectives. Clinical and Translational Radiation Oncology. 2022: 38: 6-14

Towbin H, Staehelin T, Gordon J. Electrophoretic transfer of proteins from polyacrylamide gels to nitrocellulose sheets: procedure and some applications. Proceedings of the national academy of sciences. 1979; 76: 4350-4354

Tran TH, Alexander P, Dharmaiah S, Agamasu C, Nissley DV, McCormick F, Esposito D, Simanshu DK, Stephen AG, Balius TE. The small molecule BI-2852 induces a nonfunctional dimer of KRAS. Proceedings of the National Academy of Sciences. 2020; 117: 3363-3364

Tsuchida N, Murugan AK, Grieco M. Kirsten Ras oncogene: significance of its discovery in human cancer research. Oncotarget. 2016; 7: 46717–46733

Tuveson DA, Neoptolemos JP. Understanding metastasis in pancreatic cancer: a call for new clinical approaches. Cell. 2012; 148: 21-31

Uprety D, Adjei AA. KRAS: From undruggable to a druggable Cancer Target. Cancer treatment reviews. 2020; 89: 102070-102070

Vasan N, Baselga J, Hyman DM. A view on drug resistance in cancer. Nature. 2019; 575: 299-309

Versteijne E, van Dam JL, Suker M, Janssen QP, Groothuis K, Akkermans-Vogelaar JM, Besselink MG, Bonsing BA, Buijsen J, Busch OR, Creemers GJ. Neoadjuvant chemoradiotherapy versus upfront surgery for resectable and borderline resectable pancreatic cancer: long-term results of the Dutch randomized PREOPANC trial. Journal of Clinical Oncology. 2022; 40: 1220-1230

Weisner J, Landel I, Reintjes C, Uhlenbrock N, Trajkovic-Arsic M, Dienstbier N, Hardick J, Ladigan S, Lindemann M, Smith S, Quambusch L. Preclinical Efficacy of Covalent-Allosteric AKT Inhibitor Borussertib in Combination with Trametinib in KRAS-Mutant

Pancreatic and Colorectal CancerPreclinical Efficacy of AKT Inhibitor Borussertib. Cancer Research. 2019; 79: 2367-2378

Woo MK, Nordal RA. Commissioning and evaluation of a new commercial small rodent x-ray irradiator. Biomed Imaging Interv J. 2006; 2: e10-e10

Xue JY, Zhao Y, Aronowitz J, Mai TT, Vides A, Qeriqi B, Kim D, Li C, de Stanchina E, Mazutis L, Risso D. Rapid non-uniform adaptation to conformation-specific KRAS (G12C) inhibition. Nature. 2020; 577: 421-425

Yan H, Chin ML, Horvath EA, Kane EA, Pfleger CM. Impairment of ubiquitylation by mutation in Drosophila E1 promotes both cell-autonomous and non-cell-autonomous Ras-ERK activation in vivo. Journal of cell science. 2009; 122: 1461-1470

Yang MH, Laurent G, Bause AS, Spang R, German N, Haigis MC, Haigis KM. HDAC6 and SIRT2 Regulate the Acetylation State and Oncogenic Activity of Mutant K-RASRegulation of K-RAS Acetylation. Molecular Cancer Research. 2013; 11: 1072-1077

Yao JC, Eisner MP, Leary C, Dagohoy C, Phan A, Rashid A, Hassan M, Evans DB. Population-based study of islet cell carcinoma. Annals of surgical oncology. 2007; 14: 3492-3500

Ye J, Mills BN, Zhao T, Han BJ, Murphy JD, Patel AP, Johnston CJ, Lord EM, Belt BA, Linehan DC, Gerber SA. Assessing the magnitude of immunogenic cell death following chemotherapy and irradiation reveals a new strategy to treat pancreatic cancer. Cancer immunology research. 2020; 8: 94-107

Ying H, Kimmelman AC, Lyssiotis CA, Hua S, Chu GC, Fletcher-Sananikone E, Locasale JW, Son J, Zhang H, Coloff JL, Yan H. Oncogenic Kras maintains pancreatic tumors through regulation of anabolic glucose metabolism. Cell. 2012; 149: 656-670

Young A, Lou D, McCormick F. Oncogenic and Wild-type Ras Play Divergent Roles in the Regulation of Mitogen-Activated Protein Kinase SignalingRegulation of Signaling by Wild-Type and Oncogenic Ras. Cancer discovery. 2013; 3: 112-123

Zhang SS, Nagasaka M. Spotlight on Sotorasib (AMG 510) for KRASG12C Positive Non-Small Cell Lung Cancer. Lung Cancer: Targets and Therapy. 2021; 12: 115-122

Zhao C, Du G, Skowronek K, Frohman MA, Bar-Sagi D. Phospholipase D2-generated phosphatidic acid couples EGFR stimulation to Ras activation by Sos. Nature cell biology. 2007; 9: 707-712

9. Acknowledgements

I would like to express my special thanks to Mr. PD Dr. Med Georg Feldmann, my MD/PhD supervisor, for giving me the opportunity to study for my MD/PhD in Germany. It was a valuable experience for me at both academic and personal levels. No matter how busy he was, his office was always available for our questions and requests for help, and he always answered our questions promptly and patiently, I feel grateful to have been his student.

I am very grateful to Mrs. Dr. Bisht Savita, my team leader, for her great help throughout my research period. I am grateful for her gentleness and kindness, which allowed me, a shy and introverted person, to seek help at the first sign of trouble, she was always generous in helping me no matter it was a professional problem or a trivial matter.

I would also like to thank Dr. Garbe and Dr. Johanna for their supports in radiotherapy techniques.

I would like to thank all my colleagues in Feldmann Group for teaching me laboratory skills at the beginning of my research, guiding me through the laboratory environment and atmosphere, they helped me to adapt to the laboratory life very quickly.

To all my colleagues in MED II and MED III, I would like to thank them for their timely help in my daily work and for the friendly cooperation between the working groups.

Finally, my heartfelt thanks to my parents and boyfriend for their endless love and support, which provided me with the motivation to never give up and pursue my goals. Without them, I would not have been able to successfully complete my studies.